Title
Remyelination failure following white matter stroke: new targets for repair identified by oligodendrocyte progenitor cell transcriptome database.

Author
Sozmen, Elif Guler

Publication Date
2013

Peer reviewed|Thesis/dissertation

UNIVERSITY OF CALIFORNIA

Los Angeles

Remyelination failure following white matter stroke: new targets for repair identified by oligodendrocyte progenitor cell transcriptome database

A dissertation submitted in partial satisfaction of the

requirements for the degree Doctor of Philosophy

in Neuroscience

Elif Guler Sozmen

2013

ABSTRACT OF THE DISSERTATION

Remyelination failure following white matter stroke: new targets for repair identified by oligodendrocyte progenitor cell transcriptome database

by

Elif Guler Sozmen

Doctor of Philosophy in Neuroscience

University of California, Los Angeles, 2013

Professor S. Thomas Carmichael, Chair

White matter stroke is a common problem in the elderly population and makes up one third of all ischemic stroke cases. Stroke causes localized process of white matter cell death but also a subsequent regenerative response with the activation of oligodendrocyte progenitor cells (OPCs). This dissertation details the OPC regenerative response and their cellular fate in a mouse model of white matter stroke. The stroke environment supports successful OPC proliferation but lacks pro-myelinating factors that lead to OPC differentiation arrest. Novel transcriptome studies are conducted for genomic comparison of progenitors across two stroke time points in order to determine the molecular systems underlying OPC differentation arrest. The resulting transcriptome database contained several previously described inhibitory mechanisms in addition to novel targets, most important of which were Matrilin 2 and Inhibin A. In-vitro studies confirmed the contrasting effects of Matrilin 2 and Inhibin A on OPC differentiation and oligodendrocyte maturation that makes them promising therapeutic targets for white matter stroke recovery.

The dissertation of Elif Guler Sozmen is approved

Michael Sofroniew

Harley I. Kornblum

Bennett G. Novitch

Seema Tiwari-Woodruff

S. Thomas Carmichael, Chair

University of California, Los Angeles

2013

TABLE OF CONTENTS

Page

This dissertation would not have been possible without the guidance and the help of several individuals who in one way or another contributed and extended their valuable assistance in the preparation and completion of this study.

First and foremost, I would like to express my sincere gratitude to my advisor Dr. Tom Carmichael for the continuous support of my doctorate study and research, for his patience, motivation, enthusiam and vast knowledge. He has been a true inspiration not just as a scientist but also as a positive role model during the five years of my graduate study.
Special thanks to the rest of my committee, Dr. Michael Sofroniew, Dr. Harley Kornblum, Dr. Ben Novitch, and Dr. Seema Tiwari-Woodruff for their support, guidance and helpful suggestions. Their guidance has served me well and I owe them my heartfelt appreciation.

My sincere thanks go to:
The Laboratory of Seema Tiwari-Woodfruff for conducting the CAP measurements.
Dr. Bennett Novitch for sharing the valuable antibodies produced in his laboratory.
Dr. Pablo Paez and Wilma Speuer for their assistance in developing primary OPC cultures.
Dr. Roman Giger for providing us the NgR-OMNI Fc.
Dr. Giovanni Coppola for analyzing the OPC transcription data.
I thank my fellow lab mates and friends across the world who shared my joys and frustrations during the years of my graduate student career.
Last but not least, I would like to thank my adoptive family of MacIsaacs who showed we can choose our families after all.

Appendix A is a reprint of: Sozmen EG, Kolekar A, Havton LA, Carmichael ST (2009) A white matter stroke model in the mouse: axonal damage, progenitor responses and MRI correlates. J Neurosci Methods 180:261-272. I would like to thank Arunima Kolekar and Dr. Leif Havton for their contributions in developing the model and characterizing the lesion through EM studies.

This work was supported by American Heart Association Pre-Doctoral Fellowship, Ruth L. Kirchstein NRSA Pre-Doctoral Fellowship from NINDS and Adelson Family Foundation.

BIOGRAPHICAL SKETCH

NAME OF FELLOWSHIP APPLICANT Sozmen, Elif, G	POSITION TITLE Graduate Student
eRA COMMONS USER NAME (credential, e.g., agency login) ESOZMEN	

EDUCATION/TRAINING

INSTITUTION AND LOCATION	DEGREE *(if applicable)*	YEAR(s)	FIELD OF STUDY
California State University, Sacramento	B.S.	2000-2003	Molecular Biology/ Microbiology
David Geffen School of Medicine, University of California, Los Angeles	M.D., Ph.D. 2015 (expected)	2006 – present	Medicine / Neuroscience

Academic Awards

2006 UCLA MSTP support by NIGMS

2009 – 2011 American Heart Association Pre-doctoral Fellowship, Western States Affiliate

2010 Neurology Science Day Poster Award - 2nd place among graduate student competitors

2011 Semel/BRI Travel Award

2011 – 2013 Ruth L. Kirschstein National Research Service Award, NINDS

Publications

Research Papers

Sozmen EG, Romero-Gallo, J Chytil A, Russell EW, Whitehead R, Parks TW, Grady WM (2005) Inactivation of TGF-beta signaling in hepatocytes results in an increased proliferative response after partial hepatectomy. *Oncogene* 24(18):3028-41.

Munoz NM, Upton M, Rojas A, Washington MK, Lin L, Chytil A, **Sozmen EG**, Madison BB, Pozzi A, Moon RT, Moses HL, Grady WM (2006) Transforming growth factor ß receptor type II inactivation induces the malignant transformation of intestinal neoplasms initiated by Apc mutation. *Cancer Res.* 66(20):9837-44.

Sozmen EG, Kolekar A, Havton LA, Carmichael ST (2009) A white matter stroke model in the mouse: axonal damage, progenitor responses and MRI correlates. *J Neurosci Methods.* 180(2):261-72.

Sozmen EG, Hinman JD, Carmichael ST (2012) Models that matter: white matter stroke models. *Neurotherapeutics.* 9(2):349-58.

Abstracts

Sozmen EG, Romero-Gallo J, Trobridge P, Yeh M, Grady WM (2005) TGF- ß signaling inactivation in hepatocytes inhibits DEN induced hepatocellular carcinoma**.** *Hepatology* 42(S1):299A- 401A. Poster presentation at 56th Annual Meeting of the American Association for the Study of Liver Diseases, San Francisco, CA. November 2005.

Sozmen EG, Kolekar A, Carmichael ST. Characterization of oligodendrocyte progenitors and white matter remyelination in subcortical stroke. Poster presentation at 2nd Biennieal Meeting of Glia in Health and Disease, Cold Spring Harbor Laboratories, Cold Spring Harbor, NY, July 2008.

Sozmen EG, Kolekar A, Havton LA, Carmichael ST. Glial response and oligodendrocyte regeneration following ischemic white matter injury: studies in a mouse subcortical stroke model. *Glia*, 2009. Poster presentation at 9th European Meeting on Glial Cells in Health and Disease, Paris, France, September 2009.

Sozmen EG, Kolekar A, Havton LA, Carmichael ST. Secondary axonal and myelin degradation following ischemic white matter injury and associated glial regenerative response in a mouse model of subcortical stroke. Poster presentation at 39th Society of Neuroscience Meeting, Chicago, IL, October 2009.

Sozmen EG, Crawford DK, Tiwari-Woodruff S, Carmichael ST. NG2+ progenitor response and lineage analysis in white matter stroke.

Poster presentation at 3rd Biennieal Meeting of Glia in Health and Disease, Cold Spring Harbor Laboratories, Cold Spring Harbor, NY, July 2010.

Sozmen EG, Crawford DK, Tiwari-Woodruff S, Carmichael ST. Cell fate determination of oligodendrocyte precursor cells following white matter stroke

Poster presentation at 40th Society for Neuroscience Meeting, San Diego, CA, November 2010.

Sozmen EG, Carmichael ST. Inhibition of OPC differentiation and alternative cell fates following white matter ischemic injury.

Poster presentation at 41st Society for Neuroscience Meeting, Washington DC, October 2011.

Sozmen EG, Carmichael ST. OPC differentiation arrest and transcriptional changes in OPCs following white matter stroke.

Poster presentation at 42nd Society for Neuroscience Meeting, New Orleans, LA October 2012.

INTRODUCTION

White matter stroke is a common clinical problem that constitutes up to one-third of all stroke cases (Schneider *et al*., 2004). Distinct histological changes are found within ischemic white matter such as: focal edema, demyelination, axonal damage, loss of oligodendrocytes, and local activation of astrocytes and microglia (Fernando *et al*., 2006; Jellinger, 2007; Sozmen *et al*., 2009). Unlike gray matter, treatment avenues for white matter stroke have not been explored, such as the opportunities for axonal rescue coupled with successful OPC differentiation and remyelination. The hallmarks of white matter stroke, namely loss of oligodendrocytes and consequent axonal demyelination, are shared features with late stage Multiple Sclerosis (MS), Traumatic Brain Injury, Spinal Cord Injury and Alzheimer's Disease. Despite the vast differences in etiology and subsequent immune responses across these diseases, white matter stroke triggers the brain's endogenous, albeit limited, repair capacity similar to MS and spinal cord injury through a distinct cell population termed oligodendrocyte progenitor cells (OPCs) (Sozmen *et al*., 2009). For all the reasons above, widespread interest has been devoted to the therapeutic potential of OPCs that are ubiquitously scattered throughout the CNS (Gensert and Goldman, 1997; Shoshan *et al*., 1999; Windrem *et al*., 2004; Rivers *et al*., 2008).

The mammalian process of axon myelination is a well-studied subject. The embryonic lineage of myelinating oligodendrocytes that describes the origin of OPCs, their migration, proliferation and postnatal development are heavily investigated. Although most OPCs successfully differentiate into myelinating oligodendrocytes, a considerable amount remains as uncommitted glia in the adult as a possible reservoir of endogenous progenitors. A fundamental question in biology is whether recapitulating development can overcome the hurdles to repair and regeneration presented in a disease state. The adult OPC is a classic example for answering such a question since this cell comprises 4-8% of the total cells found in the CNS as

persists in a progenitor state (Dawson *et al*., 2003). Much of the current information regarding repair mechanisms after white matter injury is derived from toxin/immune-mediated demyelination and spinal cord injury models.

Many studies indicate that experimental demyelination initiates a robust regenerative response that includes cues for resident OPCs to proliferate, migrate and partially differentiate into myelinating oligodendrocytes (Franklin, 2002). For instance, spontaneous remyelination is documented in the early stages of MS as shown in its primary animal model, experimental autoimmune encephalomyelitis (EAE), as well as in cuprizone- and lysolecithin-mediated demyelination (Tripathi *et al*., 2010). Studies conducted in Shiverer mice elegantly demonstrate the extent of OPC myelinating potential in this myelin-deficient mouse strain upon progenitor transplants (Windrem *et al*., 2004). However, as robust as the OPC regenerative response appears to be, post-mortem MS and experimental studies consistently indicate that the failure of OPC differentiation *in vivo* is the major roadblock to recovery after demyelination (Kuhlmann et al., 2008). It is currently unclear how complex cell fate decisions are controlled, not only during development but also after a demyelinating injury, as some OPCs complete maturation while some remain undifferentiated or in a progenitor state. Far less is known about the consequences of focal white matter stroke on OPC repair potential and remyelinating events as compared to toxin or immune-mediated damage.

OPCs as Adult Progenitors

The OPC is a mysterious cell type that resides in the parenchyma in a quiescent state unless activated. OPCs are often identified by the cell surface proteoglycan NG2, and high levels of the receptor Platelet Derived Growth Factor Receptor alpha (PDGFRα) (Sim *et al*., 2006). During perinatal developmental oligodendrogenesis, the NG2 marker is replaced with expression of the transcription factor Nkx2.2 and cytoplasmic translocation of another

transcription factor named Olig 1 (Arnett *et al*., 2004). This is followed with expression of GST-π, CC1 and myelin specific proteins like CNPase, MOG, PLP and MBP as indicators of a developmental progression toward mature oligodendrocytes (Dimou *et al*., 2008). Although they share the same list of markers, adult OPCs differ from their perinatal counterparts in cell cycle duration, rates of migration, differentiation and diverse responses to growth factors (Simon *et al*., 2011).

In comparison to other cell types in the brain, OPCs contain unique molecular signaling systems. These may provide an opportunity for novel drug targets in white matter repair. Particularly, receptor/ligand systems play major roles in interactions with the local white matter environment and shape OPC commitment toward proliferation or differentiation. For example, OPCs highly express protein tyrosine phosphatase zeta (PTPζ), fibroblast growth factor receptor 3 (FGFR 3), PDGFRα and a unique profile of bone morphogenic protein (BMP) 4 inhibitors that differentially prime these cells for proliferation and maintain the precursor state (McClain *et al*., 2012). Similarly, OPCs use constitutive Notch1 signaling to activate downstream genes like Mash1 and Hes1 to sustain a less differentiated state (Stidworthy *et al*., 2004; Zhang *et al*., 2009). At the later oligodendrocyte stage, additional receptor/ligand systems become important that can potentially improve the repair process. For instance, endogenous Leukemia Inhibitory Factor (LIF) and Ciliary Neurotrophic Factor (CNTF) receptor signaling are shown to promote survival of oligodendrocytes and limit damage in demyelinating injuries (Butzkueven *et al*., 2002; Tripathi and McTigue, 2008; Deverman and Patterson, 2012). All these mentioned systems have been defined in culture systems, or in inflammatory white matter disease models. There has been no systematic work on OPC or mature oligodendrocyte signaling systems in white matter stroke. However, such signaling systems are in a position to synergistically regulate regenerative responses in OPC-mediated white matter repair.

Major Differences between White Matter Stroke and Immune-mediated Demyelination

Multiple Sclerosis (MS) is defined as the selective degeneration of myelin sheaths with relative initial sparing of axons due to dysregulated immune system, at least during the primary demyelination stage of the disease. An important pathological feature of MS is gathered from post-mortem studies regarding the early remyelination taking place in the shadow plaques. In these areas of myelin rarefaction, degenerated myelin sheaths are seldom completely replaced and repair is restricted to the rim of the bordering lesion (Patrikios *et al*., 2006). It is currently unclear when oligodendrocytes are lost after the primary demyelination in MS. The degree of axonal degeneration varies during the course of the disease: it is initiated at the early lesions when acute inflammatory episodes are present, yet continues during later stages even in the absence of overt inflammation (Androdias *et al*., 2010).

Unlike immune-mediated demyelination, white matter stroke does not involve toxic oligodendrocyte cell death. The fact that ischemia affects all cell types leads to white matter lesions exhibiting non-specific cell death in the affected area. For instance oligodendrocyte and OPC death are observed shortly after focal white matter stroke produced in mice (Souza-Rodrigues *et al*., 2008). Vasoconstriction of small caliber vasculature leads to initial apoptotis followed by necrosis that expands gradually into a chronic lesion with penumbral tissue and necrotic core (Tanaka *et al*., 2008). This is followed by the loss of myelin and concurrent axonal swelling and dystrophy within the first week of injury. The extent of long-term axonal degeneration and repair has not been assessed in the context of white matter stroke.

In animal models of MS or primary white matter injury (cuprizone, lysolecithin), OPCs respond with cell division, migration to lesion sites and differentiation into myelin producing mature oligodendrocytes (Franklin and Ffrench-Constant, 2008). This response has led to the

characterization of injury-induced OPCs as “reactive OPCs” (Arnett *et al*., 2004). Environmental signals govern the behavior of reactive OPCs following injury (Sim *et al*., 2006). Because each injury and lesion paradigm varies in terms of cause and overall cellular responses, the specific signals that induce NG2+ OPC division likely vary between conditions. For instance, demyelination induced changes in the microenvironment, such as upregulated production of BMP4, FGF-2, PDGF, IGF-1 and heparin-binding growth factor Pleiotrophin, can be the prominent factors for OPC migration and proliferation (Franklin and Hinks, 1999; Arnett *et al*., 2003; Sim *et al*., 2006). Yet studies in spinal cord injury models indicate non-demyelinating inflammatory injury can also initiate significant OPC amplification and differentiation (Gensel *et al*., 2008). In contrast to MS, white matter stroke does not induce a prolonged T and B cell response, which likely translates into a different set of chemokines found in the ischemic white matter lesion. Despite the differences of near complete loss of axons, ischemia-induced global cell death and the nature of immune response, OPC differentiation remains limited after white matter stroke in the mouse.

Promoters of OPC Differentiation

In vitro studies of OPCs illustrate that this cell type is highly responsive to external stimuli, in which cell differentiation can be induced by merely changing the culture medium from PDGF and FGF2 rich to a more complex multi-factorial cocktail (Wang et al., 2007b). There are few single factors that are capable of inducing OPC differentiation *in vitro* such as: several subtypes of integrin (Baron *et al*., 2005) and vitronectin (Gutowski *et al*., 1999) (both are components of the extracellular matrix), glutamate release on OPCs (Ziskin *et al*., 2007), and secreted factors as in Retinoic Acid (Barres *et al*., 1994; Huang *et al*., 2011), Neurotrophin 3 (Wilson *et al*., 2003) and many others. However, a combination of factors is required for successful OPC differentiation and remyelination *in vivo*. Moreover, the multifactorial environment permissive to white matter repair appears to show redundancy. For instance extrinsic regulatory systems such

as the extracellular matrix protein dystroglycan, secreted factors CNTF and LIF, and chemokines such as CXCL12 have been shown to enhance oligodendrocyte survival and myelination, yet they are often insufficient to promote remyelination on their own (Tripathi and McTigue, 2008; Deverman and Patterson 2005; Gresle *et al*., 2012; Woodruff *et al*., 2004).

Based on the studies investigating acute and chronic injury states of demyelination, the concept of a permissive window to enhance white matter repair emerges as fundamentally important in white matter stroke. The most obvious temporal changes occurring in white matter stroke are astrocytic and microglia responses that are likely to change the milieu of the peri-infarct white matter into an inhibitory environment to the remyelination process. It is as yet unclear if a window of opportunity exists after white matter stroke, in addition to neutralizing the effects of excitatoxic injury, so that OPC responses can be modulated to favor differentiation.

Inhibitors of Oligodendrocyte Regeneration

A number of studies have identified specific OPC differentiation inhibitors in post-mortem MS lesions, MS models of disease, models of spinal cord injury and neonatal hypoxic-ischemic injury (Table 1). It is likely that white matter stroke lesions contain some of the mentioned changes in the microenvironment that can negatively impact the oligodendrocyte regeneration and remyelination.

PSA NCAM

Polysialylated neural cell adhesion molecule (PSA-NCAM) is an unusual example of an anti-myelination molecule derived by injured axons. Post-mortem examination of chronic MS lesions indicates demyelinated axons paradoxically express high levels of PSA-NCAM that may play a role in stunting OPC differentiation (Charles *et al*., 2002). Congruent with this finding, oligodendrocyte regeneration and the formation of Nodes of Ranvier could be enhanced when

specific antibodies were used to mask PSA NCAM or when the functional PSA domain was cleaved with endoneurominidase N *in vitro* (Charles *et al*., 2002). Additionally, Koutsoudaki and colleagues demonstrate that elimination of the PSA synthesizing enzyme in a transgenic mouse line successfully promotes remyelination above baseline in cuprizone-mediated demyelination (Koutsoudaki *et al*., 2010). It remains unknown if white matter stroke leads to injured axons expressing PSA NCAM similar to inactive MS lesions.

Hyaluronan

Healthy brain tissue contains a steady amount of Hyaluronan, an extracellular matrix glycosaminoglycan, for scaffolding and cell support. However, an excessive amount of high molecular weight Hyaluronan is produced by reactive astrocytes upon injury that is implicated in the inhibition of OPC differentiation (Back *et al*., 2005). *In vitro* studies show high molecular weight Hyaluronan reduces the expression of mature oligodendrocyte marker MBP and the complexity of myelin sheaths when added to differentiating rat OPCs. Similarly, degradation of Hyaluronan with the enzyme Hyaluronidase reverses the inhibitory effects on OPC differentiation in the OPC-astrocyte co-culture system (Back *et al*., 2005). Accumulated high molecular weight Hyaluronan acts on cell surface receptor CD44 to relay intracellular signaling. It is proposed that Hyaluronan-CD44 autocrine signaling regulates astrocytosis after injury to maintain quiescence. For instance, administration of hyaluronidase into quiescent astrocyte cultures *in vitro* or into normal rat spinal cords *in vivo* induces proliferation of astrocytes (Struve *et al*., 2005). Conversely, addition of high molecular but not low molecular weight Hyaluronan into proliferating astrocyte cultures inhibit mitotic activity. Besides astrocytes, OPCs are also shown to express receptor CD44, which appears to have an anti-myelinating effect rather than cell-cycle control. For instance, CD44 overexpression in myelinating glia in the CNPase-CD44 transgenic mice induces non-inflammatory dysmyelination and progressive demyelination (Tuohy *et al*., 2004).

Still little is known about the underlying mechanism through which Hyaluronan blocks OPC maturation. In addition to CD44, several other cell surface receptors bind to Hyaluronan such as Toll-Like Receptor (TLR) 2 and 4, during the process of dendritic cell, microglia and macrophage activation (Scheibner *et al*., 2006; Taylor *et al*., 2007). Furthermore, Hyaluronan binding to TLRs stunts differentiation of several cell types as in osteoblasts and keratinocytes (Passi *et al*., 2004; Falconi and Aubin, 2007). In the same way, Hyaluronan acting as a TLR2 ligand is able to inhibit OPC differentiation *in vitro,* which can be partially reversed by TLR2 binding antibodies and completely prevented in OPCs derived from TLR2 null mouse pups (Sloane *et al*., 2010). When Hyaluronan was injected into lysolecithin-induced lesions in TLR2 mutant mice, remyelination took place in a similar fashion to lesions generated in wild-type animals that did not receive Hyaluronan (Sloane *et al*., 2010). In sum, CD44 and TLR2 are candidate receptor signaling targets of Hyaluronan in white matter injury that may synergistically contribute to the remyelination failure in disease.

Relevant to the findings mentioned above, an elevated amount of Hyaluronan was found in chronic MS lesions as well as in mice with EAE (Back *et al*., 2005). Increased CD44 expression was also detected in the glial scar astrocytes within the chronic MS lesions (Tuohy *et al*., 2004). Further studies in post-mortem chronic MS lesions show the presence of TLR2 in cells of oligodendrocyte lineage (Sloane *et al*., 2010). The potential role of Hyaluronan or the changes in Hyaluronan binding receptors have not been investigated in the setting of white mater stroke.

Myelin Associated Inhibitors

A direct consequence of demyelinating lesions is the remaining myelin debris that accumulates as a result of myelin sheath disintegration. Within the resulting myelin debris,

various molecules have been identified as detrimental to axonal elongation, which are collectively named Myelin-associated inhibitory (MAI) proteins. MAI factors include: Nogo A, MAG, OMgp, Ephrin B3, Semaphorins and Netrins (Prinjha *et al*, 2000; Mukhopadhyay *et al*, 1994; Wang *et al*, 2002; Benson *et al*, 2005; Moreau-Fauvarque *et al*, 2003; Low *et al*, 2008). Nogo A binding to the multisubunit receptor complex of: Nogo receptor 1 (NgR1), NgR adaptor LINGO-1 and its effectors p75/Troy at the surface of neurons leads to actin depolymerization and neurite retraction (Fournier *et al*, 2001; Mi *et al*, 2004; Shao *et al*, 2005; Yamashita *et al*, 2005). Although MAG and OMgp share no sequence homology or structural similarity with Nogo A, they can elicit the same molecular cascade by associating with NgR-p75 complex (Wang *et al*, 2002). NgRs have been detected in oligodendrocyes but not in OPCs, although the progenitors express the important co-receptors of the NgR complex namely LINGO-1 and p75 (Chang *et al*., 2000; Wong et al., 2002). In healthy CNS, NgR1 complex activation plays a role in activity-dependent synaptic refinement (Raiker *et al*., 2010), however its role in white matter disease is not clear.

Recent studies indicate that myelin proteins not only induce growth-cone collapse but they also exert inhibitory effects on OPC differentiation. An essential function of macrophages in demyelinating lesions such as MS is the phagocytosis of myelin and myelin proteins following degradation. Regions of remyelination, particularly the lesion borders, strongly overlap with zones where macrophages are active in clearing the myelin debris (Patrikios 2006). As such, the hypothesis of myelin debris having detrimental effects in remyelination emerged and later was verified in a multitude of ways. For example, differentiation of rat OPCs *in vitro* was blocked by the addition of CNS myelin preparations. Later, treatment of myelin extracts with proteinase as opposed to lipase suggested the inhibitory function is due to the protein component of the myelin debris (Syed *et al*, 2008). On the other hand, OPCs grown on the most prominent inhibitors of axon regeneration including Nogo A, OMgp and MAG failed to hinder OPC

differentiation *in vitro* (Syed *et al*, 2008). In fact, these factors are proven to be essential during white matter development. For instance, Nogo A expression increases in developing OPCs and Nogo A null mice show markedly delayed optic nerve myelination due to interruption of OPC differentiation (Pernet *et al*., 2008). Myelination in the cerebellum and optic nerve is further delayed in Nogo A and MAG double KO animals (Pernet *et al*., 2008). Similarly, OMgp null mice display hypomyelination compared to wild-type animals and OMgp deficient OPCs fail to mature properly *in vitro* (Lee *et al*., 2011). Therefore, myelin debris may include unknown proteins detrimental to remyelination that are distinct from the well-known MAI factors. Nevertheless, studies focusing on LINGO-1 expression in OPCs and oligodendrocyes show NgR complex plays an active role in remyelination albeit the ligands may be undetermined.

Mi and colleagues demonstrated LINGO-1 negatively regulates oligodendrocyte maturation in addition to axon myelination (Mi *et al*, 2005 and 2007). LINGO-1 neutralizing antibody or downregulation of LINGO-1 expression by a lentivirus construct showed blocking NgR1 complex enhances OPC differentiation *in vitro.* In DRG-OPC co-culture, the differentiated rat oligodendrocytes developed more complex processes as well as myelin structure when LINGO-1 action was suppressed (Mi *et al*., 2005). Furthermore, a LINGO-1 antagonist was effective in improving EAE scores in rat models by significantly reducing spinal cord demyelination and increasing remyelination (Mi *et al*., 2007). Likewise, neutralizing LINGO-1 was sufficient to improve functional recovery in lysolecithin and cuprizone models of demyelination (Mi *et al*., 2009). LINGO-1 activation induces the downstream effectors of RhoA and Fyn kinase in oligodendrocytes, which are the same factors inhibiting axonal outgrowth in neurons by limiting process elongation (Mi *et al*., 2005). Blocking Nogo A function in rat OPCs with antibodies targeting the extracellular domain of the protein was shown to increase LINGO-1 expression in rat OPCs *in vitro* along with stunted process extention (Zhao *et al*., 2007).

Conflicting data emerged recently suggesting that siRNA-mediated Nogo A know-down in rat OPCs enhances oligodendrocyte branching complexity (Zhao *et al*., 2011). This finding supports the results of Chong and colleagues, who demonstrated competitive interactions between oligodendrocytes are driven by Nogo signaling by using a mutant strain deficient in all forms of Nogo. In this study, oligodendrocytes lacking Nogo showed higher myelinogenic potential, and lysolecithin induced demyelination in Nogo KO mice resulted in extensive remyelination without changing OPC differentiation potential (Chong *et al*., 2012).

Together, these results indicate NgR components such as LINGO-1 are promising targets against remyelination failure in white matter disease, although Nogo variants may play a role in limiting myelinogenic potential once OPCs differentiate. Given the unknown protein repertoire of myelin as indicated by Syed and colleagues, lingering myelin debris may still be a factor in OPC differentiation block after white matter ischemia.

Semaphorins

Semaphorins comprise a large family of guidance molecules that can be membrane bound and secreted (De Winter *et al*., 2002). Similar to NgR complex activation, semaphorins were originally identified as repulsive axon guidance molecules during development. Their role in OPC differentiation and remyelination was not investigated until recent years. Post-mortem analysis of MS lesions demonstrated Sema transcripts were upregulated in active lesions, whereas chronic lesions had low expression levels comparable to healthy white matter (Williams *et al*., 2007). Particularly, the increase in Sema 3A expression in active MS lesions coupled with the expression of Sema receptor Neuropilin-1 in plaque area OPCs suggest thar semophorin-mediated signaling may be involved in remyelination failure in MS (Williams *et al*., 2007).

Sema 3A can induce a variety of cellular responses including apoptosis, redirection of processes, and exerting negative guidance cues in diverse cell types like astrocytes, immune cells, and neurons (De Winter *et al*., 2002; Spassky *et al*., 2002; Ji *et al*., 2009). Syed and colleagues found OPCs plated on Sema 3A substrate underwent a reversible differentiation block that was tied to suppression of myelin genes and impaired process formation (Syed *et al*., 2011). The observed differentiation block was not due to increased cell death and could be reversed in 48 hours after switching to normal culture media. Furthermore, in a toxin-mediated spontaneously remyelinating injury model, exogenous Sema 3A infusion did not alter the number OPCs within the lesion but significantly decreased the number of mature oligodendrocytes (Syed *et al*., 2011). The differentiation arrest observed in Sema 3A treated lesions appears to happen at the premyelinating oligodendrocyte stage. Although the demyelinated axons were contacted by immature oligodendrocytes, the axons remained denuded while the premyelinating OPCs failed to form compact myelin sheaths (Syed *et al*., 2011).

The source of Sema 3A in lesions is not known since neurons, astrocytes and OPCs themselves may be the origin. Its expression during the critical stage of MS similar to other factors such as Notch-1, makes Sema 3A an interesting target to change the course of remyelination. This is in contrast with the markers of chronic disease such as Hyaluronan and PSA-NCAM that also inhibits OPC differentiation, yet neutralizing their negative effects may be less successful in repair by missing the critical window.

Sema 4D is another example among the semaphorin family that is involved in oligodendrocyte generation. Sema 4D deficient mice develop a higher number of cortical mature oligodendrocytes without depleting the OPC reservoir, which implies Sema 4D exerts negative effects on oligodendrogenesis (Taniguchi *et al*., 2009). More relevant finding is that transient

MCA occlusion in wild-type animals resulted in an increase of Sema 4D positive cells in the peri-infarct cortex, which persisted until 14 days following stroke. When Sema 4D null mice were subjected to stroke, not only the OPC differentiation rate was markedly increased but the total number of newly generated oligodendrocytes was higher compared to wild-type animals (Taniguchi *et al*., 2009). Taken together, Sema 4D may be involved in maintaining the appropriate density of mature oligodendrocytes in the cortex. Sema 4D effects in the white matter or the phenotype of Sema 4D positive cells were not investigated. Class 4 semaphorins partner with receptors Plexin B1 and B2 to exert their effects (Masuda *et al*., 2004). Whether OPCs express either receptor types remains elusive.

Although the physiologic functions are speculative, and the fact that conflicting semophorin-induced myelinogenic effects are reported, the semaphorin family of proteins may be relevant targets for promoting remyelination after white matter stroke. It is to be determined if white matter stroke induces an increase in various classes of semaphorins and whether newly born OPCs possess corresponding receptors following white matter ischemia.

Notch-1 Signaling Pathway

During white matter development, Notch1 receptor interaction with ligands Delta and Jagged activates the canonical Notch pathway, which favors OPC proliferation by inducing *Hes1* and *Hes5* gene expression (D'Souza *et al*., 2008). Downstream effects of canonical Notch signaling when bound to Jagged-1 have also been implicated in remyelination failure during early stages of MS (John *et al*., 2002). Astrocytes have been suggested as a potential source of OPC Notch1 activation, since Jagged-1 production was increased in cultured astrocytes in response to TGF-β and hypertrophic astrocytes in MS lesions are shown to express Jagged-1 (John *et al*., 2002). The most convincing evidence regarding an anti-remyelination role of the Notch1-Jagged1 system comes from the study conducted by Zhang and colleagues (Zhang *et*

al., 2009) using a transgenic mouse line, in which targeted inactivation of Notch1 is driven by oligodendrocyte lineage specific *Olig1* promoter. When Notch1 was inactivated, both OPC differentiation and remyelination processes were accelerated following lysolecithin injury (Zhang *et al*., 2009). Consistent with the developmental studies, the inhibitory effects of Notch1-Jagged1 signaling appear to be significant during the early stages of oligodendrocyte development in disease, given that conditional ablation of Notch1 under the control of oligodendrocyte-specific *PLP* promoter does not result in further remyelination (Stidworthy *et al*., 2004).

In contrast to Notch-Jagged interaction, the noncanonical Notch pathway activation via axon-derived ligand F3/Contactin coordinates the commitment of cells of the oligodendrocyte lineage by inducing differentiation of OPCs into mature myelinating oligodendrocytes (Hu *et al*., 2003). A recent study examining chronic human MS lesions paradoxically found increased levels of Contactin and of Notch1 positive OPCs (Nakahara *et al*., 2009). Further investigation suggests that nuclear localization of the Notch1-intracellular domain necessary for myelogenesis was interrupted in these inactive lesions by abnormal OPC expression of TIP30, an importin inhibitor (Nakahara *et al*., 2009).

Collectively, both canonical and noncanonical Notch signaling might be influencing OPC differentiation after white matter stroke. Whether such inhibition takes place due to increased production of Jagge-1 by hypertrophic astrocytes, a lack of Contactin on demyelinated axons, or aberrant expression of TIP30 in OPCs remains to be elucidated in ischemic white matter disease.

Wnt Signaling Pathway

Canonical Wnt-catenin pathway is involved in many developmental processes. It is not surprising that canonical Wnt signaling, and the expression of its intranuclear mediator Tcf4, also play role in oligodendrogenesis during development, and are implicated in effective myelin repair after multiple modes of injury (Fancy *et al*., 2009). Several lines of evidence indicate Wnt pathway acts cell autonomously in OPCs. Particularly, Tcf4/β-catenin mediated Wnt signaling functions in the timing of OPC differentiation. When Tcf4 is associated with beta-catenin, it forms a complex that is typically associated with activation of Wnt downstream genes (van de Wetering *et al*., 2002) and acts as a negative regulator of myelin gene expression (He *et al*., 2007). Fancy and colleagues demonstrated that Tcf4 is upregulated in OPCs residing in active MS plaques, in developing rodent brain and in lesioned adult rodent white matter (Fancy *et al*., 2009). It is suggested that the binding of Wnt ligands to OPCs promotes the stabilization of the beta-catenin/Tcf4 complex, maintaining the OPCs in an undifferentiated state. This hypothesis is confirmed by their use of a transgenic mouse line expressing a constitutively active form of beta-catenin in OPC lineage of cells, which results in hypomyelination during development and impaired remyelination after injury. Follow-up remyelination experiments conducted in APC^{Min} mice, which lack the negative regulatory function of beta-catenin antagonist APC, confirm the anti-myelinating role of Wnt pathway (Fancy *et al*., 2009).

Another autoregulatory check point is accomplished by Wnt induced *AXIN2* expression, which in turn controls the degradation of beta-catenin in various tissue types (Lustig *et al*., 2002). Therefore, *AXIN2* expression serves as a read-out of Wnt pathway activation as well as an indication of inhibitory feedback. Fancy and colleagues reported abundant *AXIN2* mRNA levels in the OPCs found in neonatal white matter injury samples and in active MS lesions (Fancy *et al*., 2011). Furthermore, deletion of *Axin2* in transgenic mice leads to delayed OPC

maturation and perturbed remyelination kinetics following spinal cord demyelination (Fancy *et al*., 2011).

It is unclear whether dysregulation of Wnt signaling is sufficient to account for OPC differentiation arrest or if Wnt signals work synergistically with other negative regulators acting in concert with myelin debris, inflammatory cells etc. Despite the more likely scenario of mutifactorial inhibition of oligodendrogenesis, delivery of an exogenous Axin2 stabilizer was enough to promote myelination in cerebellar slice cultures after acute hypoxia and repair in spinal cords after lysolecithin administration (Fancy *et al*., 2011). For the purpose of post-stroke white matter repair, it remains to be to determined if the Wnt pathway is dysregulated in newly born OPCs that can negatively affect white matter stroke recovery.

Alternative Glial Fate of OPCs

OPCs are inherently multipotential. In culture conditions A2B5 positive astrocytes can become oligodendrocytes and astrocytes, also depending on cellular microenvironments (Tanner *et al*., 2011). Multiple experiments suggested bipotential capacity of OPCs in-vivo. For instance, when OPC cell line CG4 was transplated into glial-depleted regions of the CNS, transplanted cells contributed to generation of both astrocytes and myelinating oligodendrocytes (Franklin *et al*., 1995). A series of fate-mapping studies further confirmed the multipotential nature OPCs as they could give rise to astrocytes during development and tissue homeostasis *in vivo*. Zhu and colleagues used NG2creBAC mice crossed with a Cre reporter Z/EG strain that demonstrated the progeny of OPCs mainly consists of myelinating oligodendrocytes, yet NG2 positive cells could form a subpopulation of protoplasmic astrocytes in the gray matter of the ventrolateral forebrain and the spinal cord (Zhu *et al*., 2008). In contrast, a similar study conducted in PDGRα-creERT2/ R26R-YFP double-transgenic mice reported that OPCs routinely produce oligodendrocytes and, surprisingly, projection neurons in the piriform cortex, but not astrocytes (Rivers *et al*., 2008). In a study using the same reporter line, OPCs gave rise

to oligodendrocytes as well as few astrocytes but barely any neurons in the spinal cords of EAE model of demyelination (Tripathi *et al*., 2010). Furthermore, lineage mapping in the Olig2-creERTM/R26R-YFP line showed OPC fate is restricted to oligodendrocytes in the white matter of early post-natal and adult mouse brain (Dimou *et al*., 2008). Within the gray matter, Olig 2 lineage cells generated few astrocytes, some oligodendrocytes but remained mostly in progenitor state, more so if the induction took place later in adulthood. Additionally, this limited progenitor response of cortical OPCs persisted after brain injury with few cortical OPCs producing mature oligodendrocytes (Dimou *et al*., 2008). In this study we show adult OPCs can generate astrocytes only in the presence of injury. Consequences of astrocytic transformation are not known but hold significance when remyelination is limited after stroke.

Our understanding of complex interactions between the white matter microenvironment in disease and the fate of oligodendrocyte progenitors has substantially increased. Rodent white matter stroke models suggest the lack of white matter repair stems from the differentiation failure of adult OPCs despite a robust proliferative response observed following the infarct. Cellular and molecular environment within the white matter infarcts are altered markedly over time. By considering time-dependent changes in white matter stroke lesions particularly, loss of axons, astrocyte activation and consequent changes in the extracellular matrix, the presence of OPC differentiation inhibitors appear more likely to play a role in white matter repair failure rather than an absence of pro-myelinating cues. An extensive list of pro- and anti-myelinating factors gathered from non-stroke studies is in a place to guide future research to determine stroke-specific key changes (Table 1). Prominently, the neuron-derived anti-myelination molecule PSA-NCAM in addition to by-products of astrocytic activation such as Hyaluronan, and myelin associated inhibitors found within the lesion are promising targets to neutralize OPC non cell-autonomous inhibitors of repair. Studies in MS and SCI clearly demonstrate how demyelinating injuries trigger the activation of important OPC differentiation programs that mimic CNS development. As such, the canonical Notch and Wnt signaling pathways are the primary

receptor-ligand mechanisms remaining to be investigated in white matter stroke to delineate OPC intrinsic changes. If administered during a permissive window of repair, antagonists targeting the prominent OPC differentiation inhibitors can be an effective way to enhance post-stroke recovery. Lastly, the misguided differentiation of OPCs into astrocytes is a potential pitfall during white matter repair, given that OPC differentiation arrest is a common occurrence in white matter stroke and immune-mediated demyelination.

In this study, we carried out comprehensive characterization of OPC regeneration response in white matter stroke, and identified novel targets through RNAseq OPC transcriptome experiments that can change the course of white matter repair in this disease, as well as other demyelinating injuries. Through this novel OPC transcription database, we anticipated to find some of the inhibitory mechanisms mentioned so far in addition to novel targets that reflect the unique transformations taking place in the stroked white matter.

Negative regulators of myelination		
High Molecular Weight Hyaluronan	TLR2	Back *et al.,* 2005; Sloane *et al.,* 2010
PSA-NCAM		Charles *et al.,* 2002; Koutsoudaki *et al.,* 2010
Notch canonical	Jagged 1	John *et al.,* 2002, Park and Appel 2003
Notch non-canonical	TIP30	Nakahara *et al.,* 2009
Semaphorin	Sema3A, Sema 4D	Syed *et al.*, 2011, Taniguchi *et al.*, 2009
Wnt	Tcf4, GSK3B	He *et al.,* 2007; Fancy *et al.,* 2009
SRF		Stritt *et al.,* 2009
Myelin Assoicated Inhibitors		Kotter *et al.,* 2006; Baer *et al.,* 2009; Syed *et al.,* 2008
LINGO	p75 NTR	Mi *et al.,* 2005; Bourikas *et al.,* 2010
NOGO	Nogo-A	Pernet *et al.,* 2008; Yang *et al.,* 2010
CXCR2		Liu *et al.,* 2010
DR6		Mi *et al.,* 2011
CNTF		Tripathi and McTigue 2008
Pro-myelinating factors		
LIF		Kerr *et al.,* 2005
IL-6		Valerio *et al.,* 2002
Retionic Acid	RXR gamma	Barres *et al.,* 1994; Huang *et al.,* 2011
Notch non-canonical	F3/Contactin	Hu *et al.,* 2003
BDNF		Chan *et al.*, 2001
Neuregulins		Wang *et al.,* 2002
MMPs	MMP 9, MMP 12	Larsen *et al.,* 2006
CXCL12		Gottle *et al.,* 2010
NT3		Wilson *et al.,* 2003
Wnt	Axin2	Fancy *et al.,* 2011

Table 1. Review of prominent negative regulators of OPC differentiation and the factors that promote myelination according to published reports.

References

Androdias G, Reynolds R, Chanal M, Ritleng C, Confavreux C, Nataf S (2010) Meningeal T cells associate with diffuse axonal loss in multiple sclerosis spinal cords. Ann Neurol 68:465-476.

Arnett HA, Wang Y, Matsushima GK, Suzuki K, Ting JP (2003) Functional genomic analysis of remyelination reveals importance of inflammation in oligodendrocyte regeneration. J Neurosci 23:9824-9832.

Arnett HA, Fancy SP, Alberta JA, Zhao C, Plant SR, Kaing S, Raine CS, Rowitch DH, Franklin RJ, Stiles CD (2004) bHLH transcription factor Olig1 is required to repair demyelinated lesions in the CNS. Science 306:2111-2115.

Back SA, Tuohy TM, Chen H, Wallingford N, Craig A, Struve J, Luo NL, Banine F, Liu Y, Chang A, Trapp BD, Bebo BF, Jr., Rao MS, Sherman LS (2005) Hyaluronan accumulates in demyelinated lesions and inhibits oligodendrocyte progenitor maturation. Nat Med 11:966-972.

Baron W, Colognato H, ffrench-Constant C (2005) Integrin-growth factor interactions as regulators of oligodendroglial development and function. Glia 49:467-479.

Barres BA, Lazar MA, Raff MC (1994) A novel role for thyroid hormone, glucocorticoids and retinoic acid in timing oligodendrocyte development. Development 120:1097-1108.

Benson MD, Romero MI, Lush ME, Lu QR, Henkemeyer M, Parada LF (2005) Ephrin-B3 is a myelin-based inhibitor of neurite outgrowth. Proc Natl Acad Sci U S A 102:10694-10699.

Butzkueven H, Zhang JG, Soilu-Hanninen M, Hochrein H, Chionh F, Shipham KA, Emery B, Turnley AM, Petratos S, Ernst M, Bartlett PF, Kilpatrick TJ (2002) LIF receptor signaling limits immune-mediated demyelination by enhancing oligodendrocyte survival. Nat Med 8:613-619.

Chan JR, Cosgaya JM, Wu YJ, Shooter EM (2001) Neurotrophins are key mediators of the myelination program in the peripheral nervous system. Proc Natl Acad Sci U S A 98:14661-14668.

Chang A, Nishiyama A, Peterson J, Prineas J, Trapp BD (2000) NG2-positive oligodendrocyte progenitor cells in adult human brain and multiple sclerosis lesions. J Neurosci 20:6404-6412.

Charles P, Reynolds R, Seilhean D, Rougon G, Aigrot MS, Niezgoda A, Zalc B, Lubetzki C (2002) Re-expression of PSA-NCAM by demyelinated axons: an inhibitor of remyelination in multiple sclerosis? Brain 125:1972-1979.

Chong SY, Rosenberg SS, Fancy SP, Zhao C, Shen YA, Hahn AT, McGee AW, Xu X, Zheng B, Zhang LI, Rowitch DH, Franklin RJ, Lu QR, Chan JR (2012) Neurite outgrowth inhibitor Nogo-A establishes spatial segregation and extent of oligodendrocyte myelination. Proc Natl Acad Sci U S A 109:1299-1304.

D'Souza B, Miyamoto A, Weinmaster G (2008) The many facets of Notch ligands. Oncogene 27:5148-5167.

Dawson MR, Polito A, Levine JM, Reynolds R (2003) NG2-expressing glial progenitor cells: an abundant and widespread population of cycling cells in the adult rat CNS. Mol Cell Neurosci 24:476-488.

De Winter F, Oudega M, Lankhorst AJ, Hamers FP, Blits B, Ruitenberg MJ, Pasterkamp RJ, Gispen WH, Verhaagen J (2002) Injury-induced class 3 semaphorin expression in the rat spinal cord. Exp Neurol 175:61-75.

Deverman BE, Patterson PH (2012) Exogenous Leukemia Inhibitory Factor Stimulates Oligodendrocyte Progenitor Cell Proliferation and Enhances Hippocampal Remyelination. The Journal of Neuroscience 32:2100-2109.

Dimou L, Simon C, Kirchhoff F, Takebayashi H, Gotz M (2008) Progeny of Olig2-expressing progenitors in the gray and white matter of the adult mouse cerebral cortex. J Neurosci 28:10434-10442.

Falconi D, Aubin JE (2007) LIF inhibits osteoblast differentiation at least in part by regulation of HAS2 and its product hyaluronan. J Bone Miner Res 22:1289-1300.

Fancy SP, Baranzini SE, Zhao C, Yuk DI, Irvine KA, Kaing S, Sanai N, Franklin RJ, Rowitch DH (2009) Dysregulation of the Wnt pathway inhibits timely myelination and remyelination in the mammalian CNS. Genes Dev 23:1571-1585.

Fancy SP, Harrington EP, Yuen TJ, Silbereis JC, Zhao C, Baranzini SE, Bruce CC, Otero JJ, Huang EJ, Nusse R, Franklin RJ, Rowitch DH (2011) Axin2 as regulatory and therapeutic target in newborn brain injury and remyelination. Nat Neurosci 14:1009-1016.

Fernando MS, Simpson JE, Matthews F, Brayne C, Lewis CE, Barber R, Kalaria RN, Forster G, Esteves F, Wharton SB, Shaw PJ, O'Brien JT, Ince PG (2006) White matter lesions in an unselected cohort of the elderly: molecular pathology suggests origin from chronic hypoperfusion injury. Stroke 37:1391-1398.

Fournier AE, GrandPre T, Strittmatter SM (2001) Identification of a receptor mediating Nogo-66 inhibition of axonal regeneration. Nature 409:341-346.

Franklin RJ (2002) Remyelination of the demyelinated CNS: the case for and against transplantation of central, peripheral and olfactory glia. Brain Res Bull 57:827-832.

Franklin RJ, Hinks GL (1999) Understanding CNS remyelination: clues from developmental and regeneration biology. J Neurosci Res 58:207-213.

Franklin RJ, Ffrench-Constant C (2008) Remyelination in the CNS: from biology to therapy. Nat Rev Neurosci 9:839-855.

Gensel JC, Almad AA, Alexander JK, Schonberg DL, Tripathi RB (2008) Does chronic remyelination occur for all spared axons after spinal cord injury in mouse? J Neurosci 28:8385-8386.

Gensert JM, Goldman JE (1997) Endogenous progenitors remyelinate demyelinated axons in the adult CNS. Neuron 19:197-203.

Gresle MM, Alexandrou E, Wu Q, Egan G, Jokubaitis V, Ayers M, Jonas A, Doherty W, Friedhuber A, Shaw G, Sendtner M, Emery B, Kilpatrick T, Butzkueven H (2012) Leukemia Inhibitory Factor Protects Axons in Experimental Autoimmune Encephalomyelitis via an Oligodendrocyte-Independent Mechanism. PLoS One 7:e47379.

Gutowski NJ, Newcombe J, Cuzner ML (1999) Tenascin-R and C in multiple sclerosis lesions: relevance to extracellular matrix remodelling. Neuropathol Appl Neurobiol 25:207-214.

He Y, Dupree J, Wang J, Sandoval J, Li J, Liu H, Shi Y, Nave KA, Casaccia-Bonnefil P (2007) The transcription factor Yin Yang 1 is essential for oligodendrocyte progenitor differentiation. Neuron 55:217-230.

Hu QD et al. (2003) F3/contactin acts as a functional ligand for Notch during oligodendrocyte maturation. Cell 115:163-175.

Huang JK, Jarjour AA, Nait Oumesmar B, Kerninon C, Williams A, Krezel W, Kagechika H, Bauer J, Zhao C, Evercooren AB, Chambon P, Ffrench-Constant C, Franklin RJ (2011) Retinoid X receptor gamma signaling accelerates CNS remyelination. Nat Neurosci 14:45-53.

Jellinger KA (2007) The enigma of vascular cognitive disorder and vascular dementia. Acta Neuropathol 113:349-388.

Ji JD, Park-Min KH, Ivashkiv LB (2009) Expression and function of semaphorin 3A and its receptors in human monocyte-derived macrophages. Hum Immunol 70:211-217.

John GR, Shankar SL, Shafit-Zagardo B, Massimi A, Lee SC, Raine CS, Brosnan CF (2002) Multiple sclerosis: re-expression of a developmental pathway that restricts oligodendrocyte maturation. Nat Med 8:1115-1121.

Kerr BJ, Patterson PH (2005) Leukemia inhibitory factor promotes oligodendrocyte survival after spinal cord injury. Glia 51:73-79.

Koutsoudaki PN, Hildebrandt H, Gudi V, Skripuletz T, Skuljec J, Stangel M (2010) Remyelination after cuprizone induced demyelination is accelerated in mice deficient in the polysialic acid synthesizing enzyme St8siaIV. Neuroscience 171:235-244.

Kuhlmann T, Miron V, Cui Q, Wegner C, Antel J, Bruck W (2008) Differentiation block of oligodendroglial progenitor cells as a cause for remyelination failure in chronic multiple sclerosis. Brain 131:1749-1758.

Lee X, Hu Y, Zhang Y, Yang Z, Shao Z, Qiu M, Pepinsky B, Miller RH, Mi S (2011) Oligodendrocyte differentiation and myelination defects in OMgp null mice. Mol Cell Neurosci 46:752-761.

Liu L, Belkadi A, Darnall L, Hu T, Drescher C, Cotleur AC, Padovani-Claudio D, He T, Choi K, Lane TE, Miller RH, Ransohoff RM (2010) CXCR2-positive neutrophils are essential for cuprizone-induced demyelination: relevance to multiple sclerosis. Nat Neurosci 13:319-326.

Low K, Culbertson M, Bradke F, Tessier-Lavigne M, Tuszynski MH (2008) Netrin-1 is a novel myelin-associated inhibitor to axon growth. J Neurosci 28:1099-1108.

Lustig B, Jerchow B, Sachs M, Weiler S, Pietsch T, Karsten U, van de Wetering M, Clevers H, Schlag PM, Birchmeier W, Behrens J (2002) Negative feedback loop of Wnt signaling through upregulation of conductin/axin2 in colorectal and liver tumors. Mol Cell Biol 22:1184-1193.

Masuda K, Furuyama T, Takahara M, Fujioka S, Kurinami H, Inagaki S (2004) Sema4D stimulates axonal outgrowth of embryonic DRG sensory neurones. Genes Cells 9:821-829.

McClain CR, Sim FJ, Goldman SA (2012) Pleiotrophin Suppression of Receptor Protein Tyrosine Phosphatase-beta/zeta Maintains the Self-Renewal Competence of Fetal Human Oligodendrocyte Progenitor Cells. J Neurosci 32:15066-15075.

McTigue DM, Tripathi RB (2008) The life, death, and replacement of oligodendrocytes in the adult CNS. J Neurochem 107:1-19.

Mi S, Lee X, Hu Y, Ji B, Shao Z, Yang W, Huang G, Walus L, Rhodes K, Gong BJ, Miller RH, Pepinsky RB (2011) Death receptor 6 negatively regulates oligodendrocyte survival, maturation and myelination. Nat Med.

Mi S, Lee X, Shao Z, Thill G, Ji B, Relton J, Levesque M, Allaire N, Perrin S, Sands B, Crowell T, Cate RL, McCoy JM, Pepinsky RB (2004) LINGO-1 is a component of the Nogo-66 receptor/p75 signaling complex. Nat Neurosci 7:221-228.

Mi S, Miller RH, Lee X, Scott ML, Shulag-Morskaya S, Shao Z, Chang J, Thill G, Levesque M, Zhang M, Hession C, Sah D, Trapp B, He Z, Jung V, McCoy JM, Pepinsky RB (2005) LINGO-1 negatively regulates myelination by oligodendrocytes. Nat Neurosci 8:745-751.

Mi S, Hu B, Hahm K, Luo Y, Kam Hui ES, Yuan Q, Wong WM, Wang L, Su H, Chu TH, Guo J, Zhang W, So KF, Pepinsky B, Shao Z, Graff C, Garber E, Jung V, Wu EX, Wu W (2007) LINGO-1 antagonist promotes spinal cord remyelination and axonal integrity in MOG-induced experimental autoimmune encephalomyelitis. Nat Med 13:1228-1233.

Mi S, Miller RH, Tang W, Lee X, Hu B, Wu W, Zhang Y, Shields CB, Miklasz S, Shea D, Mason J, Franklin RJ, Ji B, Shao Z, Chedotal A, Bernard F, Roulois A, Xu J, Jung V, Pepinsky B (2009) Promotion of central nervous system remyelination by induced differentiation of oligodendrocyte precursor cells. Ann Neurol 65:304-315.

Moreau-Fauvarque C, Kumanogoh A, Camand E, Jaillard C, Barbin G, Boquet I, Love C, Jones EY, Kikutani H, Lubetzki C, Dusart I, Chedotal A (2003) The transmembrane semaphorin Sema4D/CD100, an inhibitor of axonal growth, is expressed on oligodendrocytes and upregulated after CNS lesion. J Neurosci 23:9229-9239.

Mukhopadhyay G, Doherty P, Walsh FS, Crocker PR, Filbin MT (1994) A novel role for myelin-associated glycoprotein as an inhibitor of axonal regeneration. Neuron 13:757-767.

Nakahara J, Kanekura K, Nawa M, Aiso S, Suzuki N (2009) Abnormal expression of TIP30 and arrested nucleocytoplasmic transport within oligodendrocyte precursor cells in multiple sclerosis. J Clin Invest 119:169-181.

Park HC, Appel B (2003) Delta-Notch signaling regulates oligodendrocyte specification. Development 130:3747-3755.

Passi A, Sadeghi P, Kawamura H, Anand S, Sato N, White LE, Hascall VC, Maytin EV (2004) Hyaluronan suppresses epidermal differentiation in organotypic cultures of rat keratinocytes. Exp Cell Res 296:123-134.

Patrikios P, Stadelmann C, Kutzelnigg A, Rauschka H, Schmidbauer M, Laursen H, Sorensen PS, Bruck W, Lucchinetti C, Lassmann H (2006) Remyelination is extensive in a subset of multiple sclerosis patients. Brain 129:3165-3172.

Pernet V, Joly S, Christ F, Dimou L, Schwab ME (2008) Nogo-A and myelin-associated glycoprotein differently regulate oligodendrocyte maturation and myelin formation. J Neurosci 28:7435-7444.

Prinjha R, Moore SE, Vinson M, Blake S, Morrow R, Christie G, Michalovich D, Simmons DL, Walsh FS (2000) Inhibitor of neurite outgrowth in humans. Nature 403:383-384.

Raiker SJ, Lee H, Baldwin KT, Duan Y, Shrager P, Giger RJ (2010) Oligodendrocyte-myelin glycoprotein and Nogo negatively regulate activity-dependent synaptic plasticity. J Neurosci 30:12432-12445.

Rivers LE, Young KM, Rizzi M, Jamen F, Psachoulia K, Wade A, Kessaris N, Richardson WD (2008) PDGFRA/NG2 glia generate myelinating oligodendrocytes and piriform projection neurons in adult mice. Nat Neurosci 11:1392-1401.

Scheibner KA, Lutz MA, Boodoo S, Fenton MJ, Powell JD, Horton MR (2006) Hyaluronan fragments act as an endogenous danger signal by engaging TLR2. J Immunol 177:1272-1281.

Schneider AT, Kissela B, Woo D, Kleindorfer D, Alwell K, Miller R, Szaflarski J, Gebel J, Khoury J, Shukla R, Moomaw C, Pancioli A, Jauch E, Broderick J (2004) Ischemic stroke subtypes: a population-based study of incidence rates among blacks and whites. Stroke 35:1552-1556.

Shao Z, Browning JL, Lee X, Scott ML, Shulga-Morskaya S, Allaire N, Thill G, Levesque M, Sah D, McCoy JM, Murray B, Jung V, Pepinsky RB, Mi S (2005) TAJ/TROY, an orphan TNF receptor family member, binds Nogo-66 receptor 1 and regulates axonal regeneration. Neuron 45:353-359.

Shi J, Marinovich A, Barres BA (1998) Purification and characterization of adult oligodendrocyte precursor cells from the rat optic nerve. J Neurosci 18:4627-4636.

Shoshan Y, Nishiyama A, Chang A, Mork S, Barnett GH, Cowell JK, Trapp BD, Staugaitis SM (1999) Expression of oligodendrocyte progenitor cell antigens by gliomas: implications for the histogenesis of brain tumors. Proc Natl Acad Sci U S A 96:10361-10366.

Sim FJ, Lang JK, Waldau B, Roy NS, Schwartz TE, Pilcher WH, Chandross KJ, Natesan S, Merrill JE, Goldman SA (2006) Complementary patterns of gene expression by human oligodendrocyte progenitors and their environment predict determinants of progenitor maintenance and differentiation. Ann Neurol 59:763-779.

Simon C, Gotz M, Dimou L (2011) Progenitors in the adult cerebral cortex: cell cycle properties and regulation by physiological stimuli and injury. Glia 59:869-881.

Sloane JA, Batt C, Ma Y, Harris ZM, Trapp B, Vartanian T (2010) Hyaluronan blocks oligodendrocyte progenitor maturation and remyelination through TLR2. Proc Natl Acad Sci U S A 107:11555-11560.

Souza-Rodrigues RD, Costa AM, Lima RR, Dos Santos CD, Picanco-Diniz CW, Gomes-Leal W (2008) Inflammatory response and white matter damage after microinjections of endothelin-1 into the rat striatum. Brain Res 1200:78-88.

Sozmen EG, Kolekar A, Havton LA, Carmichael ST (2009) A white matter stroke model in the mouse: axonal damage, progenitor responses and MRI correlates. J Neurosci Methods 180:261-272.

Spassky N, de Castro F, Le Bras B, Heydon K, Queraud-LeSaux F, Bloch-Gallego E, Chedotal A, Zalc B, Thomas JL (2002) Directional guidance of oligodendroglial migration by class 3 semaphorins and netrin-1. J Neurosci 22:5992-6004.

Stidworthy MF, Genoud S, Li WW, Leone DP, Mantei N, Suter U, Franklin RJ (2004) Notch1 and Jagged1 are expressed after CNS demyelination, but are not a major rate-determining factor during remyelination. Brain 127:1928-1941.

Struve J, Maher PC, Li YQ, Kinney S, Fehlings MG, Kuntz Ct, Sherman LS (2005) Disruption of the hyaluronan-based extracellular matrix in spinal cord promotes astrocyte proliferation. Glia 52:16-24.

Syed YA, Baer AS, Lubec G, Hoeger H, Widhalm G, Kotter MR (2008) Inhibition of oligodendrocyte precursor cell differentiation by myelin-associated proteins. Neurosurg Focus 24:E5.

Syed YA, Hand E, Mobius W, Zhao C, Hofer M, Nave KA, Kotter MR (2011) Inhibition of CNS remyelination by the presence of semaphorin 3A. J Neurosci 31:3719-3728.

Taniguchi Y, Amazaki M, Furuyama T, Yamaguchi W, Takahara M, Saino O, Wada T, Niwa H, Tashiro F, Miyazaki J-i, Kogo M, Matsuyama T, Inagaki S (2009) Sema4D deficiency

results in an increase in the number of oligodendrocytes in healthy and injured mouse brains. Journal of Neuroscience Research 87:2833-2841.

Tanner DC, Cherry JD, Mayer-Proschel M (2011) Oligodendrocyte progenitors reversibly exit the cell cycle and give rise to astrocytes in response to interferon-gamma. J Neurosci 31:6235-6246.

Taylor KR, Yamasaki K, Radek KA, Di Nardo A, Goodarzi H, Golenbock D, Beutler B, Gallo RL (2007) Recognition of hyaluronan released in sterile injury involves a unique receptor complex dependent on Toll-like receptor 4, CD44, and MD-2. J Biol Chem 282:18265-18275.

Tripathi RB, Rivers LE, Young KM, Jamen F, Richardson WD (2010) NG2 glia generate new oligodendrocytes but few astrocytes in a murine experimental autoimmune encephalomyelitis model of demyelinating disease. J Neurosci 30:16383-16390.

Tuohy TM, Wallingford N, Liu Y, Chan FH, Rizvi T, Xing R, Bebo B, Rao MS, Sherman LS (2004) CD44 overexpression by oligodendrocytes: a novel mouse model of inflammation-independent demyelination and dysmyelination. Glia 47:335-345.

Valerio A, Ferrario M, Dreano M, Garotta G, Spano P, Pizzi M (2002) Soluble interleukin-6 (IL-6) receptor/IL-6 fusion protein enhances in vitro differentiation of purified rat oligodendroglial lineage cells. Mol Cell Neurosci 21:602-615.

van de Wetering M, Sancho E, Verweij C, de Lau W, Oving I, Hurlstone A, van der Horn K, Batlle E, Coudreuse D, Haramis AP, Tjon-Pon-Fong M, Moerer P, van den Born M, Soete G, Pals S, Eilers M, Medema R, Clevers H (2002) The beta-catenin/TCF-4 complex imposes a crypt progenitor phenotype on colorectal cancer cells. Cell 111:241-250.

Wang KC, Koprivica V, Kim JA, Sivasankaran R, Guo Y, Neve RL, He Z (2002) Oligodendrocyte-myelin glycoprotein is a Nogo receptor ligand that inhibits neurite outgrowth. Nature 417:941-944.

Wang SJ, Peyrollier K, Bourguignon LY (2007a) The influence of hyaluronan-CD44 interaction on topoisomerase II activity and etoposide cytotoxicity in head and neck cancer. Arch Otolaryngol Head Neck Surg 133:281-288.

Wang Z, Colognato H, Ffrench-Constant C (2007b) Contrasting effects of mitogenic growth factors on myelination in neuron-oligodendrocyte co-cultures. Glia 55:537-545.

Williams A, Piaton G, Aigrot MS, Belhadi A, Theaudin M, Petermann F, Thomas JL, Zalc B, Lubetzki C (2007) Semaphorin 3A and 3F: key players in myelin repair in multiple sclerosis? Brain 130:2554-2565.

Wilson HC, Onischke C, Raine CS (2003) Human oligodendrocyte precursor cells in vitro: phenotypic analysis and differential response to growth factors. Glia 44:153-165.

Windrem MS, Nunes MC, Rashbaum WK, Schwartz TH, Goodman RA, McKhann G, 2nd, Roy NS, Goldman SA (2004) Fetal and adult human oligodendrocyte progenitor cell isolates myelinate the congenitally dysmyelinated brain. Nat Med 10:93-97.

Wong ST, Henley JR, Kanning KC, Huang KH, Bothwell M, Poo MM (2002) A p75(NTR) and Nogo receptor complex mediates repulsive signaling by myelin-associated glycoprotein. Nat Neurosci 5:1302-1308.

Yamashita T, Fujitani M, Yamagishi S, Hata K, Mimura F (2005) Multiple signals regulate axon regeneration through the Nogo receptor complex. Mol Neurobiol 32:105-111.

Zhang Y, Argaw AT, Gurfein BT, Zameer A, Snyder BJ, Ge C, Lu QR, Rowitch DH, Raine CS, Brosnan CF, John GR (2009) Notch1 signaling plays a role in regulating precursor differentiation during CNS remyelination. Proc Natl Acad Sci U S A 106:19162-19167.

Zhao X, Wu J, Kuang F, Wang J, Ju G (2011) Silencing of Nogo-A in rat oligodendrocyte cultures enhances process branching. Neurosci Lett 499:32-36.

Zhao XH, Jin WL, Ju G (2007) An in vitro study on the involvement of LINGO-1 and Rho GTPases in Nogo-A regulated differentiation of oligodendrocyte precursor cells. Mol Cell Neurosci 36:260-269.

Ziskin JL, Nishiyama A, Rubio M, Fukaya M, Bergles DE (2007) Vesicular release of glutamate from unmyelinated axons in white matter. Nat Neurosci 10:321-330.

METHODS

Mice

Heterozygous Ng2::CreER^{T2} (Zhu *et al*., 2008) were crossed with the R26R-EYFP reporter mice (JAX mice) to obtain OPC reporter mouse line NG2-CreERT2/R26R-EYFP animals. Mice were bred further to achieve R26R-EYFP homozgosity to be used in fate mapping, NgR-OMNI Fc and Human IgG Fc experiments and CAP recordings. Mice older than 2.5 months received intraperitonial injections of tamoxifen derivative 4OHT (10 mg; dissolved at 10 mg/ml in a 1:9 ethanol/ corn oil mixture) twice for 5 days. Mice were subjected to white matter stroke or sham procedure 10 days after the last dose of 4OHT. Brains were collected at 4, 7, 10 and 14 days after stroke or sham for cell fate-mapping experiments (n=5-6 per cohort). In NgR-OMNI Fc/ Human IgG Fc study, the OPC mice were treated with 4OHT in the same manner later brains were isolated 14 days after stroke or sham for fate-mapping (n=5 per cohort). PLP-GFP reporter and YFP-H transgenic mice were used to assess the loss of mature oligodendrocytes and axons respectively (JAX mice). Wild-type C57BL/6 were used to conduct the initial CAP recordings, OPC proliferation study, SVZ origin experiments, transcriptome studies and to generate primary OPC cultures. For OPC proliferation experiments, EdU (Invitrogen) was administered intraperitoneally at 0.3 mg /10 g mouse weight (1 mg/ml) twice 24 hours before sacrifice time points of 4, 7, 10 and 14 days after stroke or sham (n=5 per cohort). In SVZ origin study, EdU was administered similarly but for 5 constitutive days before white matter stroke induction, and animals were sacrificed at day 7 and 14 after stroke or sham (n=3 per time point per cohort). Initial CAP recordings were performed on animals 7 and 28 days after stroke (n=5). CAP recordings in NgR-OMNI or Human IgG injected animals were performed 28 days after stroke (n=3). All experiments were performed in accordance with National Institutes of Health animal protection guidelines and were approved by the University of California at Los Angeles Animal Research Committee.

White Matter Stroke

Mice aged 2.5 to 3 months underwent white matter stroke as described with modifications (Sozmen *et al*., 2009). The vasoconstrictor N5-(1-Iminoethyl)-L-ornithine (L-NIO; 27mg/ml in sterile physiological saline; Calbiochem) was injected via micropippette through the cortex at an angle of 36° with a dorso-medial to ventro-lateral injection path, into the white matter underlying the forelimb motor cortex. This procedure promotes intense vasoconstriction at the site of injection, leading to focal ischemia (Horie *et al*., 2008; Hinman *et al*., 2013). Three stereotaxic injections (each of 200 nL of L-NIO solution) were made in the following coordinates: A/P: +0.22, +0.74, +1.24, M/L: +0.20, +0.17, +1.15, D/V: -2.20, -2.25, -2.30. The pipette was left *in situ* for 5 min post-injection to allow proper diffusion. Control animals underwent a sham procedure during which a craniotomy was done similar to stroke animals, with no subsequent injections.

Immunohistochemistry

Animals were perfused transcardially with 0.1 M phosphate buffered saline followed by PLP fixative containing 2% paraformaldehyde (Suzuki *et al*., 2002). Following cryoprotection in 30% sucrose brains were frozen and sectioned using a cryostat (Leica CM 0530) into 35 - 40 µm sections. For immunohistochemistry, the sections were blocked in 5% donkey serum, incubated with a primary antibody over night at 4°C, incubated with a secondary antibody for 1-2 hours at room temperature, and coverslipped with DPX. For immunostaining with antibodies raised in the mouse, M.O.M. kit was used to eliminate nonspecific binding (Vector). Primary antibodies were: goat anti GFP (1:5000, gift from Dr. Nathaniel Heintz, Rockefeller University), rabbit anti Iba-1 (1:1000, Wako Chemicals), rabbit NG2 (1:200, Millipore), rat anti-myelin basic protein (MBP, 1:1000, Millipore), rabbit anti Olig2 (1:500, Millipore), rat anti Olig 1 (gift from Dr. Bennett Novitch, UCLA), rabbit anti GST-π (1:500, Abcam), rabbit anti CC1 (1:100, Millipore). rabbit anti Aldh1 (1:1000, Abcam), rabbit anti Caspr (1:500, Abcam), mouse anti βIV-spectrin (1:200,

Neuromab), Hyaluronan binding protein (1:1000, Cape Cod Associates), rabbit anti Pleiotrophin (1: 250, Millipore), rabbit anti Matrilin 2 (1:200, Abcam), mouse anti Inhibinα (1:500, Abcam). All secondary antibodies were donkey F(ab)2 fragments conjugated to cy2 cy3 or cy5 (Jackson Immunoresearch) and were used at a dilution of 1:500. EdU incorporation was detected by Click-iT® EdU cell proliferation assay following to the kit protocol (Invitrogen).

NgR-OMNI Fc Delivery

NGR-OMNI Fc, a soluble chimeric form of Nogo receptor fused with Fc portion of human IgG1, was created by Dr. Roman Giger and his group (University of Michigan). NgR-OMNI Fc binds to Nogo66, OMgp and MAG with high affinity (Robak *et al*., 2009). 1.05 ug of NgR-OMNI Fc (a gift from Dr. Roman Giger) or Human IgG Fc (Jackson Immunoreserach) were delivered into white matter stroke lesions 2 days after stroke induction at the following coordinates: A/P: +0.50, +1.05, M/L: +1.95, +1.75, D/V: -1.30, -1.35. All injections were delivered at 90° angle unlike the white matter stroke induction.

Lentivirus Constructs and Delivery

For laser capture microdissection purposes, PDGFRα/lckGFP construct was generated in the Carmichael laboratory by using PDGFRα promoter from a published lentiviral construct (Geller *et al*., 2008) to drive the expression of membrane targeted lck-GFP (received from Dr. Steven Green, University of Iowa). PDGFRα/lckGFP was packaged into lentivirus vectors at the UCLA Vector core facility. High titers of PDGFRα/lckGFP lentivirus was delivered in thin glass pulled pipettes into lesioned or uninjured white matter by two stereotaxic injections (each of 600 nL) at the following coordinates: A/P: +0.50, +1.05, M/L: +1.95, +1.75, D/V: -1.30, -1.35. All injections were delivered at 90° angle unlike the white matter stroke induction.

SVZ Origin Experiments

To assess SVZ contribution in post-stroke recovery, we targeted SVZ with CMV-GFP lentivirus that leads to expression of GFP in all cell types. The CMV-GFP lentivirus was provided in high titer by UCLA Vector core. The SVZ was labeled by stereotaxic delivery of the CMV-GFP lentivirus (2 injections, each of 200 nL) at the following coordinates modified from (Menn *et al*., 2006): A/P: +0.2, +1.0, M/L: +1.2, +1.0, D/V: -1.6, -2.0.

Microscopy and Stereology

High-resolution confocal images and Z-stacks were acquired in the Nikon C2 confocal system. To carry out stereology, Z-stacks were imported into Stereoinvestigator software (Stereoinvestigator, MBF Bioscience). Cells of interest were stereologically quantified using the optical fractionator probe and neuroanatomical quantification. Briefly, a counting area was drawn to include the lesion with adjacent peri-infarct white matter of each section analyzed. 3 to 4 serial sections spaced 240 µm apart were used to estimate the total number of cells of interest in each brain. For all fate-mapping studies, OPC proliferation experiments, and the SVZ origin study, means ± standard deviations of each cohort were compared with one-way ANOVA with Tukey multiple comparison test assuming equal variances (Prism Graph Pad).

Compound Action Potential Recordings

Compound action potential (CAP) recordings and conduction measurements were performed by the Laboratory of Dr. Seema Tiwari-Woodruff as previously described (Crawford *et al*., 2009a). Briefly, each mouse was anaesthetized with isoflurane, decapitated and the brain rapidly removed. Coronal slices that were 300 µm thick were cut in ice-cold artificial cerebrospinal fluid with a vibrating-knife microtome (Leica, model VT1000S). Slices were then transferred to a

holding chamber containing oxygenated artificial cerebrospinal fluid at room temperature and were allowed to equilibrate for at least 1 hour prior to recording. Brain slices that contained white matter stroke lesion visible to the naked eye were used for electrophysiology recording, as previously described (Crawford *et al.*, 2009b). Stimulation used for evoked CAPs was constant current stimulus-isolated square wave pulses. For analyses of the CAP amplitude, standardized input–output functions were generated for each slice by varying the intensity of stimulus pulses (200 μs duration, delivered at 0.2 Hz) in steps from approximately threshold level to an asymptotic maximum (0.3–4.0 mA) for the short-latency negative CAP component. To enhance the signal-to-noise ratio, all quantitative electrophysiological analyses were conducted on waveforms that were the average of four successive sweeps. Evoked CAPs were amplified and filtered (bandpass = DC to 10 kHz) using an Axopatch 200A amplifier (Molecular Devices), digitized at 200 kHz and stored on disk for offline analysis.

Laser Capture Microdissection and RNA-Seq Transcriptome Studies

Mice (n= 6 per group) were subjected to white matter stroke in wild-type animals and were survived to 5 and 15 days. Specific OPC labeling after stroke induction was achieved by injection of PDGFRα/lckGFP lentivirus 4 days before the designated sacrifice time point. Control group brains received PDGFRα/lckGFP lentivirus in the absence of stroke and were isolated 4 days after the lentivirus delivery. Brains were isolated, snap frozen and stored in - 80° C until the day of LCM. One brain at a time, cryosections (20 μm) were collected on PET-membrane slides (Leica) the day of LCM isolation, fixed in 90% ethanol (vol/vol) for 2 minutes and kept in 100% ethanol. Peri-infarct white matter OPCs were detected under 40X magnification by positive GFP signal and were isolated in Leica LMD 7000 system. Laser captured tissue fragments were collected in Lysis Buffer of NucleoSpin RNA Isolation kit (Clontech). The rest of the protocol was completed to isolate total RNA according to the kit instructions, designed for low yield tissue isolation experiments. Possible DNA comtamination was eliminated by an

additional DNAseI digestion step at room temperature for 15 minutes (Clontech). Mock collection of a large section area was isolated and RNA from this tissue was run in Bioanalyzer Picochip (Agilent) to ensure the quality of RNA. This was done because the actual collected samples were below the Picochip detection range.

Total RNA was amplified and converted into double-stranded DNA, which are typically between 200 and 300 bp, by using the Ovation RNA-seq System (Nugen, v2) that was further processed with Ovation UltraLow kit (Nugen). The Nugen technology employs a single primer isothermal amplification (SPIA) method to amplify RNA target into double stranded cDNA under standardized conditions that markedly deplete rRNA without preselecting mRNA. The end product of each sample was also run on the Picochip assay to ascertain successful amplification. Later cDNA were submitted to UCLA core facility Southern California Genotyping Consortium, to be used for Illumina sequencing library preparation using Encore NGS Library System I (Nugen). Amplified double-stranded cDNA was fragmented into 300 bp using a Covaris-S2 system. DNA fragments (200 ng) were then end-repaired to generate blunt ends with 59 phosphatase and 39 hydroxyls and adapters were ligated. The purified cDNA library products were evaluated using the Agilent bioanalyzer and diluted to 10 nM for cluster generation in situ on the HiSeq paired-end flow cell using the CBot automated cluster generation system. Three sample at a time, all samples were multiplexed into single pools and run in 9 lanes total of Paired-End 2 x 100 bp flow cells in HiSeq 2000 (Illumina).

Bioinformatics

RNA-Seq analysis and bioinformatics were carried out in colloboration with Dr. Giovanni Coppola at UCLA. RNA-Seq reads were separately aligned to the mouse genome using the software TopHat. The resulting alignment data from Tophat were then fed to an assembler Cufflinks to assemble aligned RNA-Seq reads into transcripts. The samples with poor exon alignments were not included in further comparisons. Transcript abundances were measured in

Fragments Per Kilobase of exon per Million fragments mapped (FPKM), which originated from the idea of RPKM (Reads per Kilobase per Million). The data were then analyzed in R computing environment with the Bioconductor package. For each time point, differential gene expression from each biological replicate was averaged and standard deviations were calculated. Gene ontology studies was conducted on genes with False Discovery Rate ≤ 0.1. Genes that were differentially expressed over two post-lesion time points and the control from the ANOVA analysis ($P < 0.1$) were submitted to Cluster 3.0 for hierarchical clustering analysis (euclidian distance, centroid linkage clustering) and visualized using Java TreeView. IPA was performed using the Ingenuity Pathways Analysis software.

Quantitative Reverse Transcription PCR (qRT-PCR)

cDNA from the two stroke samples and control white matter were submitted to Fluidigm Corporation for qRT-PCR reaction. The data set was fed to Fluidigm software to retrieve ΔΔCt values that was later used to calculate fold changes by Relative Expression Software Tool.

Primary Mouse OPC Cultures

Cerebral hemispheres from 1-day-old mice were mechanically dissociated and were plated on poly-d-lysine-coated flasks in DMEM (Dulbecco's modified Eagle's medium) and Ham's F12 (1:1, v/v) (Life Technologies), containing 100 μg/ml gentamycin and supplemented with 4 mg/ml dextrose anhydrous, 3.75 mg/ml Hepes buffer, 2.4 mg/ml sodium bicarbonate and 10% (v/v) FBS (fetal bovine serum) (Omega Scientific). After 24 h, the medium was changed, and the cells were grown in DMEM/Ham's F12 supplemented with 5 μg/ml insulin, 50 μg/ml human transferrin, 30 nM sodium selenite, 10 mM d-biotin, 0.1% BSA (Sigma), 1% (v/v) horse serum and 1% (v/v) FBS. After 9 days, OPCs were purified from the mixed glial culture by the differential shaking and adhesion procedure of Suzumura *et al*., (1984) and were allowed to grow on poly-D-lysine (PDL) coated coverslips in defined culture medium (Agresti *et al*., 1996)

plus 10 ng/ml PDGF-AA and 10 ng/ml bFGF (Sigma). OPCs were kept in mitogens (PDGF and bFGF) for 4 days, passaged once, allowed to proliferate further for 2 days and then induced to exit from the cell cycle and differentiate by switching the cells to a mitogen-free co-culture media (Oh *et al*., 2003). Co-culture media is DMEM/Ham's F12 supplemented with 4.5 g/l d-glucose, 5 µg/ml insulin, 50 µg/ml human transferrin, 30 nM sodium selenite, 15 nM T_3 (tri-iodothyronine), 10 mM d-biotin, 10 nM hydrocortisone, 0.1% BSA, 1% (v/v) horse serum and 1% (v/v) FBS.

In-vitro OPC Differentiation Assay

The effects of Matrilin 2 and Inhibin A on OPC differentiation were assessed in primary OPC cultures. For the control condition, 22 mm glass coverslips that were coated with PDL (10 µg/mL, overnight incubation at room temperature), washed once in distilled water and air-dried. After being passaged once, OPCs were plated on PDL or PDL + Matrilin 2 coated coverslips depending on the experimental group. Coverslips were coated with Matrilin 2 in the same way as PDL. Briefly, PDL coated coverslips were incubated in carrier free recombinant mouse Matrilin 2 (20 µg/mL, BD Bioscience), washed and dried. To induce differentiation, OPCs were grown in regular co-culture media in PDL control and PDL+ Matrilin 2 surface group. Media supplemented with Matrilin 2 (10 µg/mL) was used in PDL + Matrilin 2 media group. Media containing carrier free mouse recombinant Inhibin A (10 µg/mL, Randox Research) was used in PDL + Inhibin A group. Lastly, co-culture containing both Matrilin 2 and Inhibin A was used in PDL + Matrilin 2 + Inhibin A media group. Each group consisted 5 individual culture plate wells as biological replicates. Cells were allowed to differentiate for 5 day in respective co-culture media and were fixed with 4% PFA, washed and stained for Olig 2 and MBP as described earlier. Olig 2+ cells and MBP+/ Olig 2+ double positive cells were quantified in five separate fields using 20x magnification. The OPC differentiation index was calculated as the percentage of double-labeled cells over the total number of Olig 2+ cells. Photomicrographs of individual MBP positive cells were taken at 100x magnification (7 - 10 per experimental group) to be used

in Scholl ring analysis as described previously (Langhammer *et al*., 2010). Each MBP positive cells were skeletonized using the Glia probe of Neurolucida software (MBF Bioscience). 20 µm intervals of Scholl rings were placed on each cell outline and process crossings were quantified. The experimental groups were compared with PDL control group to assess changes in oligodendtocyte maturation. One-way ANOVA statistical analysis with Bonferonni's multiple comparisons post-hoc test was used to report the differences (GraphPad Prism).

References

Agresti C, D'Urso D, Levi G (1996) Reversible inhibitory effects of interferon-gamma and tumour necrosis factor-alpha on oligodendroglial lineage cell proliferation and differentiation in vitro. Eur J Neurosci 8:1106-1116.

Crawford DK, Mangiardi M, Tiwari-Woodruff SK (2009a) Assaying the functional effects of demyelination and remyelination: revisiting field potential recordings. J Neurosci Methods 182:25-33.

Crawford DK, Mangiardi M, Xia X, Lopez-Valdes HE, Tiwari-Woodruff SK (2009b) Functional recovery of callosal axons following demyelination: a critical window. Neuroscience 164:1407-1421.

Geller SF, Ge PS, Visel M, Flannery JG (2008) In vitro analysis of promoter activity in Muller cells. Mol Vis 14:691-705.

Hinman JD, Rasband MN, Carmichael ST (2013) Remodeling of the axon initial segment after focal cortical and white matter stroke. Stroke; a journal of cerebral circulation 44:182-189.

Horie N, Maag AL, Hamilton SA, Shichinohe H, Bliss TM, Steinberg GK (2008) Mouse model of focal cerebral ischemia using endothelin-1. Journal of neuroscience methods 173:286-290.

Langhammer CG, Previtera ML, Sweet ES, Sran SS, Chen M, Firestein BL (2010) Automated Sholl analysis of digitized neuronal morphology at multiple scales: Whole cell Sholl analysis versus Sholl analysis of arbor subregions. Cytometry A 77:1160-1168.

Menn B, Garcia-Verdugo JM, Yaschine C, Gonzalez-Perez O, Rowitch D, Alvarez-Buylla A (2006) Origin of oligodendrocytes in the subventricular zone of the adult brain. J Neurosci 26:7907-7918.

Oh LY, Denninger A, Colvin JS, Vyas A, Tole S, Ornitz DM, Bansal R (2003) Fibroblast growth factor receptor 3 signaling regulates the onset of oligodendrocyte terminal differentiation. J Neurosci 23:883-894.

Robak LA, Venkatesh K, Lee H, Raiker SJ, Duan Y, Lee-Osbourne J, Hofer T, Mage RG, Rader C, Giger RJ (2009) Molecular basis of the interactions of the Nogo-66 receptor and its homolog NgR2 with myelin-associated glycoprotein: development of NgROMNI-Fc, a novel antagonist of CNS myelin inhibition. J Neurosci 29:5768-5783.

Sozmen EG, Kolekar A, Havton LA, Carmichael ST (2009) A white matter stroke model in the mouse: axonal damage, progenitor responses and MRI correlates. J Neurosci Methods 180:261-272.

Suzuki M, Katsuyama K, Adachi K, Ogawa Y, Yorozu K, Fujii E, Misawa Y, Sugimoto T (2002) Combination of fixation using PLP fixative and embedding in paraffin by the AMeX method is useful for histochemical studies in assessment of immunotoxicity. J Toxicol Sci 27:165-172.

Suzumura A, Bhat S, Eccleston PA, Lisak RP, Silberberg DH (1984) The isolation and long-term culture of oligodendrocytes from newborn mouse brain. Brain Res 324:379-383.

Zhu X, Bergles DE, Nishiyama A (2008) NG2 cells generate both oligodendrocytes and gray matter astrocytes. Development 135:145-157.

RESULTS

Despite the high incidence rate of white matter stroke in our progressively aging population, post-stroke white matter repair remains a relatively understudied problem. The main cause for this gap in stroke research is a lack of suitable models for isolated white matter ischemia, as opposed to larger cerebral ischemia models that involve mostly gray matter. A new subcortical white matter model is established in the Carmichael Laboratory that addresses this need (Sozmen *et al*., 2009). This published study demonstrated that white matter lesions induced in the present model are akin to lacunar infarcts seen in patients with subcortical white matter stroke (Gouw *et al*., 2008). Please refer to the manuscript included in Appendix A for figures and details.

White matter stroke model using the vasoconstrictive agent endothelin-1

White matter strokes were originally produced by stereotaxic microinjection of a vasoconstrictive agent endothelin-1 (ET-1) below forelimb motor cortex in adult male mice. Endothelin-1 was selected due to its potent vasoconstrictive effects on vascular smooth muscles by binding to receptor ET-A (Fujise *et al*., 1997).

A clinical case of white matter stroke is illustrated in Figure 1A of the article, in which the lesions are demarcated by the hallmark white matter hyperintensities on FLAIR T2-weighted MRI (Appendix A). The same disease process is replicated in mice after ET-1 injection (Fig.1B Appendix A) with focal damage in subcortical white matter that can be visualized by hyperintensity (Fig. 1C Appendix A). 7 days after stroke, axons are clearly lost within the stroke cavity as visualized in the YFP-H mice (Fig. 1D Appendix A). Oligodendrocyte apoptosis occurs early in the stroke core and in the interfascicular oligodendrocytes that extend away from the infarct (Fig. 2 Appendix A). Corresponding to this time, activated microglia and astrocytes infiltrate the ischemic white matter and persist in close association with the white matter tracts and injured axons (Fig. 3F Appendix A). Myelin loss was observed in the stroke center starting

at day 7, which progressively transformed into a larger demyelinated region by day 28 (Fig. 4B Appendix A). Similarly, progressive axonal injury took place in ischemic white matter; however axons remained partially preserved in the peripheral zone of the infarct despite the demyelination (Fig. 4F, 4H Appendix A). At 7 days post lesion, dystrophic axonal bulbs were present (Fig. 5B in Appendix A) and degenerating axons with separating myelin sheaths were confirmed ultrastructurally by EM (Fig. 5E, 5F Appendix A). The stroke disconnected widespread neuronal circuits in bilateral sensory and motor cortices (Fig. 6 Appendix A).

Improved vasonstrictive agent

Soon after the model was established, new studies emerged suggesting that other cell types besides vascular smooth muscles possess endothelin receptors. In particular, astrocytes respond to ET- 1 and the differentiation potential of glial progenitors can be altered upon such exposure (Gadea *et al*., 2008). More importantly, ET-1 binding to ET-B receptors on OPCs was found to contribute to the maintenance of the progenitor state (Gadea *et al*., 2009). Such direct interaction of ET-1 on cells that are expected to have a role in white matter repair makes the use of ET-1 as a stroke agent problematic. We replaced ET-1 with a potent selective vasoconstrictor, the inhibitor of endothelial cell nitrous oxide synthase, L-NIO. This approach targets endothelial cells alone and eliminates any receptor-mediated effects of the ET-1 system on astrocytes and OPCs that might influence the outcome of white matter stroke. L-NIO is not directly toxic and the selected dose was determined by preliminary dose-escalation experiments. L-NIO injections induced white matter lesions far more efficiently compared to the ET-1 model, with a larger stroke volume and more robust glial response.

L-NIO injection generates focal ischemic lesions and leads to functional deficit

L-NIO mediated vasospasm leads to a focal lesion that is largely contained within the white matter, although minor leakage is occasionally present through the striatal white matter

tracts (Fig 1A). The resulting lesion creates a stroke core devoid of oligodendrocytes as demonstrated in the oligodendrocyte reporter mouse line PLP-GFP that expresses GFP under the control of myelin gene PLP (Fig. 1B). Loss of oligodendrocytes is followed by demyelination starting at 7 days after stroke induction (Fig. 1D).

To investigate axon degeneration in lieu of demyelination, we used the YFP-H mouse line originally described by Feng *et al* (2000). In this transgenic line, high levels of soluble YFP is produced in motor and sensory neurons, particularly in layer V neurons, under the direction of regulatory elements derived from the mouse *Thy1* gene (Feng *et al*., 2000). YFP filled axons densely populate the white matter at the site of stroke (Fig. 2A). At 7 day time point of white matter stroke, we observed concurrent loss of YFP positive axons that produced a prominent stroke core with complete lack of YFP signal (Fig. 2B). Unlike the stroke core, the rim of ischemic lesion contains retraction balls, the hallmark of diffuse axonal injury, suggesting a relatively preserved zone within the peri-infarct white matter (Fig. 2B).

The entire length of myelinated axons is organized into a series of polarized domains that center around nodes of Ranvier, which are crucial for normal saltatory conduction. These domains consist of distinct multiprotein complexes of cell adhesion molecules, ion channels, and scaffolding molecules. Therefore, demyelination may have important consequences on the overall structure and/or stability of the axonal cytoskeleton. In order to delineate potential zone differences in white matter infarcts, markers for nodes of Ranvier axonal domains were used to assess the changes in axon-myelin ultrastructure. The contactin-associated protein (Caspr) is expressed in axons that bind to myelin counterpart Neurofascin 155 to form paranodes. Mice lacking paranodal junctions undergo severe axon degeneration in the cerebellum, confirming that neuron-glia interactions are required for axon integrity. Consistent with this finding, the reduction in Caspr has been suggested as an early marker of demyelination (Salzer, 2003). Furthermore, clustering of voltage-gated ion channels in the nodes were disrupted in demyelinated MS plaques, whereas the remyelinated lesions were characterized by

reestablished aggregates of Na_v (Coman *et al*., 2006). The axonal cytoskeletal protein βIV-spectrin and its association with scaffolding protein Ankyrin G regulate healthy accumulation of ion channels (Yang *et al*., 2004). Collectively, these findings indicate that loss and restoration of nodal markers can be a sensitive measure of axonal health and the extent of remyelination. Both paranodal Caspr and nodal βIV-spectrin levels were significantly decreased in the stroke core at 7 days (Fig. 2D). This finding is consistent with the complete loss of axons in the infarct core. In contrast, the lesion rim where the YFP+ retraction balls were observed, both markers labeled reduced number of axons (Fig. 2E) that displayed noncontiguous organization compared to healthy white matter (Fig. 2C). As such, the peri-infarct white matter consists of lightly demyelinated axon bundles with signs of deteriorating axonal integrity. We hypothesized, this zone is similar to shadow plaques seen in MS and may be a candidate site of post-stroke remyelination.

The small infarct generated by L-NIO injection was expected to produce motor function deficits that could be monitored by behavioral tests like cylinder and gridwalking. Both behavioral assays are routinely carried out in the models of gray matter stroke in the Carmichael Laboratory. The behavior tests showed a trend of modest deficit after stroke and recovery to baseline by day 7, although was not statistically significant. To further understand the functional implications of the infarct, we used measurements of compound action potentials (CAP) across the lesion. Given the disruption of axonal circuits and the perturbed nodes of Ranvier architecture in the peri-infarct white matter, we hypothesized CAP recordings would provide a direct measure of axon conduction deficits early and late in the disease. Indeed, 7 days after injury the CAP amplitude of myelinated axons (N1 component) and the slower conduction across non-myelinated axons (N2 component, Fig2. F) were both diminished. At the later time point following stroke, CAP recordings revealed improved conduction across the lesion with a modest restoration of CAP amplitudes without complete recovery. Overall, the late stage results indicate that white matter stroke has long-term implications on axon conduction. The reason

behind the lack of behavioral test read-out may be due to compensation mechanisms in the motor cortex (Cirstea and Levin, 2000). It is important to note that the volume of white matter infarcts is a predictor of clinical outcome in ischemic stroke patients (Arsava *et al*., 2009). Also, the accumulation of multiple white matter lesions is correlated with progressive decline in quality of daily living (Wang *et al*., 2006). Therefore, it is possible that bilateral L-NIO injections can translate into readily detectable motor deficits. We have not investigated this possibility, since CAP recordings can be performed with ease and it assays white matter function directly without any compensatory mechanism complicating the results.

OPC regeneration response following white matter stroke

Multiple modes of experimental demyelination demonstrate that white matter injury initiates a robust regenerative response by "activating" OPCs to proliferate, migrate and partially differentiate into myelinating oligodendrocytes (Franklin and Ffrench-Constant, 2008). We investigated if white matter stroke triggers a similar response.

To measure the OPC proliferation rate, brief pulses of EdU were given shortly before sacrifice time points. This method was favored over continous administration of EdU in order to identify the peak window of OPC proliferation. In all post-stroke time points many Olig 2 positive cells were also co-labeled with EdU (Fig. 3A,B). The adult white matter consists of quiescent OPCs that are shown to have an incredibly long cell-cycle period in the absence of injury (Jafari *et al*., 2012). Our findings are consistent with this published data as EdU incorporation in non-stroked white matter OPCs was negligible (Fig. 3C). OPC proliferation was peaked at the earliest time point used, at 4 days after stroke (4d: 32.04% ± 5.93 vs 7d: 11.08% ± 9.51, $P < 0.001$, 14d: 9.56% ± 6.68, 4d vs 14d $P < 0.001$) (Fig 3C). Nonetheless, the lesion induced persistent and prolonged OPC mitotic activity that was not observed in other demyelination studies. Due to the brief EdU pulse paradigm, we predict these double positive cells are at the progenitor stage, although a slight overestimation of proliferative response is still possible if a

minority of cells had already differentiated by the time of sacrifice. In short, post-stroke white matter consists of OPCs with heightened proliferative capacity comparable to other demyelinating injuries.

Cell fate determination of newly born OPCs following injury

In order to investigate the extent of white matter repair after stroke, the NG2CreERT2/Rosa-YFP OPC reporter line was used. This reporter line expresses tamoxifen-activated Cre recombinase under the control of the *NG2* promoter, and upon *Cre* induction turns on the *EYFP* reporter in NG2 cells (Fig. 4A). This way, OPCs present at the time of induction and their progeny are genetically labeled with YFP expression. The $CreER^{T2}$ containing constructs produce reliable cell-specific recombination and are used often to temporally control mapping of various CNS cell types (Rivers *et al*., 2008; Erdmann *et al*., 2007). Five day long administration of tamoxifen derivative 4OHT results in detectable YFP expression in the reporter cells. In non-stroked animals, the reporter cells were positive for NG2 or PDGFRα or for both markers (Fig. 4B), while the astroyctes, microglia/macrophage and neurons did not show reporter activity (not shown). It is important to note that not all detected OPCs were YFP positive, therefore only a subset (~60%) of the OPC pool was labeled through this method. To eliminate the potential risk of "leaky" Cre expression, mice were given the carrier oil instead of 4OHT, which failed to induce YFP expression. Lastly, 4OHT administration was followed by a 10 day long wash period before stroke induction so any estrogen-like protective effect of 4OHT against ischemia could be avoided. In short, the current paradigm allows reliable labeling of a subset of quiescent OPCs prior to injury and their progeny in white matter stroke.

White matter stroke produces lesions that are densely populated by OPC reporter cells (Fig. 4C). Olig 2 co-labeling of the cells revealed that the majority of the reporter cells remain in oligodednrocyte lineage but a small percentage (10-15%) of reporters were not positive for Olig 2 (Fig. 4D). To further investigate the phenotype of OPC reporter cells, stroked and control brain

were labeled with NG2 to identify undifferentiated OPCs (Fig. 5A) and the differentiated cells were detected by cytoplasmic translocation of Olig 1 (Fig 5C). The majority of the reporter pool were uncommitted NG2 positive OPCs in both control and stroked white matter at all time points (54 – 82%, n=5-6) (Fig. 5B). Only at day 14 time point, a significant decrease was observed in the percentage of NG2 positive reporter cells relative to the control group (14d control: 77.8% ± 4.52, 14d stroke: 58.9% ± 7.15, $P < 0.001$). The bHLH transcription factor Olig 1 is expressed in OPC lineage cells from progenitor stage to maturity. However, the cytoplasmic translocation of the gene product marks the transition from the immature state towards differentiation (Arnett *et al*., 2004). The differentiation rate of reporters was low after white matter stroke at all time points (< 15%) and did not significantly deviate from the baseline rate of OPC differentiation shown in the control group (Fig. 5D). This was confirmed by using different oligodendrocyte markers such as CC1, GFT-π and transferrin.

In the healthy adult white matter, the resident OPCs remain quiescent unless activated by injury (Sim *et al*., 2006). Non-stroke demyelination studies report, the OPCs proliferate within 7 days of injury and differentiate into oligodendrocytes by day 14 (Tanaka *et al*., 2003). Unexpectedly, white matter stroke samples showed differentiation rate similar to control, despite a decrease in immature reporter cell percentage at day 14. The fact that stroked brains exhibit approximately the same progenitor maintenance profile as the control group indicates that the newly born OPCs persist without differentiating into oligodendrocytes in the lesion.

Alternative glial cell fate of OPCs in white matter stroke

In order to clarify the phenotype of the remaining reporter cells, the samples were labeled for astrocytic marker Aldh1. This gene product is highly enriched in astrocytes (Cahoy *et al*., 2008) and its labeling provides cell body filling so that quantification is possible, a feature that is not achieved by the traditional GFAP immunohistochemistry (Fig. 6A). White matter stroke induces a robust astrocytic response evident by numerous Aldh1 positive astrocytes filling the

lesion, particularly the lesion rim (Fig. 6A). We assessed the alternative glia fate of OPC reporter cells in white matter stroke and control brains. In absence of injury, there was no evidence of astrocytic fate among the OPC lineage cells (Fig. 6D). In contrast, white matter stroke caused glial fate divergence as indicated by Aldh1 positive reporter cells (Fig. 6B) comprising 4-13% of the total reporter pool across all time points. Astrocytic transformation of progenitors was further confirmed by GFAP labeling of stroke samples, in which a subset of OPC reporter cells contained GFAP positive processes (Fig. 6C). This finding is in agreement with other published reports that demonstrated bipotential nature of OPCs *in vivo* both in the absence and presence of injury (Zhu *et al*., 2008; Tripathi *et al*., 2010). The misguided differentiation of OPCs can contribute to the differentiation arrest in white matter stroke.

Glial activation and changes in the microenvironment as a result of white matter stroke

Changes in microenvironment play a large role in OPC fate determination. Besides the loss of axons, other prominent changes in stroked white matter are astrocytic and microglia responses that are likely to change the milieu of the peri-infarct white matter into an inhibitory environment. Astrocytes fill the ipsilatereal white matter, dorsal striatum and overlying cortex that span an area far larger than the stroke volume (Fig. 7A). The infarct also leads to persistent accumulation of Iba positive microglia/macrophages (Fig. 3F Appendix A). Neither astrocyte accumulation nor microglia activation was resolved when 60 day stroke samples were compared with early time points of the disease. With the mentioned temporal changes in mind, we surveyed the stroked white matter for known inhibitory factors. Hyaluronan deposition is a direct cosequence of astrocyte activation in response to white matter lesions that contributes to OPC differentiation failure (Back *et al*., 2005). Consistently, high molecular weight hyaluronan is produced and secreted by astrocytes following white matter stroke (Fig. 7B) that was prominent relative to healthy white matter (Fig. 7E). Furthermore, elevated levels of secreted Pleiotrophin was found in the lesioned white matter (Fig. 7C) while the baseline levels were low in the control

brains (Fig. 7F). OPCs are shown to express high levels of Pleiotrophin receptor RTPz that plays a role in maintaining OPCs in proliferative state during development and myelination (Canoll *et al*., 1996). The source of Pleiotrophin in white matter stroke is not known but astrocytes, microglia/macrophage and regenerating microvasculature were shown to secrete Pleiotrophin after acute ischemia in rats (Yeh *et al*., 1998). Collectively, these results indicate permanent changes taking place in the lesioned white matter that potentially contribute to OPC differentiation block.

The origin of responsive OPCs in white matter stroke

NG2 positive OPCs are distributed throughout the adult CNS, comprising 4-8% of cells in white matter. In addition to the resident pool of progenitors, Type B cells in the SVZ also generate OPCs that migrate to corpus callosum, striatum and fimbria fornix in response to injury, and succesfully differentiate into myelinating oligodendrocytes (Menn *et al*., 2006). The origin of OPCs in stroke has not been studied but has clinical relevance. White matter OPC pool is positioned to respond effectively to lesions in close proximity yet has a more limited differentiation potential compared to SVZ-derived OPCs *in vitro* (Windrem *et al*., 2002). On the other hand, if OPCs are derived from the SVZ in stroke they might have a limited role in humans because, unlike the rodent, the SVZ is separated by substantial distances from many white matter stroke lesions. For the reasons mentioned above, we investigated if SVZ contributes to regenerative response following white matter stroke.

Initially, the SVZ-derived cells were tracked by global labeling of ipsilateral SVZ with CMV-GFP lentivirus injection (Fig 8A). SVZ labeling prior to stroke or saline control allowed us to identify cells of SVZ origin that have migrated into the lesioned white matter. In the absence of injury, SVZ-derived cells formed the stream of cells that are a part of rostral migratory stream, which were negative for OPC marker NG2 (Fig 8B). The collection of GFP labeled cells spanned 600 – 650 μm away from the SVZ in control conditions. At 7 day after stroke, no GFP

lebeled SVZ cells were found in the proximity of the lesion (Fig. 8C) even when the infarct was created in close proximity to the labeled SVZ (Fig. 8D). This is in contrast with other experimental demyelination studies, which demonstrated SVZ-derived cells are recruited to the lesion site and gave rise to astrocytes and oligodendrocytes (Nait-Oumesmar *et al*., 1999). However, white matter stroke did not induce recruitment from the SVZ. In fact, the GFP labeled cells were accumulated medial to the lesion away from the stroke site without signs of successful infiltration (Fig. 8D).

Next, we sought to confirm the lack of SVZ contribution to OPC regeneration by labeling the proliferating SVZ pool. Systemic administration of thymidine analog EdU was selected to label constitutively cycling SVZ progenitors. SVZ inhabits slowly dividing Type B cells that give rise to transit-amplifying Type C primary precursors, which in turn generate Type A neuroblasts (Doetsch *et al*., 1999). Incorporation of tymidine analogs has been used before to successfully map the fate and projection of SVZ progenitors (Nait-Oumesmar *et al*., 1999). Bidaily administration of EdU for 5 days prior to stroke induction provided information that re-inforced our previous findings. Although, the SVZ cells contained a high number of cells incoporating EdU, the stroke site contained few EdU labeled cells (Fig. 8E). Furthermore, the EdU labeled cells were mostly of microglia/macrophages phenotype (Fig. 8F). Additionally, EdU incorporating cells were rarely positive for Olig 2 during in white matter stroke that comprised less than 2% of the total EdU positive pool. In summary, white matter stroke in the mouse does not induce recruitment of SVZ-derived cells in the OPC lineage. This leaves the resident OPC pool as the most likely contributor to the observed post-stroke OPC response.

Inhibition of Nogo signaling system and implications in OPC differentiation

The degree of axonal repair can be improved after white matter stroke by establishing new connections that are lost due to ischemic insult. Similar to spinal cord injury and other demyelinating diseases, stroked white matter contains inhibitors of neurite outgrowth.

We investigated if inhibition of NgR complex could ameliorate OPC differentiation block. Nogo signaling was chosen for its dual role in axon regeneration failure and reported inhibitory effect of LINGO-1 on OPC maturation (Mi *et al*., 2007). NGR-OMNI Fc, a soluble hybrid form of NgR that is fused with Fc portion of human IgG1, was created by Roman Giger and his group that binds to Nogo66, OMgp and MAG with high affinity (Robak *et al*., 2009). We hypothesized; sequestration of the major NgR ligands by the engineered NgR-OMNI Fc would help to neutralize the axon inhibitory cues in the lesion and would improve axon regeneration after stroke. Combined with reduced LINGO-1 activation in premyelinating OPCs, targeting NgR activation is a promising way to improve post-stroke white matter matter repair.

NgR-OMNI Fc or Human IgG Fc control (1.05 ug) was delivered into the ipsilateral white matter shortly after stroke induction (Fig. 9A). *In vivo* delivery of NgR-OMNI Fc has not been reported before so the selected dose of the protein was solely empirical considering its binding profile *in vitro* (Robak *et al*., 2009).

To characterize the functional consequences of NgR-OMNI Fc mediated NgR antagonization, we used CAP recordings at 1 month after stroke. The recordings revealed axon conduction deficit in the Human IgG Fc group compared to healthy white matter with significantly attenuated response to stimulation in both N1 and N2 components (Fig. 9B). NgR-OMNI Fc infused lesions generated N1 amplitutes similar to healthy white matter at lower currents but resulted in attenuated conduction when increased stimulation was used (Fig. 9B). In contrast, N2 component recordings suggest NgR-OMNI Fc was not effective in reducing non-myelinated axon conduction deficit, since there was no improvement in N2 amplitudes relative to Human IgG Fc control. A closer look at the individual recordings demonstrated that the Human IgG infused lesions induce latency shifts to the right in both N1 and N2 peaks in addition to the muted amplitudes (Fig. 9C). In the NgR-OMNI Fc plots these latency shifts were not as prominent, were shifted to the left, compared to the Human IgG Fc baseline, and exhibited modestly improved amplitutes. A shift to the left could theoretically be due to an increse in axon

conduction velocity as a consequence of improved myelination. In summary, NgR-OMNI Fc provides some improvement in terms of functional recovery but is not sufficient to completely restore the axon conduction deficit.

Next we investigated if antagonizing NgR complex leads to changes in OPC fate after stroke. For this set of experiments, NgR-OMNI Fc or Human IgG was delivered into the lesions created in OPC reporter mice. Comparison of the reporter cell phenotypes at 14 day time point indicated a significant increase in the rate of OPC differentiation in the NgR-OMNI Fc group (Fig. 10B). Furthermore, astrocytic cells of OPC lineage were markedly reduced in NgR-OMNI Fc injected brains (Fig. 10C). Both groups were similar for the percentage of immature reporter cells (Fig. 10A). Taken together, sequestration of NgR ligands by NgR-OMNI Fc has advantageous effects on OPC differentiation, useful in maintaining the newly born cells within the oligodendrocyte lineage. Even if the current dose was not effective in restroring axon conduction, NgR-OMNI Fc delivery is successful in overcoming OPC differentiation block. Nevertheless, myelin levels in NgR-OMNI Fc treated lesions (Fig. 10D') were not apparently different than the control group (Fig. 10D). However, we observed improved clearance of myelin debris when NgR ligands were bound to NgR OMNI Fc. The consequences of NgR-OMNI Fc action in white matter stroke remain to be determined further.

White matter stroke OPC transriptome study

To date, the majority of OPC studies, whether they are in MS models or in neurodevelopment, have been focused on studying a small number of molecular systems at a time. The few exceptions like the studies by (Sim *et al*. 2006, Cahoy *et al*., 2008 and Huang *et al*., 2011) have proven the power of a global approach in identifying unique OPC molecular pathways in health and disaese. Importantly, it has only been through a global approach that these OPC signaling systems appeared context and tissue dependent.

Our findings suggested that white matter stroke injury is unique compared to the other focal white matter injuries in terms of near complete loss of axons, limited OPC differentiation potential, OPC fate divergence and the lack of SVZ involvement. We hypothesized; the stroke environement that initiates high rate of OPC proliferation early in the disease is markedly changed during the later time points, as the infarct evolves with increased glia activation and altered composition of extracellular matrix. Such changes were already evident by deposition of two inhibitory factors, Hyaluronan and Pleiotrophin, during day 14 time point of stroke. OPC lineage cells are expected to change their repertoire of autocrine and paracrine signaling within the ischemic white matter in response to these changes that can be profiled by comprehensive transcriptome experiments. For this purpose, peri-infarct white matter OPCs were isolated by laser capture microdissection (LCM) during the peak window of proliferation and the time of failed differentiation, 5 and 15 day respectively. OPCs from non-stroked control white matter were isolated as the third group to provide a baseline expression profile of adult OPCs. Specific cell labeling for LCM isolation was achieved by the PDGFRα/lckGFP lentivirus that encodes membrane targeted GFP under the control of PDGRα promoter (Figs 10A, 10B). This lentivirus was delivered shortly after stroke induction into the lesioned white matter. The isolation conditions generated RNA samples high in RNA integrity (Fig. 10C) but small in quantity, ranging between 10 – 50 pg of RNA. Each RNA sample was amplified and converted into cDNA for RNAseq library preparation (Fig. 10D). Originally 6 independently lesioned or control brain samples were submitted as biological replicates to be run in 100bp paired-end sequencing on Illumina Hiseq system. However, samples that did not provide sufficient gene mapping were disqualified from the analysis. This was the case in all of the non-lesioned control samples. The poor quality of control sample libraries was attributed to the significantly low baseline of PDGRα/lckGFP label in the control brain OPCs. This in turn reduced the number of cells available for isolation and caused a significant drop in total start-up RNA amounts. Further

quality control disqualified some of the 5d and 15d stroke libraries that showed insufficient exon mapping. At the end, two biological replicates remained to perform pairwise comparisons.

We identified 1,733 differentially expressed genes between two stroke time points with false discovery rate < 0.1 (831 with $P < 0.05$) over the two white matter stroke time points (Fig. 12). The genes with the highest fold change were reviewed for biological relevance and selected as targets for further studies (Fig. 12). We focused on secreted factors and receptor-ligand signaling systems. The changes in expression were confirmed by qRT-PCR. We found the following genes significantly upregulated at day 5 after stroke: *Ppard, Ripk1, IGFBP3, TNF, Gpc4, Spbn1, Efnb2, Sema4b, Ninj1, Slfn4, Jag1, Foxp3, Runx3, Bambi, Matn2, Lama5* and *Plxna4.* At 15 day the following genes were enriched: *Bmp2, Mmp21, Hapln4, Cxcl13, Ccr7, Lama3, Spock2,* and *Gria4.* For subsequent studies, we focused on *Matn2* after qRT-PCR analysis showed the most dramatic fold change of this gene among others. Ingenuity pathway analysis predicted inhibition of Inhibin A, the upstream negative regulator of Matrilin 2, during the early time point of white matter stroke (Fig. 13A). For these reasons, we investigated the possible roles of both gene products in white matter stroke.

Matrilin 2 and Inhibin A production in white matter stroke lesions

Matrilin 2 is a widely distributed ECM adaptor protein found throughout the body that has binding partners such as collagen, laminin, fibrilin 1 and 2. Matrilin 2 can also form homo oligomers as well as heteromultimers with other matrilin family members by their coiled-coiled oligomerization domains. (Piecha *et al*., 1999; Frank *et al*., 2002). Information on Matrilin 2 function within the nervous system is greatly limited. The only report to date is published by Malin and colleagues that provided extensive information regarding Matrilin 2 function in PNS injury and repair (Malin *et al*., 2009). Matrilin 2 is expressed in the DRG and in Schwann cells along peripheral nerves throughout murine development (Malin *et al*., 2009). *In vitro*, Matrilin 2 coated coverslips promotes Schwann cell adhesion and migration exceeding the effects of

known migratory factors like laminin and fibronectin (Malin *et al*., 2009). In cultures derived from Matrilin 2 deficient mice, the migratory ability of embryonic Schwann cell was decreased but could be rescued by addition of exogenous Matrilin 2 in the medium or on culture plate. Apart from its effects in glia *in vitro*, Matrilin 2 is also shown to increase axonal outgrowth of embryonic DRG neurons without affecting axonal branching. Upon embryonic development, Matrilin 2 expression is downregulated, remaining in low levels in the peripheral nerves. However, peripheral nerve injury significantly upregulates *Matrilin 2* expression, particulary in Schwann cells close to the nerve transection (Malin *et al*., 2009). Such injury in the Matrilin 2 KO mice results in delayed peripheral nerve repair and functional recovery after transection. Repair promoting function of Matrilin 2 is thought to be due to Schwan cell secretion of Matrilin 2, which allows a permissive medium for axonal outgrowth. Considering the enriched expression of Matrilin 2 early in the disease and its effects in PNS, we hypothesized Matrilin 2 plays a role in OPC fate determination and axonal repair.

Inhibins and Activins belong to TGFβ superfamily hormones that were discovered for their respective roles as suppressors (*i.e.* inhibins) or stimulators (*i.e.* activins) of pituitary FSH synthesis and secretion. The receptors for inhibins were not discovered until recently. Other TGFβ superfamily ligand interact with type I and type II receptors, which are serine-threonine kinase recptors (Massague *et al.,* 2000). Two cell surface molecules that bind inhibin with high affinity and compete with activin signaling have been identified so far (Matzuk *et al*., 2000). The first molecule is betaglycan that acts together with activin type II receptor (ActRII) to bind inhibin with high affinity (Lewis *et al.,* 2000). The second is a cell adhesion molecule, p120, that binds to inhibin in association with activin type I receptor (ActRI) (Chong *et al.,* 2000). Activin receptors are prototypes of single-pass transmembrane serine-threonine kinases and their association with betaglycan, p 120 and inhibins antagonize the activin-mediated signal transduction (Tsuchida *et al.,* 2009). Similar to other TGFβ superfamily receptor-ligand signaling, activin-mediated signal transduction requires ligand binding to type II receptors that in

turn recruits and activates the type I receptor. Following the receptor dimerization and activation, Activin/TGFβ specific Smads, Smad 2/3/4 complexes are activated by phosphorylated type I receptor. In the nucleus, Smad 2/3/4 regulate gene expression with additonal transcriptional cofactors. Smad-independent pathway is also reported, such as MAPK activation with downstream targets of Erk1/2, p38 MAPK and JNK (Tsuchida *et al.,* 2009). Inhibin exerts its effects by binding to betaglycan and p120 to antagonize the activin receptor dimerization, to limit the activin induced intracellular signaling and subsequent alterations in gene expression. It is currently unknown if activins induce *Matrilin 2* expression in target cells but decreased levels of Matrilin 2 can be explained by Inhibin A antagonizing activin signaling to downregulate gene expression of activin gene targets if Matrilin 2 is one of them.

Since the function of Matrilin 2 is not investigated thoroughly in CNS, the interplay between Inhibin A and *Matrilin 2* expression comes from studies in systems outside of the nervous system. Inhibin A has tumor suppressor functions within the female reproductive system. In fact, deletion of the Inhibinα (*Inha*) subunit results in the development of sex cord-stromal tumors in adult mice at an early age that shows upregulation of *Matn2* mRNA (Matzuk *et al*., 1992). A microarray study of stromal tumors conducted by Nagaraja and colleagues in the INHA KO mice reported significant changes in the expression of ECM genes including Matrilin 2 (Nagaraja *et al*., 2010). Changes in ECM genes can impact diverse processes such as cell communication, migration, differentiation among many others (Leask and Abraham, 2006). In line with the published reports, we predicted Inhibin A production in cells other than OPCs would have negative consequences on OPC differentiation process.

Consistent with the transcriptome data, Matrilin 2 levels are significantly increased in the newly born OPCs and in some astrocytes early in the disease (Fig. 13B). In contrast, 14 day brains did not contain any white matter cells labeled with anti-Matrilin 2 antibody, neither did the non-injured white matter. Meanwhile, Inhibin A had a complementary profile following white matter stroke. The early time point lesions did not include any cells positive for Inhibin A (Fig.

13C), which dramatically changed at day 15 after stroke (Fig. 13C'). An antibody raised against the Inhibin A subunit Inhibitα detected numerous cells that filled the stroke core and peri-infarct white matter, which were phenotyped strictly as astrocytes (Fig. 13C''). Such cells were absent early in the diease and in healthy white matter (Fig. 13C). We hypothesized that white matter stroke leads to activated astrocytes that upregulate their production and secretion of Inhibin A. Once the reactive astroyctes fill the lesioned white matter, Inhibin A binding to activin receptors, betaglycan and p 120 on OPCs antagonizes activin mediated *Matn2* expression that may play a role in OPC fate determination. We propose a model of Inhibin A action based on the literature in systems outside of CNS (Fig. 15). In short, complementary temporal changes in Matrilin 2 and Inhibin A production suggest a novel interaction between white matter OPCs and and reactive astrocytes.

Opposing effects of Matrilin 2 and Inhibin A on OPC differentiation

Following up on the transcriptome and immunohistochemistry results, we investigated how Matrilin 2 and Inhibin A affect the OPC differentiation process *in vitro.* Primary mouse OPC cultures were used to carry out OPC differentiation assays. OPCs thrive in conditions enriched with growth factors PDGF and FGF that maintain them in the proliferating progenitor state. Cell differentiation can be induced by merely changing the composition of the culture media by replacing the growth factors with T3 thyroid hormone and insulin among other factors (Wang *et al*., 2007). The differentiation media, named as co-culture media, transforms the OPCs into oligodendrocytes that express myelin genes within 7 days. Since the *in vitro* effects of Matrilin 2 and Inhibin A were not known, we analyzed the OPC differention rate at day 5 to minimize the risk of co-culture media neutralizing the effects.

The primary OPC cultures contain predominantly Olig 2 positive cells as expected (Fig.14 A) in the presence of FGF and PDGF, although few astrocytes were observed that did not label with OPC lineage markers. Upon changing the media to co-culture recipe, OPCs become

positive for MBP and goes through a range of morphological changes in the process of differentiation from simple to mature phenotype (Fig 14. B – D). We compared the rate of OPC differentiation and oligodendrocte maturation in 5 experimental groups: PDL coated surface (10 µg/mL) control group, Matrilin 2 coated surface (20 µg/mL), Matrilin 2 added in media (10 µg/mL), Inhibin A added in media (10 µg/mL), and finally media containing both Matrilin 2 and Inhibin A. All test groups also included PDL on the culture surface (n=5).

We compared OPC differentiation rate calculated as the percentage of MBP+ Olig 2+ double labeled cells over the total number of Olig 2 + cells. Matrilin 2 coated surface or addition of soluble Matrilin 2 into the media did not alter the differentiation potential of OPCs relative to the PDL surface control (Fig. 14E). In contrast, Inhibin A containing media significantly decreased the number of MBP+ cells (PDL: 45.5% ± 9.06, PDL + Inhibin A media: 27.30% ± 5.44, $P< 0.001$). Furthermore, this effect was attenuated when Matrilin 2 and Inhibin A were both present in culture media. (Fig 14E, 32.95% ± 6.34, $P< 0.01$ relative to PDL control).

Subsequently, in order to compare the extent of oligodendrocyte maturation, we used Scholl ring analysis on the MBP+ cell images in each conditon (n= 7-10). Presence of Matrilin 2, particularly in soluble form, increased the average number process crossing per Scholl ring indicating increased complexity of oligodendrocyte arbors (Fig. 14F, PDL: 4.94 ± 1.05, PDL + Matrilin surface 2: 11.24 ± 2.0, $P< 0.001$; PDL + Matrilin 2 media: 19.13 ± 5.49, $P< 0.00001$). Inhibin A administration alone did not alter the average incidence of ring crossing relative to the PDL control group (Fig. 14F). However, Inhibin A decreased the total number of processes, maintaining the cells in simple morphology (Fig. 14G, PDL: 45.80 ± 11.12, PDL + Inhibin A media: 9.67 ± 3.56, $P < 0.01$). In contrast, Matrilin 2 containing media markedly increased the complexity of oligodendrocytes (224.60 ± 66.70, $P < 0.00001$) that also neutralized the negative effects of Inhibin A on oligodendrocyte process formation (Fig. 14G). Furthermore, oligodendrocyte process extension was significantly limited by administration of Inhibin A (PDL: 208 ± 38.99, PDL + Inhibin A: 84 ± 26.08, $P < 0.001$), which was neutralized by the presence of

Matrilin 2 (Fig 14H). In summary, soluble Matrilin 2 significantly increased the process extension and arborization in oligodendrocytes even though it did not facilitate higher OPC differentiation. Conversely, Inhibin A had inhibitory effects on OPC differentiation and oligodendrocyte maturation by limiting oligodendrocyte process formation and the complexity of present arbors. Some of these negative effects were overcome in the experimental group where Matrilin 2 was present in lieu of Inhibin A (Fig 14I).

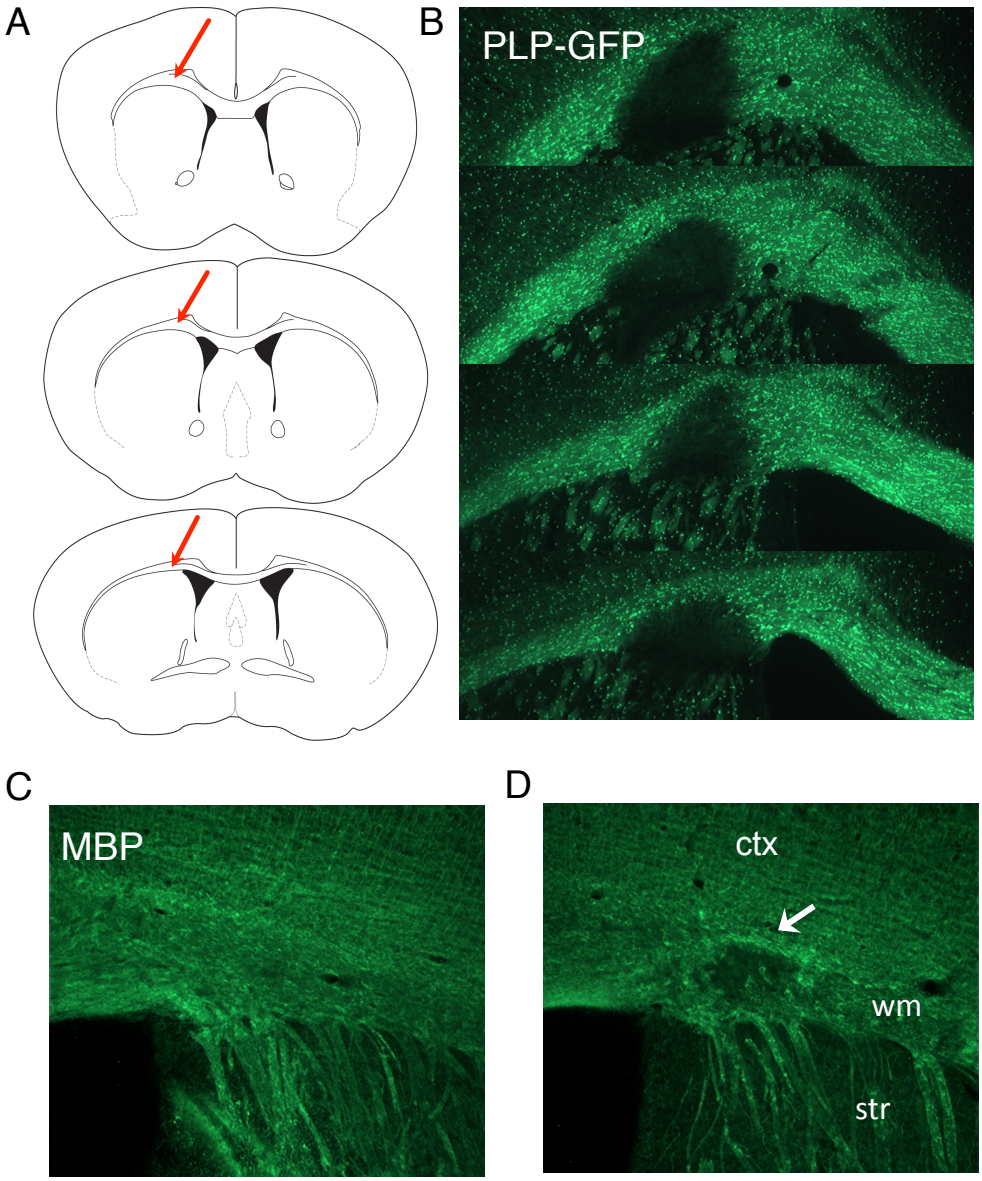

Figure 1. L-NIO injections result in focal ischemic white matter injury. A. Schematic representation of the coordinates where vasoconstrictive agent L-NIO Is injected into the white matter below forelimb motor cortex. Red arrows represent the trajectory of the pulled pipette needle. **B.** 7 days after L-NIO administration, the ischemic lesion exhibits loss of GFP labeled oligodendrocytes in the PLP-GFP transgenic line. **C, D.** Myelin is labeled by MBP immunohistochemisty in control (C) and in 7 day stroke brain (D). The arrow points out the site of myelin rarefaction. ctx – cortex, wm – white matter, str – striatum.

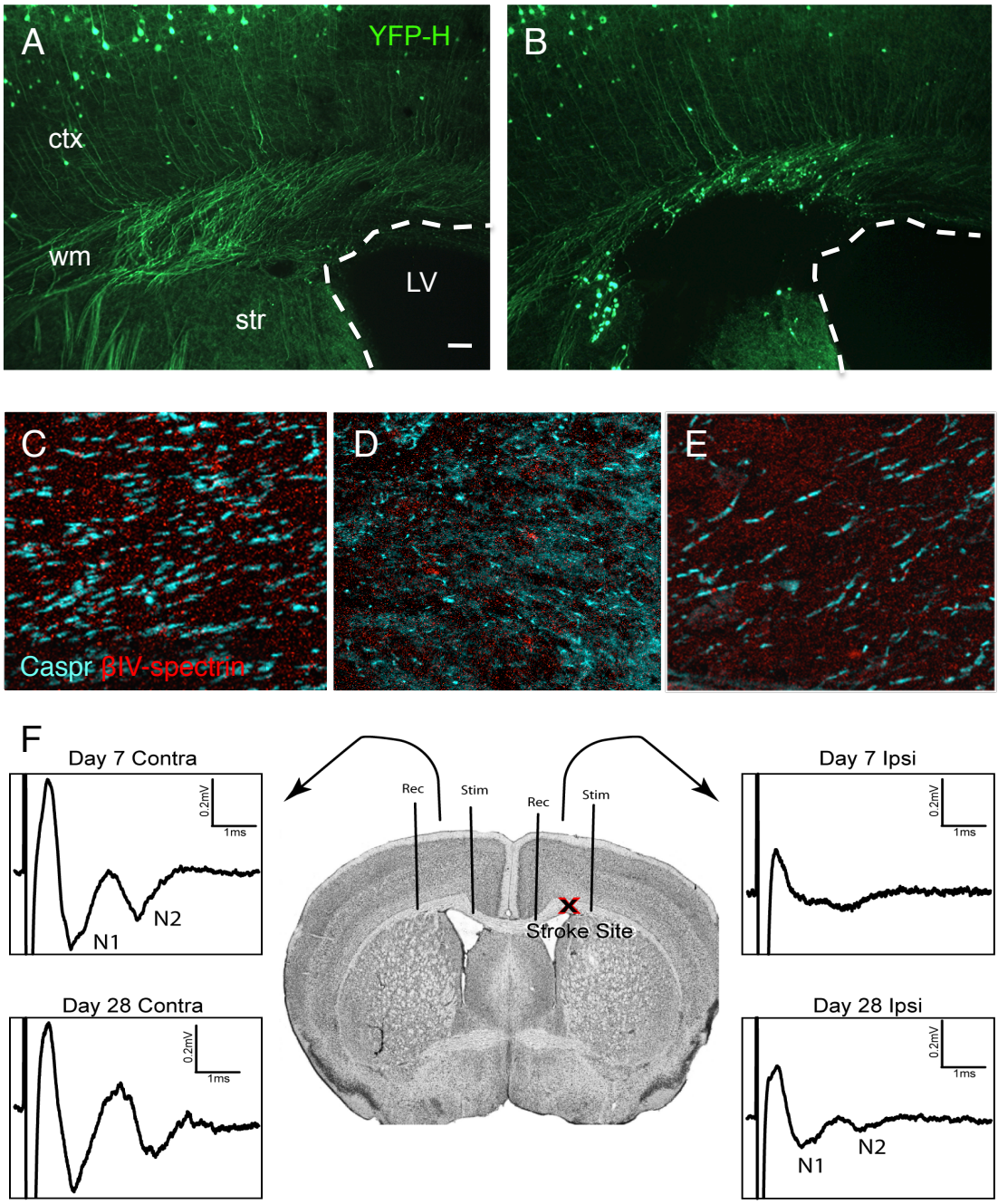
A
YFP-H
ctx
wm
str
LV
B
C
Caspr βIV-spectrin
D
E
F
Day 7 Contra
0.2mV
1ms
N1
N2
Day 28 Contra
Rec
Stim
Rec
Stim
Stroke Site
Day 7 Ipsi
Day 28 Ipsi

Figure 2. White matter stroke results in axonal injury and functional deficits. **A, B.** Ischemic stroke (B) in YFP-H mouse brain expressing soluble YFP along axons shows a lesion core devoid of axons compared to control (A). Retraction balls, a hallmark of diffuse axonal degeneration, are seen as bright varicosities in white matter projections. **C - E.** Paranodes and nodes of Ranvier are visualized by Caspr and βIV-spectrin respectively. The stroke core (D) lacks both markers consistent with axonal loss. The peri-infarct white matter (E) exhibits relatively preserved nodal architecture that are non-contiguous compared to healthy white matter (C). **F.** Compound action potentials (CAPs) generated across the white matter stroke lesion demonstrate decreased amplitude of each CAP component at 7 day after injury. A modest recovery in CAP amplitude was observed at day 28. N1 component of CAP is generated due to fast depolarization in myelinated axons. N2 component represents slower depolarization across non-myelinated axons.
ctx – cortex, wm – white matter, str – striatum, LV – lateral ventricle. Bar: 50 μm.

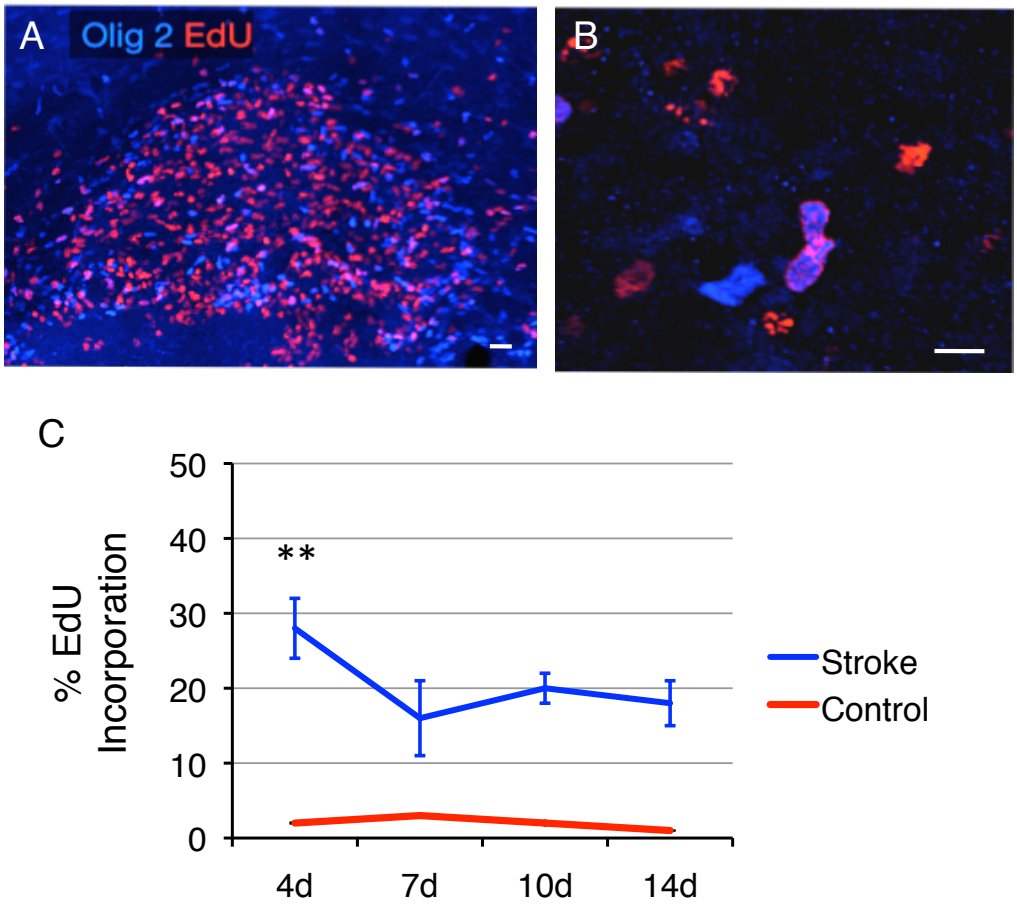

Figure 3. OPC regenerative response following white matter stroke. Brief pulses of EdU administered 24 hours prior to each time point revealed Olig 2+ cells proliferate at a high rate after white matter stroke. **A.** Labeling in 7 day stroke section is displayed. **B.** Higher magnification image shows numerous cells of OPC lineage that incorporated EdU. Bar: 20 µm **C.** OPC proliferation index is calculated as the percentage of Olig2+ cells that incorporated EdU over the total number of Olig2+ cells. Stroked brains (blue) show significantly higher rate of proliferation compared to control (red). p< 0.0001 in all time points. ANOVA, Tukey multiple comparison post-test 4d vs 7d $P < 0.001$, 4d vs 14d $P < 0.001$. n=5.

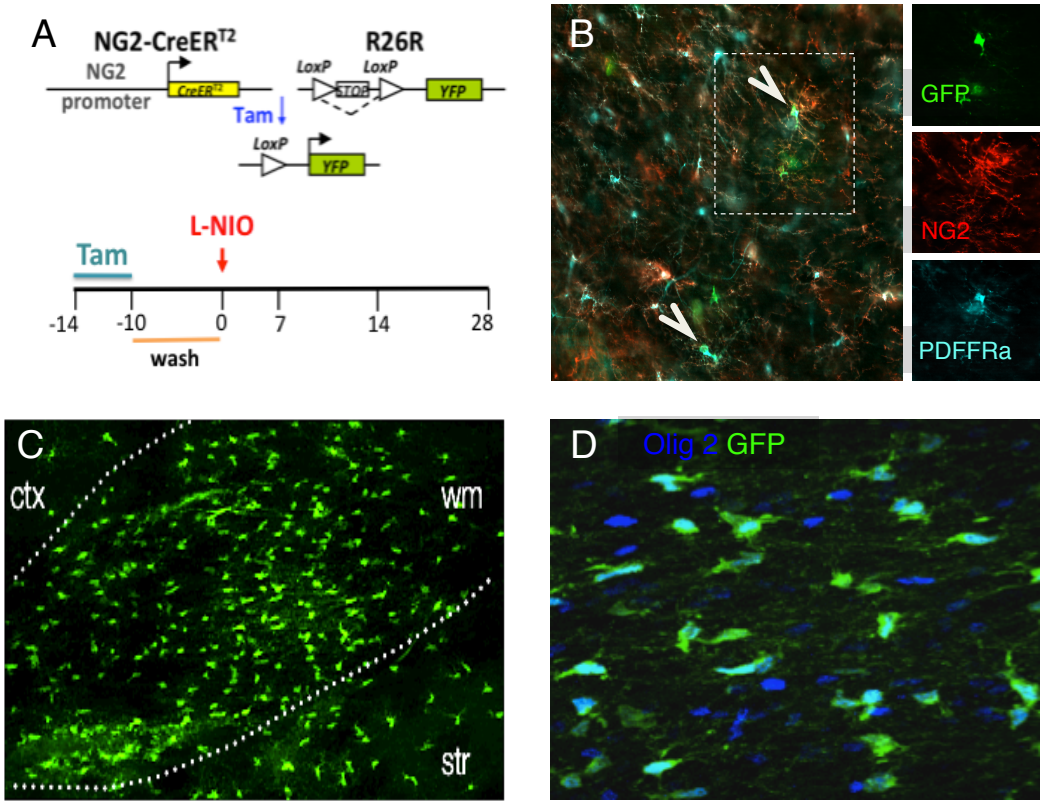

Figure 4. Cell fate determination of OPCs after white matter stroke with the inducible OPC reporter line. A. Tamoxifen inducible NG2CreER^{T2} line is crossed with Rosa-YFP mice to generate the OPC reporter mouse line. Bidaily injection of Tamoxifen was given for 5 days to induce recombination. infarcts were created after a 10 day wash period. Reporter cell phenotypes were investigated on multiple time points after stroke. **B.** In the absence of injury, reporter activity is found only in cells expressing at least one of the prominent OPC markers: NG2 and PDGFRα. Arrowheads indicate triple labeled OPCs in the control brain sample after the wash-out period. **C.** 7 days after stroke, YFP expressing cells populate the lesion **D.** The responsive reporter cells largely remain in Olig 2+ oligodendrocyte lineage.

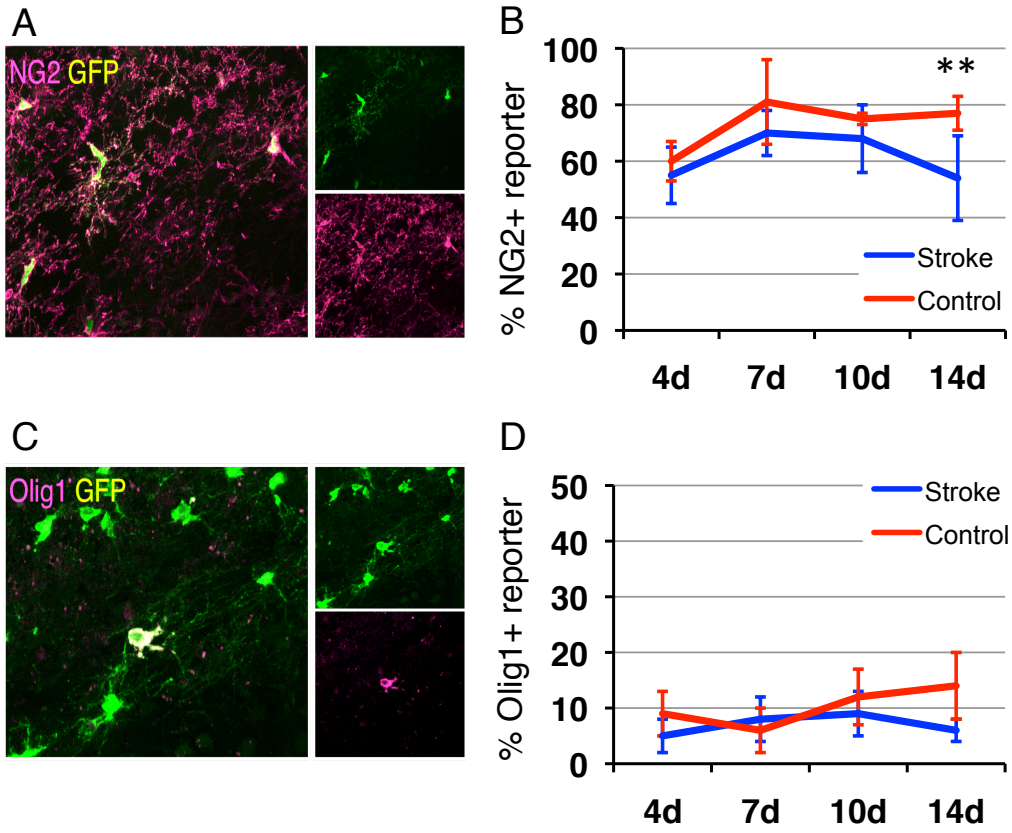

Figure 5. Newly born OPCs persist in the progenitor state with limited capacity for differentiation after white matter stroke. A. YFP expressing OPC reporter cells are colabeled with anti-NG2 antibody to identify undifferentiated cells at 4 day after lesion. **B.** Undifferentiated OPC reporter cells are represented as the percentage of NG2+ YFP+ reporters over the total number YFP+ cells. Quantification across post-stroke time points suggest the majority of induced reporters remain in progenitor stage in both stroke (blue) and control (red) brains. At day 14 after stroke, a significant decrease in undifferentiated reporter percentage was observed relative to control. 14d stroke vs. 14d control p< 0.001. **C.** OPC reporters that underwent successful differentiation into oligodendrocytes were detected by cytoplasmic translocation of Olig1. Labeling of day 14 after stroke is shown **D.** The rate of reporter cell differentiation is calculated as the percentage of Olig1+ YFP+ reporters over the total number of YFP + cells. White matter stroke (blue) does not significantly alter the rate of OPC differentiation relative to control (red) condition. OPC differentiation remained low in both groups. n= 5 - 6. ANOVA, Tukey multiple comparison post-test 14d stroke vs. 14d control $P < 0.001$. n=5.

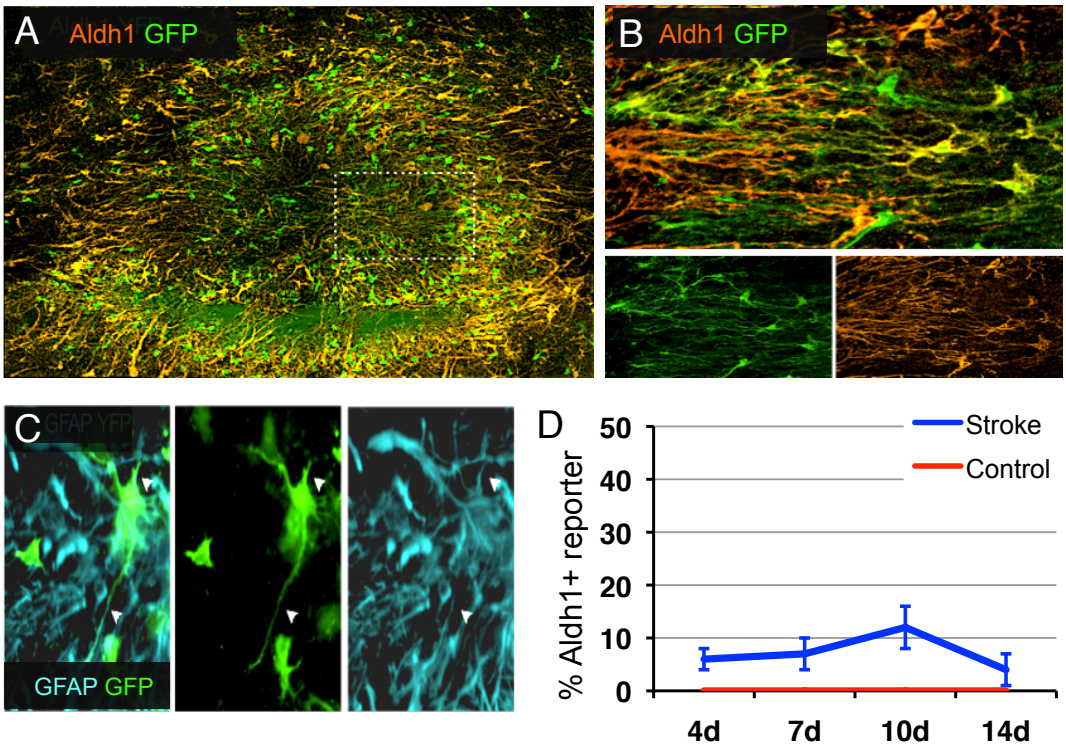

Figure 6. White matter stroke leads to astrocytic transformation of newly born OPCs. A, B. YFP expressing OPC reporter cells are colabeled with astrocyte marker Aldh1 to identify newly born OPCs that diverged into astrocytic fate. A representative sample is shown of 7 day time point (A). Higher magnification of the image reveals Aldh1+ reporter cells with astrocyte morphology. **C.** The astrocytic phenotype was confirmed by GFAP labeling of stroke samples. The arrowheads point out a reporter cell with processes positive for GFAP. **D.** The rate of astrocytic transformation is calculated as the percentage of Aldh1+ reporters over the total number of reporters across the post-stroke time points. In the absence of injury (red) none of the reporter cells were differentiated into astrocytes. A small percentage of newly born OPCs became astrocytes at all time points after stroke. n= 5 - 6.

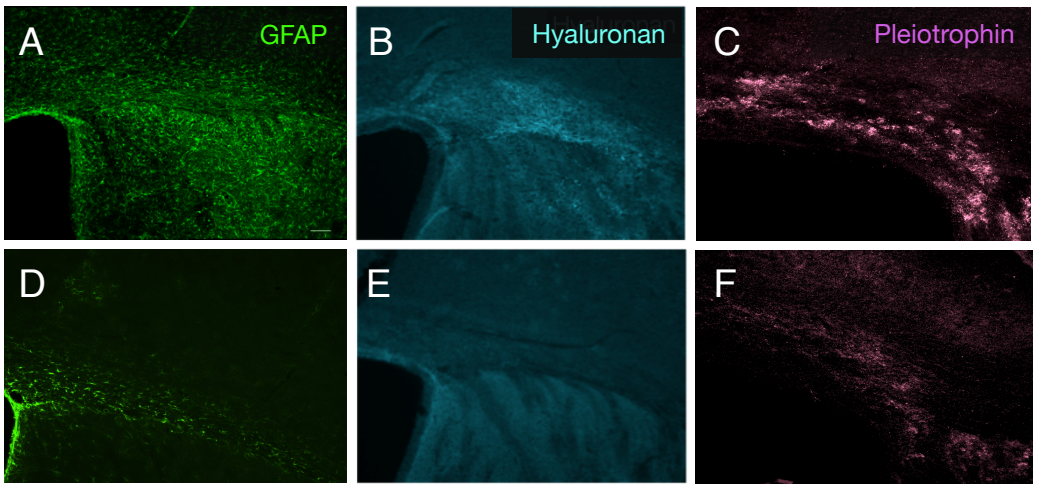

Figure 7. White matter stroke leads to dramatic changes in astrocyte density and induces an increase in secreted factors implicated in OPC differentiation block. A – C. 14 day white matter stroke **D – F.** Control samples **A.** GFAP+ astrocytes fill the ipsilatereal white matter, dorsal striatum and overlying cortex that span an area far larger than the stroke volume. This is in contrast with normal white matter that shows resident white matter astrocytes (D). **B.** High molecular weight Hyaluronan that is produced by reactive astrocytes was detected by hyaluronan binding protein, indicating its deposition in extracellular matrix following white matter stroke. Control groups (E) lacked detectable signal above background. **C.** Secreted Pleiotrophin levels were markedly increased in the stroked white matter compared to control (F).

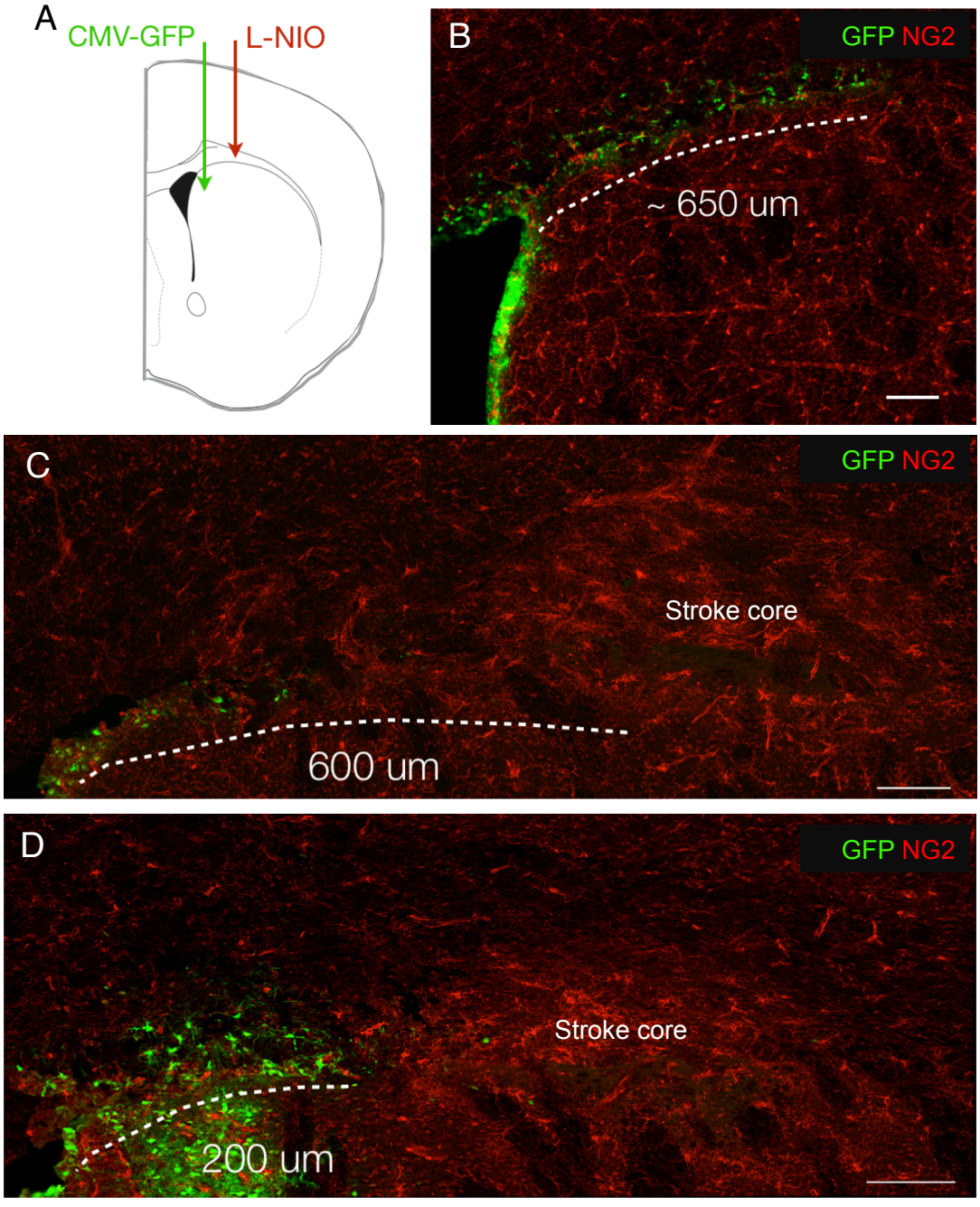
A
CMV-GFP
L-NIO
B
GFP NG2
~ 650 um
C
GFP NG2
Stroke core
600 um
D
GFP NG2
Stroke core
200 um

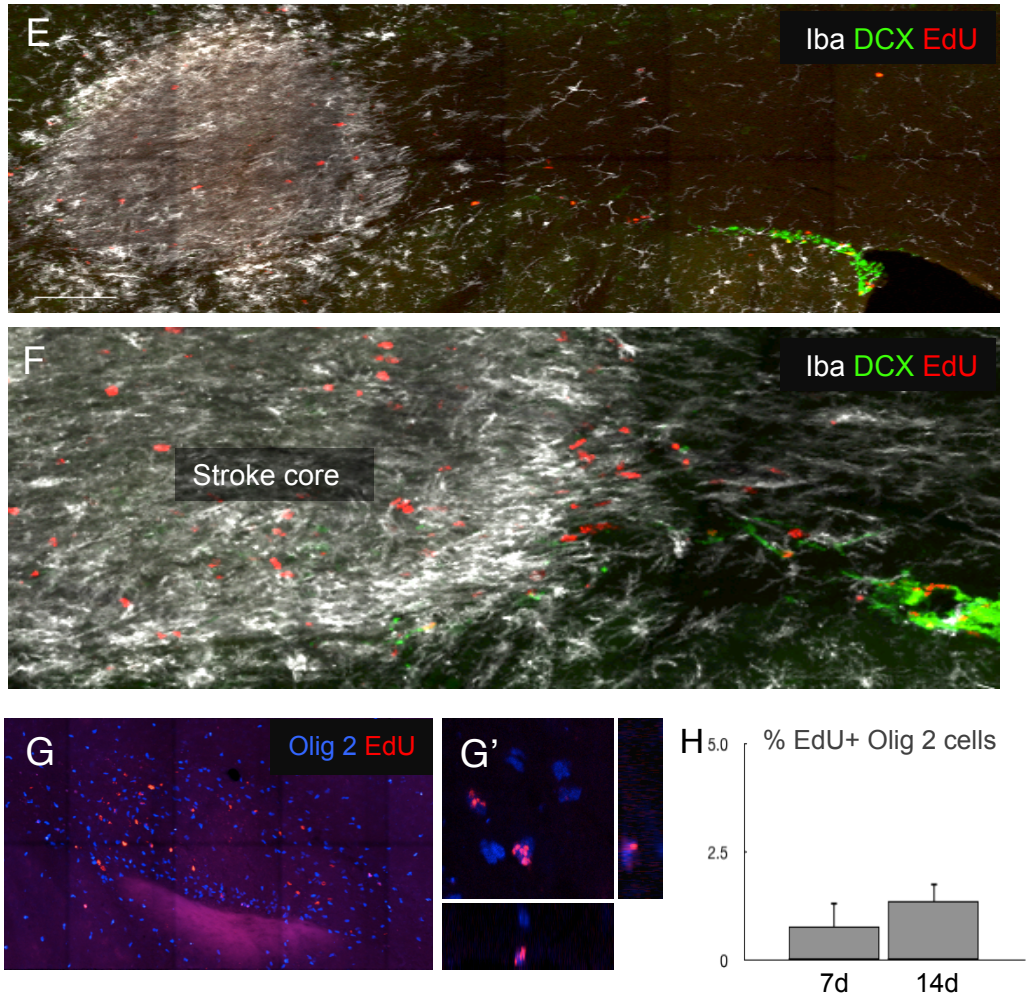

Figure 8. SVZ does not significantly contribute into OPC regeneration response in white matter stroke **A.** Schematic representation of SVZ labeling paradigm. SVZ was targeted by CMV-GFP lentivirus injection 4 days prior to stroke induction. GFP+ cells were phenotyped at days 7 and 14 after stroke or saline control. **B.** In the absence of injury, GFP+ cells stream at the border of white matter and dorsal striatum ranging 600 - 650 μm from SVZ. Cells of SVZ origin were not positive for OPC marker NG2**. C, D**. GFP+ cells migrating from ipsilateral SVZ do not infiltrate into the lesion or peri-infarct white matter regardless of the proximity of white matter stroke to the SVZ. No GFP+ NG2+ cells were found at day 7 or day 14 stroke samples. Bar: 100 μm. **E – H.** Bidaily injection of EdU for 5 days prior to stroke was used to label the progenitor pool in SVZ. **E.** EdU uptake was prominent in ipsilateral SVZ, particularly in DCX+ neuroblasts. Few EdU+ cells were detected in the lesion, largely in the Iba+ microglia/macrophages. **F.** Higher magnificaiton image of (E). **G, G'.** EdU incorporating cells were assessed for OPC lineage by anti-Olig 2 antibody labeling at day 7. EdU incorporating cells were rarely observed (G'). **H.** EdU+ Olig 2+ double cells make up less than 2% of total EdU+ cell population in stroke samples. n=3.

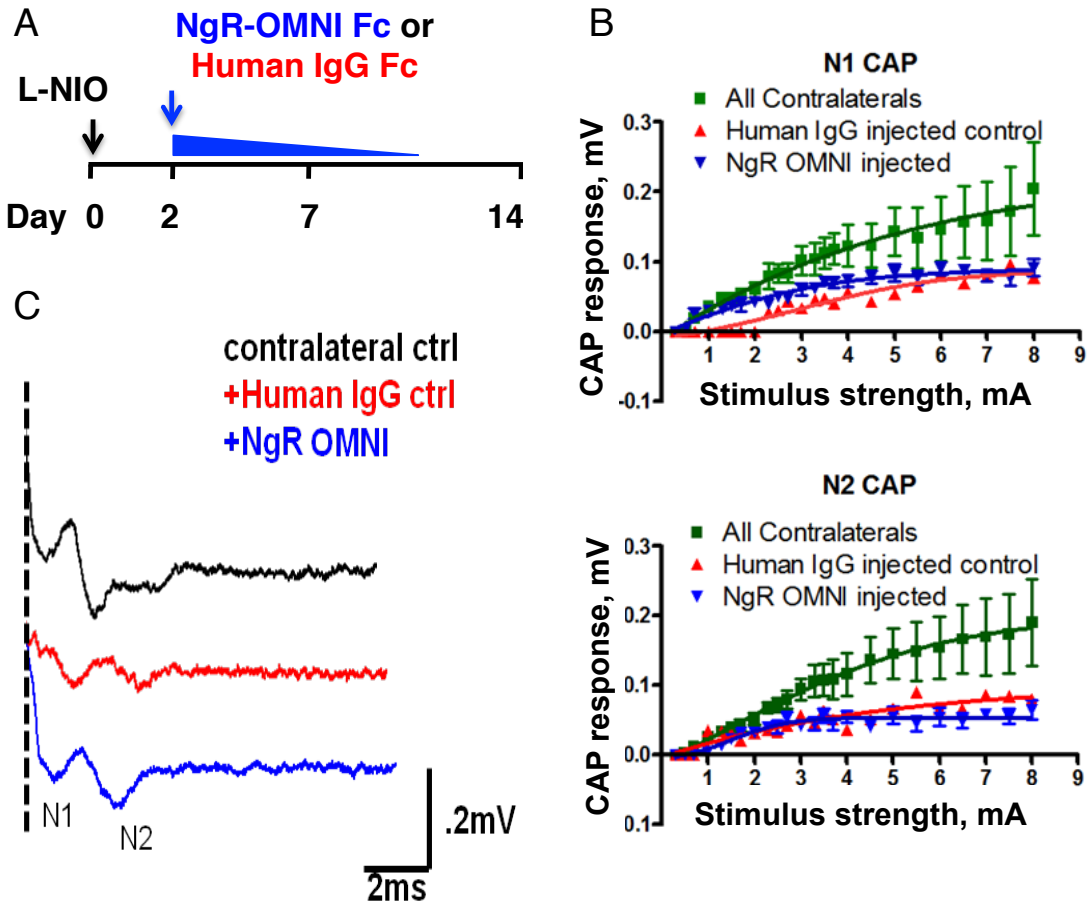

Figure 9. NgR-OMNI Fc infusion into ipsilateral white matter reduces the conduction deficit after stroke. A. Two days following stroke, 1.05 ug NgR-OMNI Fc or Human IgG Fc was delivered into ipsilateral white matter. CAP recordings were carried out at day 28 after stroke to assess long-term effects on axon conduction. n=3 **B.** N1 component (top panel) represents fast depolarization from myelinated axons. The contralateral healthy white matter (green) produced higher N1 amplitude with increased stimulation. Human IgG Fc control group (red) shows the baseline conduction deficit that is significantly attenuated in response to stimulation. NgR-OMNI Fc infused lesions (blue) generated N1 amplitutes similar to healthy white matter at lower stimuli but had attenuated conduction with increased stimulation. N2 component recordings (bottom panel) representing depolarization from non-myelinated axons suggest NgR-OMNI Fc was not effective in improving non-myelinated axon conduction deficit. **C.** Representative individual recordings are graphed together for comparison. Both stroke groups show muted CAP amplitudes. Human IgG control group exhibits N1 and N2 peak latency. NgR-OMNI Fc leads to modest improvement relative to Human IgG Fc group but is not sufficient to restore the axon conduction deficit.

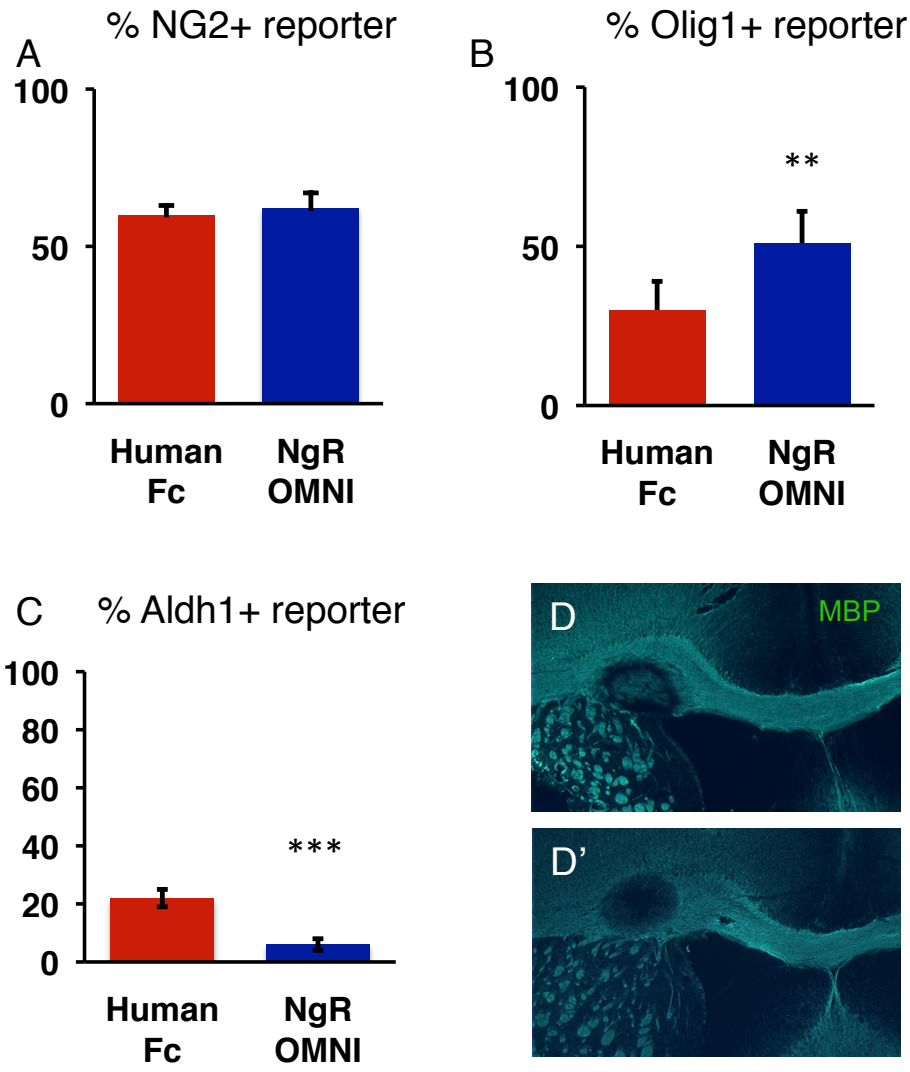

Figure 10. NgR-OMNI Fc delivery stimulates OPC differentiation and reduces astrocytic transformation. A – C OPC reporter mice injected with NgR-OMNI Fc or Human IgG Fc after stroke induction were sacrificed on day 14. n= 5 **A.** The percentage of reporter cells remaining in OPC stage was not altered by NgR-OMNI Fc delivery. **B.** OPC differentiation rate was significantly increased in presence of NgR-OMNI. $p< 0.001$. **C.** NgR-OMNI Fc also markedly decreased the rate of astrocytic fate in newly born OPCs. $p< 0.0001$. **D.** The extent of demyelination was not different between Human IgG Fc (D) and NgR-OMNI Fc (D') injected samples but myelin debris clearance was improved in NgR-OMNI Fc infused lesions.

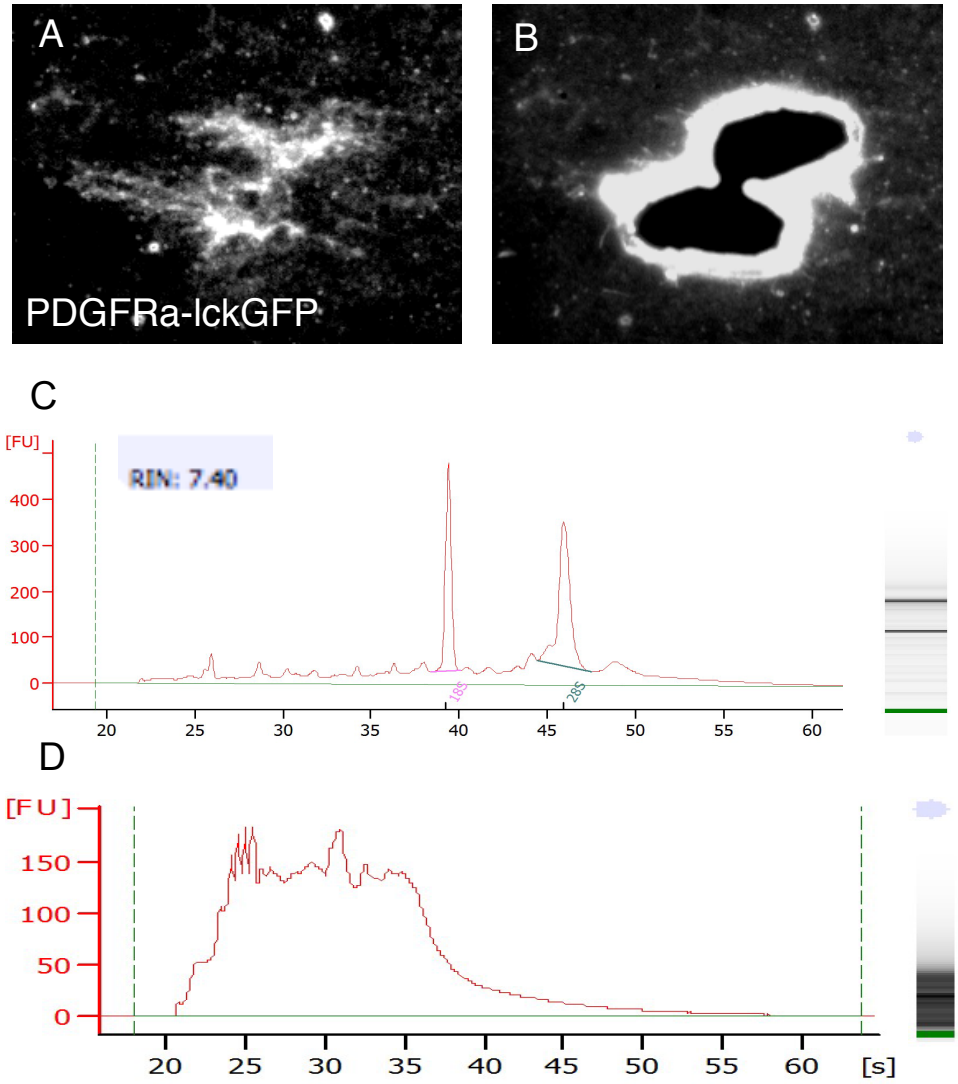

Figure 11. Laser capture microdissection (LCM) and cDNA preparation for OPC transcriptome study. A, B. A lentivirus expressing membrane-targeted GFP under the control of PDGFRα promoter was used to label peri-infarct OPCs. 5 day stroke section showing GFP+ OPCs before (A) and after LCM (B). **C.** RNA quality of tissue collected by LCM was assessed in Bioanalyzer Picochip indicating preserved RNA integrity. **D.** RNA isolated from LCM tissue was amplified and converted into cDNA that produces 200-300 bp fragments to be used in RNAseq library generation.

A

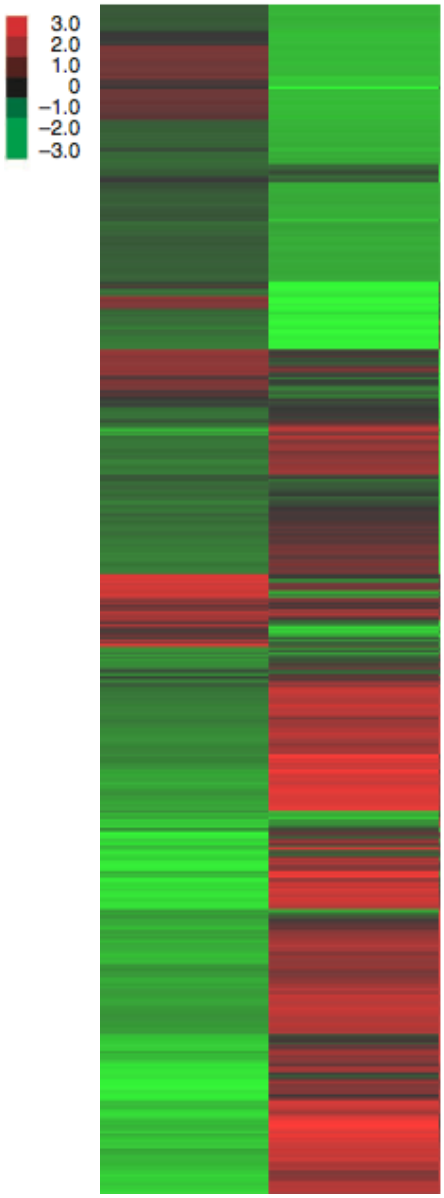

B

Up at 5 versus 15 dpl	Fold Change
Ppard	13.88880052
Ripk1	13.42683913
IGFBP3	12.81514245
Tnf	12.73905842
Gpc4	12.73244192
Spbn1	12.69737375
Efnb2	12.65210862
Sema4b	12.63211213
Ninj1	12.51846775
Slfn4	12.26255215
Jag1	12.21563447
Foxp3	12.09417257
Runx3	11.88328405
Bambi	11.09945473
Matn2	11.03972047
Lama5	10.29472829
Plxna4	7.571781947

Up at 15 versus 5 dpl	Fold Change
Bmp2	13.5687827
Mmp21	12.9850960
Hapln4	12.9147295
Cxcl13	9.3355721
Ccr7	8.9149765
Lama3	7.5952761
Spock2	7.2630688
Gria4	5.7888115

Figure 12. Differential expression of genes in peri-infarct OPCs early vs. late in white matter stroke. A. Hierarchical clustering and graphical analysis of differentially expressed genes in 5 and 15 days post lesion samples ($P < 0.05$). **B.** Top most upregulated genes of interest are listed at one time point relative to the other time point.

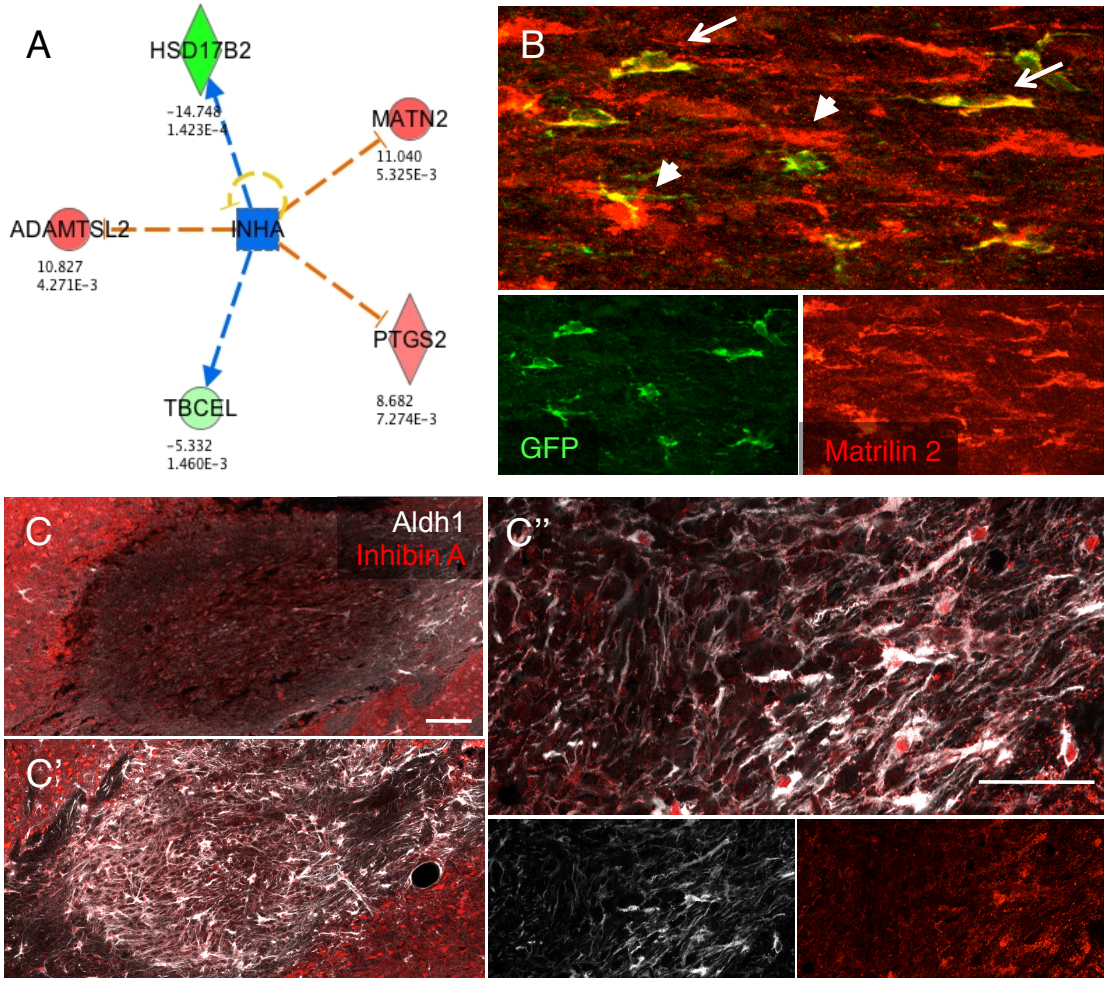

Figure 13. Matrilin 2 and its negative regulator Inhibin A have complementary profiles in early and late time points. A. Ingenuity pathway analysis predicted inhibition of growth factor Inhibin A at 5 days versus 15 days post lesion. Z score = -2.236. **B**. Matrilin 2 levels were increased in 5 day stroke samples, shown here in OPC reporter brain. GFP+ OPCs colabel with Matrilin 2 (arrows) in addition to other cell types (arrowheads). On 15 day, Matrilin 2 levels were comparable to non-stroked white matter. **C – C''** Inhibin A subunit Inhibinα is used as a marker to compare tissue levels of the growth factor. At 5 days post lesion (C), there is no detectable Inhibinα signal whereas labeling of 15 day stroke sections (C') revealed high levels of Inhibinα+ cells filling the lesion. The majority of Inhibinα label coincides with Aldh1+ astrocytes shown in higher magnification (C''). Bar: 100 μm.

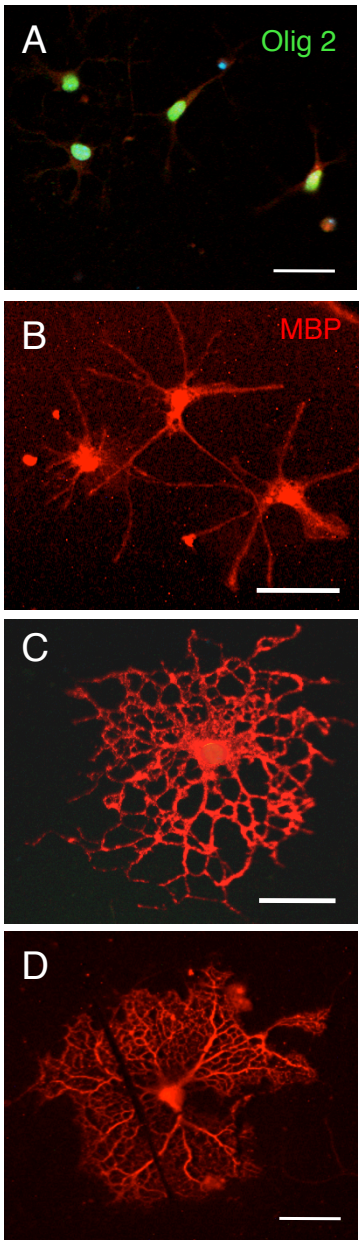
A
Olig 2
B
MBP
C
D

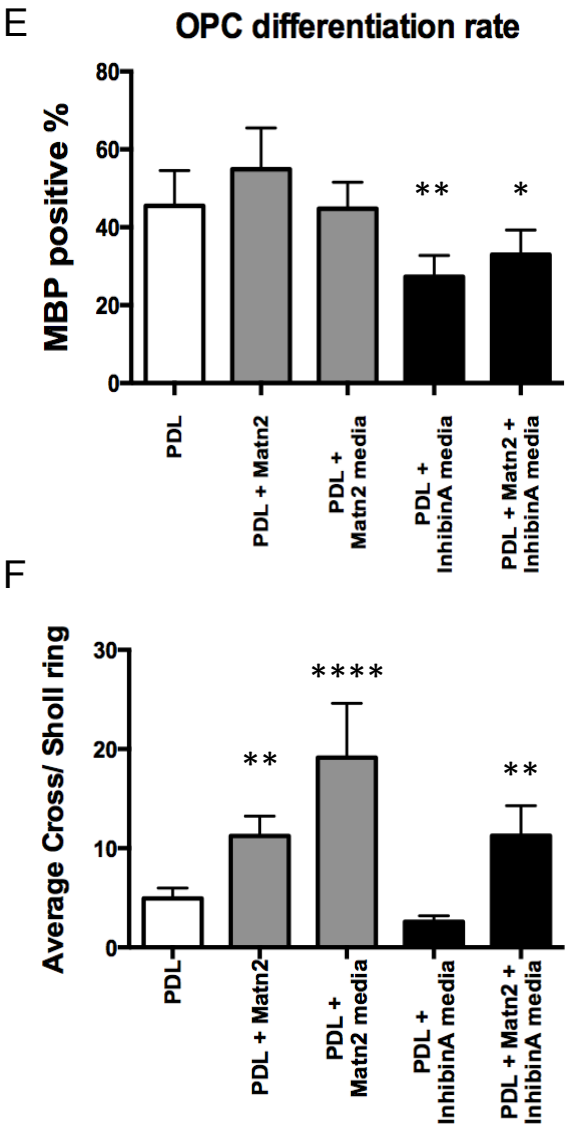
E
OPC differentiation rate
MBP positive %
80
60
40
20
0
**
*
PDL
PDL + Matn2
PDL + Matn2 media
PDL + InhibinA media
PDL + Matn2 + InhibinA media
F
Average Cross/ Sholl ring
30
20
10
0
**
****
**
PDL
PDL + Matn2
PDL + Matn2 media
PDL + InhibinA media
PDL + Matn2 + InhibinA media

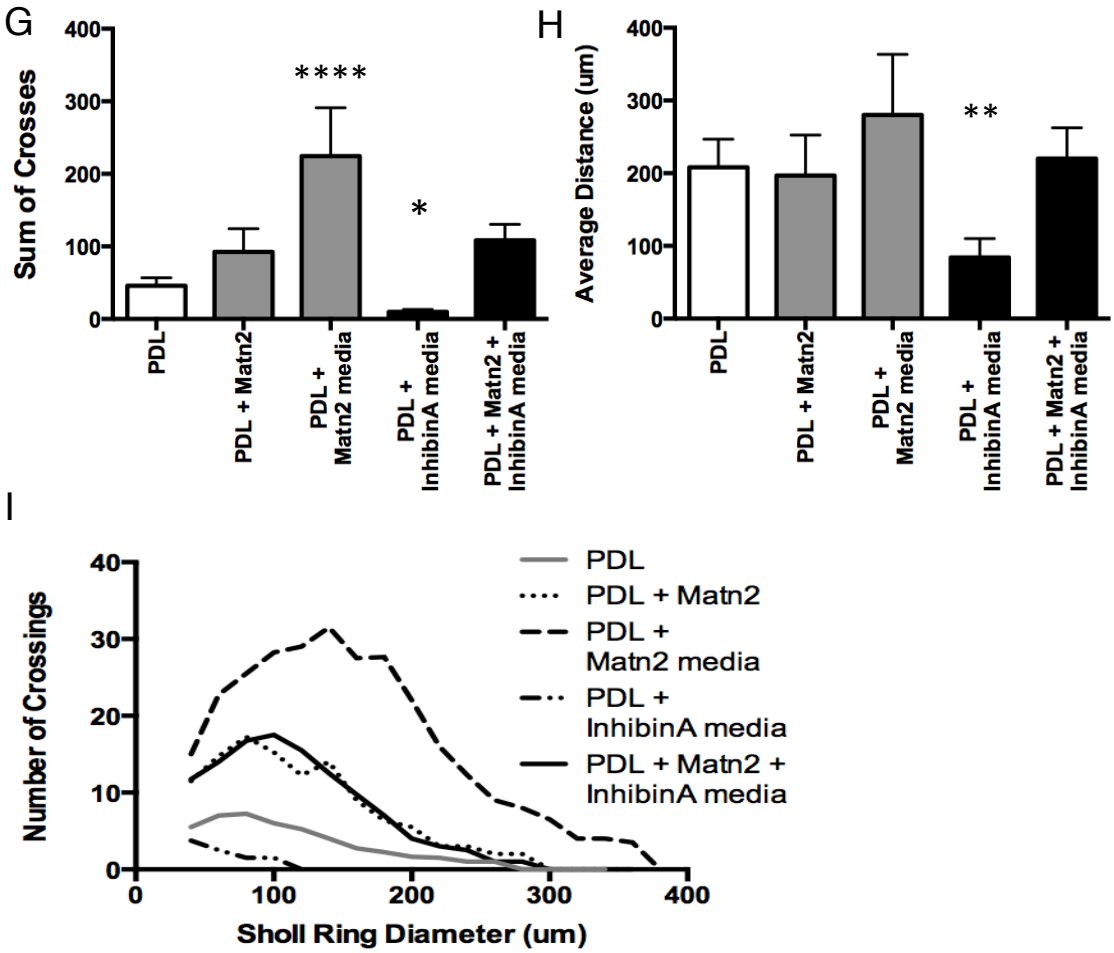

Figure 14. Matrilin 2 and Inhibin A have opposing effects on OPC differentiation and maturation A. Mouse primary OPC cultures labeled with Olig 2 antibody. **B - D**. MBP+ cells exhibit different morphology indicative of maturation state depending on culture conditions. Representative images of simple (B), complex (C) and mature (D) oligodendrocytes. Bar: 50 µm. **E.** OPC differentiation index is calculated as the percentage of MBP+ Olig2+ double labeled cells over the total number of Olig2+ cells. Matrilin 2 coated (20 µg/mL) surface or addition of soluble Matrilin 2 (10 µg/mL) into media did not affect the differentiation potential of OPCs relative to PDL surface control. Inhibin A containing media (10 µg/mL) significantly decreased the number of MBP+ cells. This effect was attenuated when Matrilin 2 and Inhibin A were both present. n= 5. **F – I** Scholl ring analysis was used to determine the extent of MBP+ cell maturation in each condition. n= 7-10. **F.** Presence of Matrilin 2, particularly in soluble form, increased the average number process crossing per Scholl ring. **G.** Addition of Inhibin A markedly decreased the total number of processes, maintaining the cells in simple morphology. In contrast, Matrilin 2 containing media increased the complexity of oligodendrocytes that also neutralized the negative effects of

Inhibin A on oligodendrocyte maturation. **H.** Oligodendrocyte process extension was significantly limited by Inhibin A which was prevented by presence of Matrilin 2. **I.** Number of process crossings per Scholl ring diameter is shown to summarize the *in-vitro* results. ANOVAs; Bonferroni's multiple comparisons post test.
* $P < 0.01$, ** $P < 0.001$, *** $P < 0.0001$, **** $P < 0.00001$

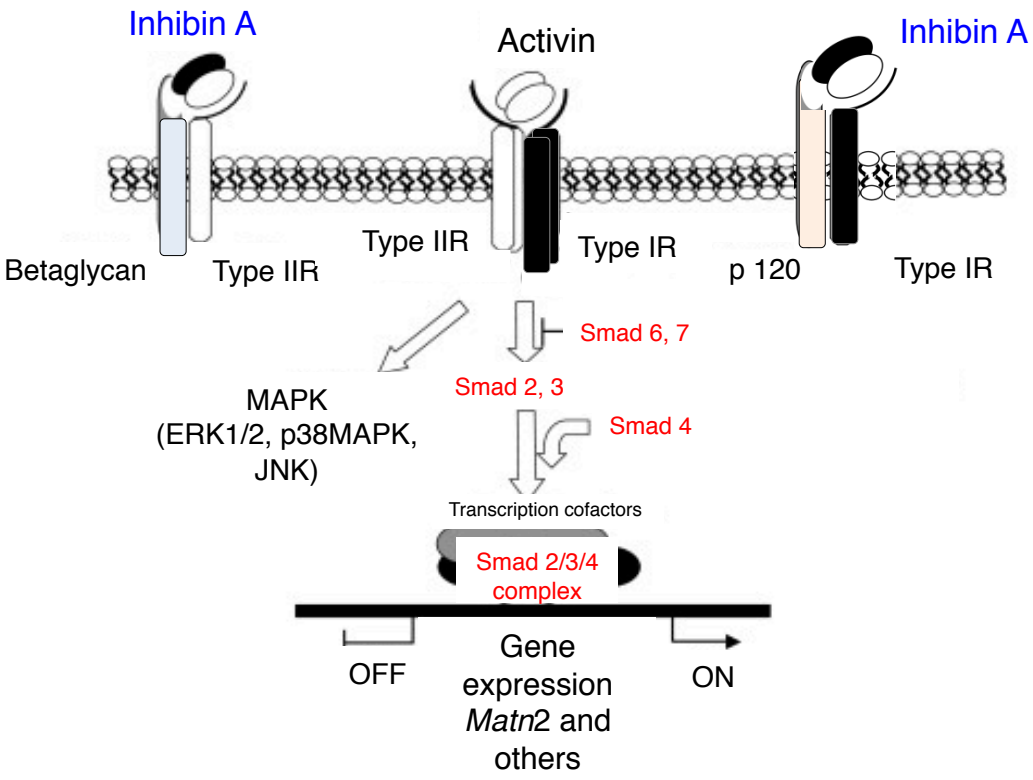

Figure 15. Proposed mechanism of action of Inhibin A on Matrilin 2 gene expression. Activins normally bind to Type II Activin receptors that in turn recruit and activate the Type I receptor to form dimers and activate Smad 2 and Smad 3 proteins by phosphorylation. Activated Smad 2/3 associates with Smad 4 to translocate into the nucleus and regulate gene activation. Activins relay signals in Smad-independent manner by MAPK pathway as well. Inhibin A binding to Betaglycan/Type II receptor as well as p 120/ Type I Activin receptor antagonizes the receptor dimer formation and downstream target activation. Inhibin A- dependent negative regulation of *Matn2* is anticipated to take place by blocking the Smad-dependent pathway.

Journal of Neuroscience Methods 180 (2009) 261–272

Contents lists available at ScienceDirect

Journal of Neuroscience Methods

journal homepage: www.elsevier.com/locate/jneumeth

A white matter stroke model in the mouse: Axonal damage, progenitor responses and MRI correlates

Elif G. Sozmen[1], Arunima Kolekar[1], Leif A. Havton, S. Thomas Carmichael*

Department of Neurology, David Geffen School of Medicine at UCLA, Neuroscience Research Building, 635 Charles Young Drive South, Los Angeles, CA 90095, United States

ARTICLE INFO

Article history:
Received 10 February 2009
Received in revised form 19 March 2009
Accepted 21 March 2009

Keywords:
Oligodendrocyte
Precursor
Myelin
NG2
Biotinylated dextran amine
Peri-infarct
Ischemia
Frontal lobe

ABSTRACT

Subcortical white matter stroke is a common stroke subtype but has had limited pre-clinical modeling. Recapitulating this disease process in mice has been impeded by the relative inaccessibility of the subcortical white matter arterial supply to induce white matter ischemia in isolation. In this report, we detail a subcortical white matter stroke model developed in the mouse and its characterization with a comprehensive set of MRI, immunohistochemical, neuronal tract tracing and electron microscopic studies. Focal injection of the vasoconstrictor endothelin-1 into the subcortical white matter produces an infarct core that develops a maximal MRI signal by day 2, which is comparable in relative size and location to human subcortical stroke. Immunohistochemical studies indicate that oligodendrocyte apoptosis is maximal at day 1 and apoptotic cells extend away from the stroke core into the peri-infarct white matter. The amount of myelin loss exceeds axonal fiber loss in this peri-infarct region. Activation of microglia/macrophages takes place at 1 day after injection near injured axons. Neuronal tract tracing demonstrates that subcortical white matter stroke disconnects a large region of bilateral sensorimotor cortex. There is a robust glial response after stroke by BrdU pulse-labeling, and oligodendrocyte precursor cells are initiated to proliferate and differentiate within the first week of injury. These results demonstrate the utility of the endothelin-1 mediated subcortical stroke in the mouse to study post-stroke repair mechanisms, as the infarct core extends through the partially damaged peri-infarct white matter and induces an early glial progenitor response.

1. Introduction

Subcortical white matter stroke constitutes 15–25% of all stroke subtypes (Bamford et al., 1991) and results in white matter lesions. These lesions encompass small infarcts in deep penetrating vessels in brain, as well as ischemic lesions in end-arterial regions of subcortical white matter (Matsusue et al., 2006; Gouw et al., 2008; Wardlaw, 2008). The infarctions in subcortical white matter are closely related to true microvascular stroke and are represented on MRI imaging as lacunar infarctions with a small stroke cavity as well as ischemic white matter hyperintensities (Gouw et al., 2008). Despite an advanced pre-clinical literature of animal modeling in large artery, "gray matter" stroke, there are few animal models of white matter ischemia. A principle problem in modeling white matter stroke in the rodent brain is that it has substantially less white matter than in higher mammals and humans.

A lack of an appropriate model for subcortical stroke presents a critical gap in stroke basic science research, as the mechanisms of cell death and of repair are likely to differ in white matter stroke from large artery gray matter strokes. For instance, oligodendrocytes undergo a different time course of cell death than neurons in large artery stroke models (Pantoni et al., 1996). Also, white matter astrocytes display a differential sensitivity to ischemic injury than those derived from gray matter (Shannon et al., 2007). In addition to this biology of cell death, the biology of the glial progenitor response is also different in cortical versus subcortical regions, and this may contribute to differing degrees of repair. Oligodendrocyte progenitor cells (OPCs) are widely scattered throughout cortical and subcortical regions in the adult brain. Using genetic labeling, it has recently been shown that OPCs in the subcortical white matter of the adult turnover at a higher rate compared to cortical OPCs (Dimou et al., 2008); and that cortical OPCs are fewer in number and experience a block at the progenitor or pre-oligodendrocyte stage (Dimou et al., 2008). Futhermore, this limited progenitor response of cortical OPCs persists after brain injury with few cortical OPCs producing mature oligodendrocytes (Dimou et al., 2008). Because of these apparently different mechanisms of cell death and of repair in cortical vs. white matter ischemia, specific animal models of subcor-

* Corresponding author. Tel.: +1 310 206 0550; fax: +1 310 825 0759.
E-mail address: scarmichael@mednet.ucla.edu (S.T. Carmichael).
[1] Authors contributed equally to this work.

0165-0270/$ – see front matter © 2009 Elsevier B.V. All rights reserved.
doi:10.1016/j.jneumeth.2009.03.017

tical white matter stroke are urgently needed. A white matter stroke model developed in the mouse would provide the added advantage that mouse genetic tools can be applied to the labeling and molecular analysis of the cells involved in white matter stroke and repair.

In this report we describe a subcortical stroke model developed in the mouse by using the vasoconstrictor peptide endothelin-1 (ET-1). ET-1 is not directly neurotoxic (Nikolov et al., 1993) and produces local vasoconstriction and loss of blood flow for up to three hours at the injection site (Fuxe et al., 1992; Hughes et al., 2003). The regulation of regional blood flow by ET-1 has been used to produce several different large artery, focal cortical or striatal infarcts. Focal injection of ET-1 into the posterior limb of the internal capsule in the rat produces a small infarction resembling a lacune (Frost et al., 2006; Lecrux et al., 2008). In the present study, ET-1 was microinjected into the subcortical white matter of the frontal lobe of the mouse, and the patterns of cell death, inflammation, gliosis, axon and myelinated fiber loss and glial progenitor responses were determined using immunohistochemical, tract tracing and electron microscopic techniques. This model produces a focal necrotic cavity in subcortical white matter and an adjacent area of axonal damage, myelin loss and oligodendrocyte gliogenesis.

2. Material and methods

2.1. Animals

All experiments were performed in accordance with National Institutes of Health animal protection guidelines and were approved by the University of California at Los Angeles Animal Research Committee. Two-month old male C57/BL6 mice (Charles-River, Shrewesbury, MA, 22–25 g) were used in this study. For axonal fiber labeling adult male YFP-H mice were used (Jackson Laboratories, Bar Harbor, ME, stock number 003782). This line expresses the fluorescent protein YFP in a soluble form that fills the entire cellular architecture of a subset of layer V and some layer II/III pyramidal neurons (Feng et al., 2000). Cohorts of animals ($n = 5$–7 per group) survived to 1, 3, 7, 14 and 28 days after stroke. Two cohorts of YFP-H mice ($n = 5$) survived to 7 and 28 days. For both wild type C57BL/6 and YFP-H mice, a cohort of unoperated control animals was processed in parallel ($n = 5$–7).

2.2. Surgical procedure and tissue processing

Mice were anesthetized with 2% isoflurane in 2:1 N_2O:O_2, and placed in a stereotaxic apparatus. Temperature was maintained at 36.5–37.5 °C using a rectal probe and heating pad. Pulled glass micropipettes (tip diameter 15–25 μm) were filled with ET-1 (Bachem, Torrance, CA; 1 μg/μL in sterile physiological saline), attached to pressure pump (Picospritzer II, General Valve, Fairfield, NJ) and mounted in a stereotaxic arm. A craniotomy was performed over the sensorimotor cortex overlying the injection sites, and the pipette containing the ET-1 was inserted through the cortex into the underlying white matter at an angle of 36° in order to minimize cortical damage. Three injections (each of 120 nL ET-1 solution) were made, targeting subcortical white matter below forelimb motor cortex (Paxinos and Franklin, 2001): AP + 0.52, ML + 0.15, DV − 2.3; AP + 0.88, ML + 0.15, DV − 2.3; AP + 1.24, ML + 0.15, DV − 2.3. The pipette was left *in situ* for 5 min post-injection to allow proper diffusion. After the post-surgery survival period, each mouse was given a lethal dose of sodium pentobarbital and perfused transcardially with 0.1 M phosphate buffered saline followed by 4% paraformaldehyde. The brains were removed, postfixed overnight in 4% paraformaldehyde and cryoprotected for 2 days in 30% sucrose. Subsequently brains were removed and frozen. Coronal tissue sections of 50 μm were prepared using a cryostat (Leica CM 0530). Adjacent series were cut and processed for immunohistochemistry, Nissl staining or cell death studies.

2.3. BDA retrograde labeling

A separate cohort of mice ($n = 5$) was given 25 mg of the neuroanatomical tracer biotinylated dextran amine (BDA, 10,000MW, Invitrogen, Carlsbad, CA) dissolved in 250 μL of saline along with ET-1 (1:1). BDA is taken up directly into neuronal cell bodies, but is only taken up by damaged axons (Veenman et al., 1992). Mice were sacrificed 7 days after stroke with paraformaldehyde fixation as above. The number of retrogradely labeled neurons from the BDA was determined in six-50 μm coronal sections spaced 175 μm apart through the stroke site.

2.4. BrdU pulse-chase

In a separate cohort, mice received bidaily intraperitoneal injections of BrdU (Sigma, 50 mg/body weight in sterile saline) for one week after ET-1 injection and were sacrificed at days 7 and 28 (early and late time points respectively, $n = 3$ for each time point). No-stroke control animals received the same BrdU pulse and euthanized at the same time points. The number and phenotype of BrdU incorporated cells were determined by stereology and immunohistochemistry.

2.5. MRI

Mice were anesthetized and placed in a Bruker 7T small animal MRI (Bruker Biospin, Switzerland). MRI imaging was performed on days 1, 2 and 8 after stroke. Respiratory rate was monitored throughout the procedure and body temperature was maintained at 37 ± 0.5 °C. A T2-weighted image set was acquired: rapid acquisition relaxation enhancement factor 8, repetition time 5357 ms, echo time 15.50 ms with an in-plane resolution of 0.086_0.172_0.35 mm with 39 contiguous slices.

2.6. Immunohistochemistry

Single and double label fluorescent immunohistochemistry was performed on free-floating sections (Ohab et al., 2006; Carmichael et al., 2008). Briefly, sections were rinsed in phosphate buffered saline (PBS), blocked in 5% donkey serum, incubated in primary antibodies for 1–4 days at 4 °C, rinsed in PBS, incubated in secondary antibodies for one hour at room temperature, rinsed in PBS, mounted on slides and air-dried, and taken through ascending alcohols and xylene and coverslipped. For BrdU/NG2 and BrdU/transferrin double labeling, the sections were incubated in NG2 or transferrin primary antibody followed by 30 min 2N HCl incubation at 37 °C and 30 min neutralization in 0.1 M sodium borate buffer at room temperature. The sections were blocked again and incubated in anti-BrdU primary antibody followed by secondary antibody incubation. All secondary antibodies were donkey F(ab)2 fragments conjugated to cy2 or cy3 (Jackson Immunoresearch, West Grove, PA) and were used at a dilution of 1:200. Primary antibodies were: rat anti-myelin basic protein (1:800, Carlsbad, CA), rabbit anti-myelin basic protein (MBP)(1:200, Abcam, Cambridge, MA), mouse anti-NeuN (1:500, Abcam), rat anti-GFAP (1:1000, Invitrogen), sheep anti-carbonic anhydrase II (1:600, Morphosys, Germany), sheep and rat anti-BrdU (1:500, Abcam), rabbit anti-transferrin (1:75, Abcam), mouse anti-apoptosis inducing factor (1:200, AIF, Santa Cruz Biotechnology, Santa Cruz, CA), mouse anti-activated Poly(ADP-ribose)polymerase 1 (PARP, 1:100, Cell Signaling, Danvers, MA), rabbit anti-NF200 (1:2000, Sigma, St. Louis, MO), mouse anti-SMI31 and anti-SMI-32 (1:1000, Abcam), rabbit anti-NG2 (1:200, Invitrogen); goat

anti-transferrin (1:100, MP Biomedicals, Solon, OH), rabbit anti-IBA1 (1:1000, Wako Chemicals, Richmond, VA) and NeuN (1:500). Control sections were run in parallel with each experiment in which the primary antibody or antiserum were omitted. For glial scar assessment, levels of astrocyte-secreted extracellular matrix polysaccharide hyaluronic acid (HA) were compared between stroke and non-stroke samples (Back et al., 2005). Hyaluronan was visualized with biotinylated hyaluronan binding protein (HABP) (1:50, Associates of Cape Cod, East Falmouth, MA) and then streptavidin-Cy3 (1:100 Jackson Immunoresearch).

2.7. Stereology and statistics

Brdu/NG2 and BrdU/transferrin double labeled cells were stereologically quantified (Ohab et al., 2006) using the optical fractionator probe on a system with a digitizing x/y/z motorized stage, Leica DMLB microscope (Leica Microsystems, Wetzlar, Germany) and neuroanatomical quantification software (Stereoinvestigator, MBF Bioscience, Williston, VT). A counting area was drawn to include all of the subcortical white matter from a point above the lateral most part of the lateral ventricle to the point at which the subcortical white matter sweeps around the lateral one-half of the striatum. For BrdU counts, 5 serial sections spaced 250 μm apart were counted through the lesion. All tissue sections were initially analyzed with observer blinded to the experimental condition. Means ± standard deviations for BrdU/NG2 and BrdU/transferrin in 7 vs. 28 days were compared with two-sample *t* test assuming equal variances (Excel, Microsoft, Redmond, WA). For quantification of retrogradely labeled neurons in the BDA:ET-1 co-injection brains, 6 serial sections spaced 175 μm apart were used through the stroke site. Similarly, the total number of neurons (NeuN stain) in the same cortical areas was determined in 3 animals and averaged to estimate the ratio of disconnected tracts.

2.8. Cell death detection

Apoptotic cell death was detected with immunohistochemical stains for apoptosis inducing factor (AIF) and caspase-cleaved (activated) PARP, which are indicators of intracellular caspase activity (Mehta et al., 2007). Additionally, double stranded DNA nicked cells, characteristic of apoptosis (van Dierendonck, 2002), were identified with *in situ* nick translation (EMD Biosciences, Gibbstown, NJ), and modified for free-floating sections with a reduction in proteinase K (0.12 μg/mL). Stained cells were counted in 11 tissue sections through the stroke site using the same counting area with the same microscope system as for immunohistochemical staining.

2.9. Confocal microscopy

100× confocal images were acquired using a Leica DM-IRBE (TCS-SP). For all images, z-sections and z-steps ranged between 0.5 and 1 μm. Images were subsequently processed using Leica Lite software or Adobe Photoshop/Illustrator (Adobe Systems).

2.10. Electron microscopy

Mice were perfused at 1–7 days after stroke ($n = 2$ each time point) with buffered 4% paraformaldehyde and 1% glutaraldehyde solution. Brains were post-fixed in the perfusion fixative overnight. Cerebral hemispheres were sectioned into 1 mm thick tissue blocks in the frontal plane and processed for electron microscopy. In short, sections were osmicated in a 1% osmium tetroxide solution, dehydrated in ethanol, and plastic-embedded in Epon. Semithin sections were cut, stained with toluidine blue, and examined in the light microscope. Sections demonstrating subcortical areas affected by ischemia were trimmed, and serial ultramicrotome sections (60–70 nm) were collected on formvar-coated one-hole copper grids. The ultrathin sections were next counterstained using uranyl acetate and lead citrate, and examined in a JOEL 100 CX transmission electron microscope.

3. Results

3.1. Overview of small ischemic stroke in frontal subcortical white matter

Subcortical white matter strokes are located in characteristic regions of the frontal and parietal lobes in humans. These lesions produce hyperintensities and/or focal cavities on MRI (Fig. 1A), myelin pallor and cell loss. Fig. 1A illustrates a recent subcortical white matter stroke in a patient, which occurs within a region of previous strokes. To model this disease process in mice, focal microinjections of the vasoconstrictor ET-1 was placed into subcortical white matter below the frontal cortex. The injection needle was angled so as to not directly manipulate or pass through the cortex above the stroke site. Three injections of 120 nL ET-1 at 1 μg/μL were made, spaced 300–400 μm apart in the A/P plane so as to extend the stroke core within the subcortical white matter in the mouse. The specific volume and concentration of ET-1 to be used were determined through preliminary studies. ET-1 solution is saturated at 1 μg/μL in saline. Of note, larger volumes resulted in difficulty in arousal from the effects of anesthesia and subsequent death of the animal. On the other hand, more dilute ET-1 solutions or smaller volumes did not produce a significant infarct. Following ET-1 injection, MR imaging in the mouse shows a hyperintensity in subcortical white matter and a small region of dorsolateral striatum, similar in location to common sites of human subcortical stroke (Fig. 1B). In this stroke model, the MRI signal is maximal at day 2 and diminished by day 8 after ET-1 injection.

Nissl stains at 7 days after the injection indicate that the focus of damage is in the subcortical white matter (Fig. 1C). A small cavity is present that is surrounded by a glial reaction. There is some neuronal loss and increase in glial density in the deep cortical layers directly above the lesion and in the very superficial aspect of the dorsolateral striatum below the white matter lesion (Fig. 1C). Notably, vehicle-only injection controls did not show any damage in the white matter, ruling out the possible mechanical damage that microinjections can produce. For that reason, the vehicle-only control brains are interchanged with mouse brains with no injection (unoperated non-stroked controls) for these studies.

In order to visualize the axonal fibers directly within the stroke region and assess the injury, ET-1 was injected into the YFP-H mouse line. The contralateral hemisphere to the injection site displays the same axonal anatomy as control non-injected mice: the subcortical white matter is filled with dense fascicles of axons, some coursing through the subcortical white matter and down through the striatum to subcortical targets (Fig. 1D, left). 7 days after subcortical white matter stroke, axons are clearly lost within the stroke cavity. Fewer axons penetrate through the striatum toward subcortical targets. Axonal retraction bulbs, visible as bright globular accumulations of YFP in dystrophic fiber endings, are present on medial and lateral sides of the stroke center (Fig. 1D, right). These cellular and fiber responses to this stroke are explored in greater detail in each subsequent section.

3.2. Cell death

Cell death after focal injection of ET-1 into subcortical white matter was tracked with immunohistochemical stains for nuclear AIF, activated PARP and *in situ* nick translation. Nuclear AIF and PARP immunoreactive cells are present as small cells, arranged in large

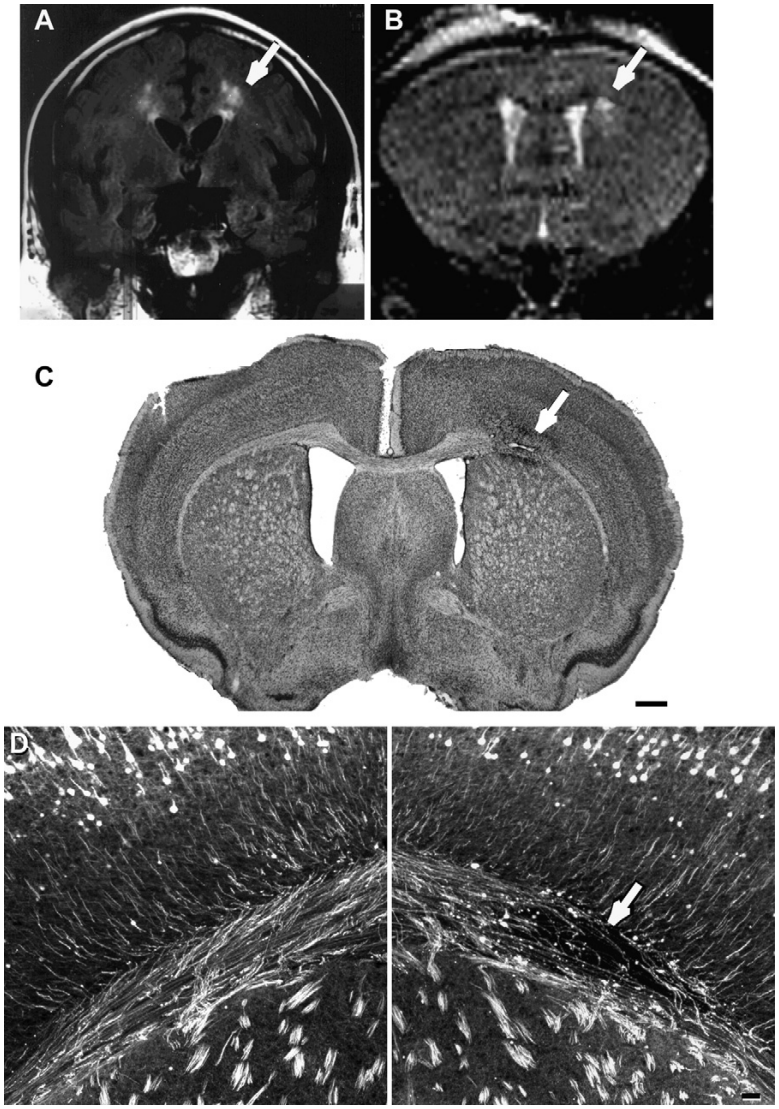

Fig. 1. Human and mouse subcortical white matter stroke. (A) Human FLAIR sequence MRI taken 2 days after left hemispheric subcortical stroke. Arrow denotes white matter hyperintensity that was new in comparison to previous scans from this patient. Case is taken from clinical service of the authors (STC). (B) Mouse MRI taken 2 days after ET-1 injection. Arrow denotes hyperintensity caused by stroke. (C) Nissl staining of subcortical white matter 7 days after stroke. Note small cavity in white matter and adjacent increase in cellularity. (D) White matter stroke in YFP-H mouse line. Left panel is contralateral and white matter is ipsilateral to the stroke 7 days after ET-1 injection. Arrow denotes infarct core, with loss of axons. Note bright axon retraction bulbs in fibers adjacent to the lesion. Bar in (C) = 350 μm. Bar in (D) = 60 μm.

clumps in the center of the lesion site. In white matter adjacent to the lesion site, AIF and PARP positive cells are present in linear rows that extend several hundred microns distant to the lesion site, resembling interfascicular oligodendrocytes (Fig. 2B and D). AIF and PARP immunoreactive cells are maximal in number at day 1 after stroke. Only occasional AIF nuclear immunoreactivity and PARP immunoreactive cells are present at day 3 and none are observed after this time point. AIF and PARP immunoreactivity co-localizes with cell phenotype markers for oligodendrocytes, including carbonic anhydrase II (Fig. 2C, Supplementary Fig. 1) and transferrin. There is a reduced number of CAII and transferrin immunoreactive cells in subcortical white matter and deep cortical layers apparent at days 7 and 14 after ET-1 injection (Fig. 2E). A small number of GFAP immunoreactive astrocytes co-localize with activated PARP or AIF

Fig. 2. Cell death in white matter one day after stroke. (A) Immunohistochemical staining for AIF in contralateral hemisphere. (B) AIF stain in the hemisphere ipsilateral to stroke. Note positive cells in white matter and deepest cortical layers, and linear rows of AIF immunoreactive cells (arrows). (C) CAII stain for oligodendrocytes (green) activated PARP immunoreactivity (red). Note multiple CAII and activated PARP double positive cells in subcortical white matter (D) *In situ* nick translation showing double stranded DNA nicking in apoptotic cells in subcortical white matter. (E) Transferrin immunoreactive oligodendrocytes in control subcortical white matter region. (F) Transferrin immunoreactive oligodendrocytes 7 days after subcortical white matter stroke. (G) NG2 immunoreactive OPCs in control subcortical white matter region. (H) NG2 immunoreactive OPCs 14 days after subcortical white matter stroke. ctx = cortex, str = striatum, wm = subcortical white matter. Bar in (B) = 50 μm and applies to (A and B); bar in (Cand D) = 40 μm, Bar in (F) = 20 μm and applies to (E–H) (for interpretation of the references to color in this figure legend, the reader is referred to the web version of the article).

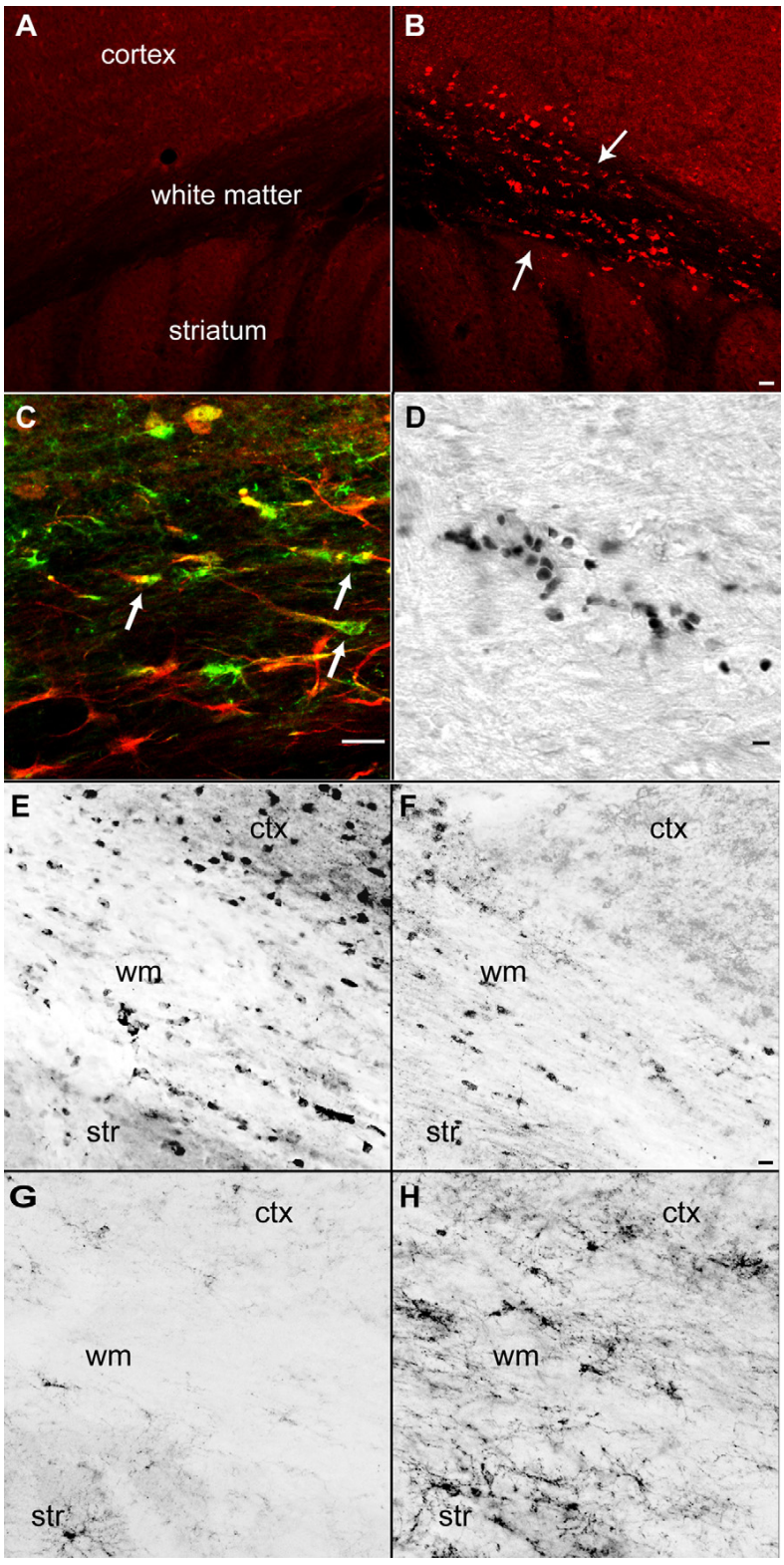
A
cortex
white matter
striatum
B
C
D
E
ctx
wm
str
F
ctx
wm
str
G
ctx
wm
str
H
ctx
wm
str

at the lesion site. To quantify apoptotic cells during their maximal occurrence, the number of stained cells in *in situ* nick translation (Fig. 2D) was counted through the lesion site in subcortical white matter 1 day after ET-1 injection: 195 cells ± 76 ($n = 5$). There are no positive cells in the control white matter.

3.3. *Inflammation, reactive gliosis*

Immunohistochemical staining for GFAP and IBA-1 was used to localize astrocyte and microglial/macrophage immunoreactive cells to ET-1 injections. In control brains, GFAP immunoreactive cells are present in the medial subcortical white matter, within the corpus callosum and that portion of the subcortical white matter dorsal to the subventricular zone (Fig. 3A). There is no change in this distribution or staining intensity of GFAP at day 1 after injection. Beginning at day 3 and reaching a maximal intensity at day 7, densely stained GFAP positive cells fill the subcortical white matter, deep cortical layers and superficial dorsolateral striatum (Fig. 3B). The GFAP positive fibers tend to run parallel to white matter fiber tracts. At 14 and 28 day time points the intensity of immunoreactivity for GFAP declines slightly but the distribution of GFAP positive cells remains the same. Tissue incubation with hyaluronic acid

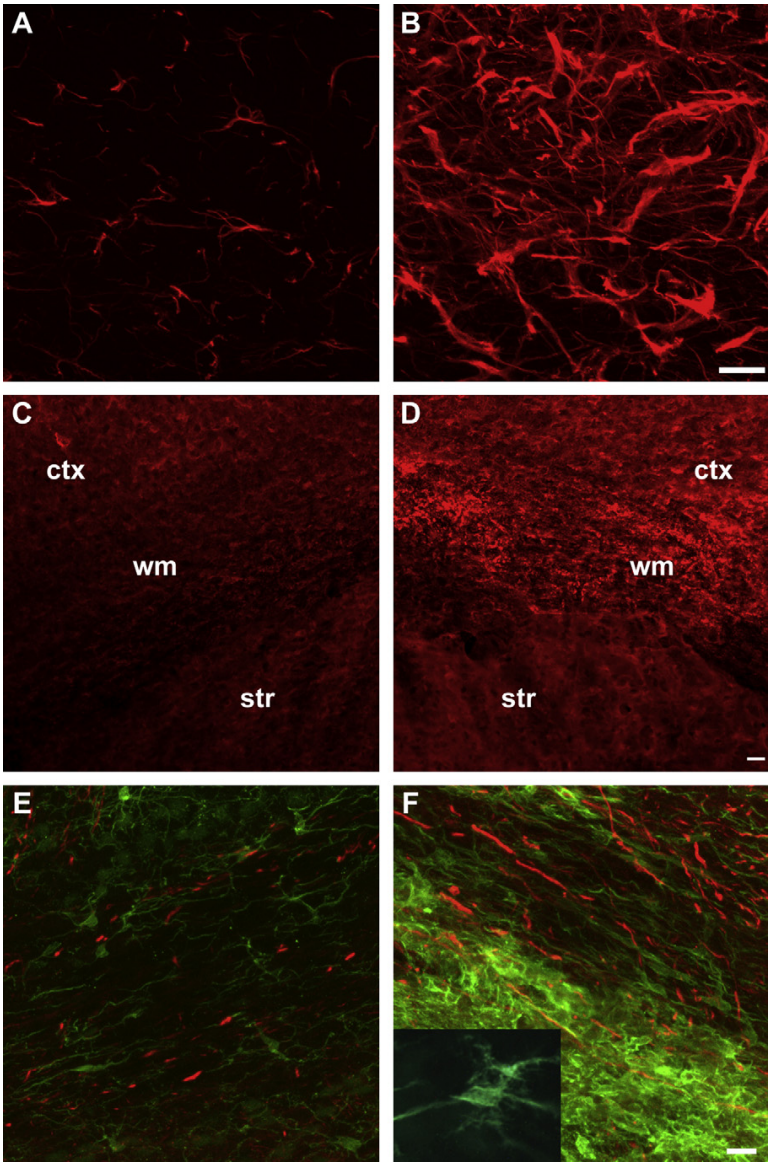

Fig. 3. Glial and inflammatory responses to white matter stroke. (A) GFAP immunoreactivity in subcortical white matter on control brains. (B) GFAP immunoreactivity in subcortical white matter 7 days after stroke. Hyaluronic acid labeling with HABP in subcortical white matter (C) in control brain and (D) in peri-infarct area 7 days after stroke. (E) SMI-32 immunoreactive axons (red) and IBA-1 immunoreactive microglia/macrophages (green) in contralateral subcortical white matter. (F) SMI-32 positive fibers (red) and IBA-1 positive microglia/macrophages (green) 7 days after stroke. Inset shows a high power view of IBA-1 positive activated microglia. Bar in (B) = 40 μm and applies to (A and B); Bar in (D) = 40 μm and applies to (C and D); Bar in (F) = 40 μm and applies to (E and F) (for interpretation of the references to color in this figure legend, the reader is referred to the web version of the article).

binding protein (HABP) localizes HA in the brain, and is maximal around the stroke cavity and closely associated with GFAP positive cells at day 7 after ET-1 injection (Fig. 3D). There is also an increase in HA labeling in the contralateral subcortical white matter. In control brains, there is low IBA-1 immunoreactivity. Faintly IBA-1 positive cells are localized predominantly in the cortex and striatum but are sparse in white matter of non-stroke control brains (Supplementary Fig. 2A). Unlike astrocyte activation, microglia activation takes place without a delay beginning on day 1 after stroke. Strongly IBA-1 positive microglia, displaying the characteristic ramified appearance of the activated state, fill the subcortical white matter ipsilateral to stroke (Supplementary Figs. 2B and 3F). IBA-1 immunoreactive cells increase up to day 7 after injection, and are associated with SMI-32 immunoreactive injured axons (Fig. 3F, see below). Interestingly, some activated microglia are found in contralateral hemisphere as well (Fig. 3E).

3.4. Axonal fiber and myelin loss

Immunohistochemical staining for neurofilament proteins and myelin basic protein identifies patterns of axonal and myelin damage over the first month after ET-1 injection. 1 day after ET-1 injection there is a small stroke core in the center of the injection site with loss of immunoreactivity for phosphorylated heavy chain neurofilament proteins, NF200 and SMI-31. This pattern of neurofilament staining remains unchanged until 14 days after the injection, after which there is a progressive decrease in NF200 and SMI-31 staining around the stroke site in the subcortical white matter (Fig. 4D and F). MBP is also lost in a small initial area in the center of the stroke at 1 day, and later develops into a larger region of diminished MBP staining from day 14 to day 28 (Fig. 4B and F). However, the region of diminished MBP staining is larger than the region of axonal neurofilament loss: the peripheral or peri-infarct zone around the stroke cavity contains areas in which NF200 and SMI-31 staining is present, but MBP is diminished (Fig. 4F and H). This mismatch of axonal and myelin staining patterns is not seen in control white matter or white matter contralateral to the stroke site (Fig. 4E and G). Additionally, stroke samples were assayed for SMI-32 immunoreactivity, which detects dephosphorylated neurofilament protein found in areas of axonal injury. At 7 days after stroke, there is an increase in SMI-32 immunoreactive fibers at the margins of the stroke site, in a zone above the striatum and just below the cortex. These fibers localize to an area of dense microglial/macrophage activity (Fig. 3F). Whereas, only a few SMI-32 immunoreactive fibers are present in subcortical white matter of control or contralateral brains (Fig. 3E).

Axonal profiles were also examined in the YFP-H mouse line and through electron microscopic observation. At 7 days after stroke, axons are lost in the stroke core (Figs. 1C and 5B). At the margins of the core, dystrophic axon bulbs are seen. Axons can be followed to directly end in these bulbs, or individual axons contain multiple large, bulb-like swellings (Fig. 5C and D). The fascicles of corticofugal axons that penetrate the striatum to eventually form the corticospinal, corticothalamic and corticobulbar tracts also contain groups of degenerating axons, with large dystrophic swellings at end of enlarged and irregular axons (Fig. 5C). At the ultrastructural level, a subset of axons at 1 day after stroke appears dark with electron dense axoplasm at the stroke site (Fig. 5E), a sign of early axonal damage. At 7 days after the stroke, there are large fields of degenerating axonal profiles with disintegrating myelin sheaths. Cells with ultrastructural characteristics of microglia are often found in close physical proximity to degenerating axons (Fig. 5F), corresponding to the observed association of microglia with injured axons in the IBA-1 and SMI-32 staining (Fig. 3F).

3.5. Neuronal circuits affected by subcortical white matter stroke

This stroke is produced in subcortical white matter below forelimb motor cortex. This region of the subcortical white matter contains fascicles of axons projecting from overlying cortex to con-

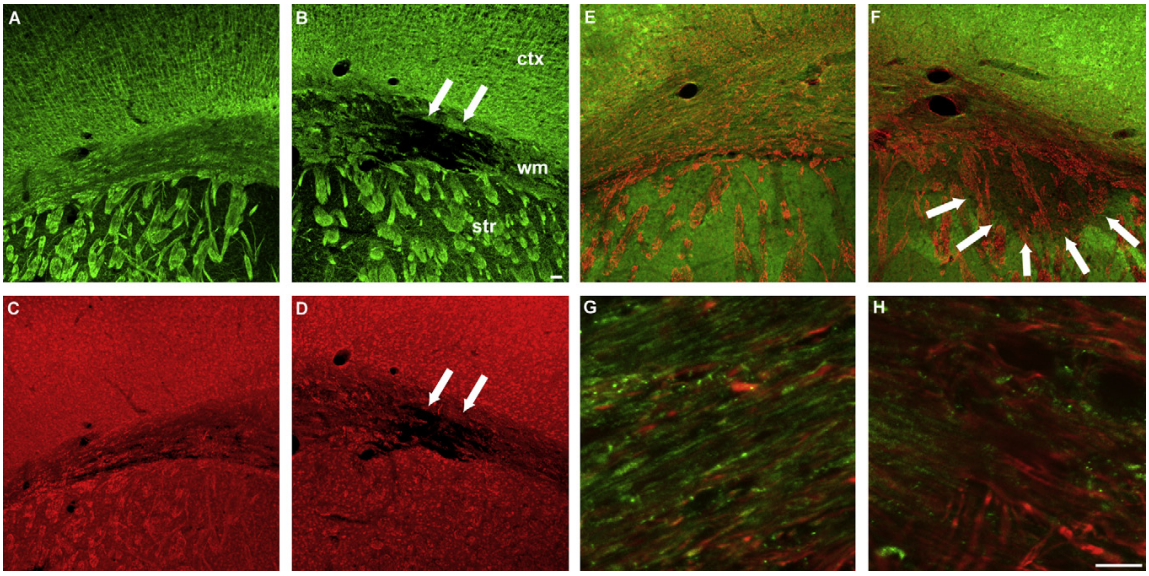

Fig. 4. Axonal and myelin damage after subcortical stroke. (A and B) MBP immunoreactivity contralateral (A) and ipsilateral (B) to stroke at 28 days after the infarct. Note area of stroke seen as a loss of myelin in a hole in subcortical white matter (arrows). (C and D) Neurofilament immunoreactivity contralateral (C) and ipsilateral (D) to stroke in same section as (A and B). The stroke site is apparent as an area of neurofilament/axonal loss (arrows). (E and F) MBP and SMI-31 stain of myelin and neurofilament patterns in contralateral (E) and ipsilateral (F) subcortical white matter 7 days after stroke. Arrows in (F) highlight the area of diminished MBP staining and preserved axonal filament staining. (G and H) High power views of peri-infarct white matter 7 days after stroke. In contralateral white matter (E) axons (red) are closely associated with myelin staining (green). At the stroke site axonal profiles (red) are present in areas of diminished myelin staining. Bar in (B) = 40 μm and applies to (A–F). Bar in (H) = 40 μm and applies to (G and H) (for interpretation of the references to color in this figure legend, the reader is referred to the web version of the article).

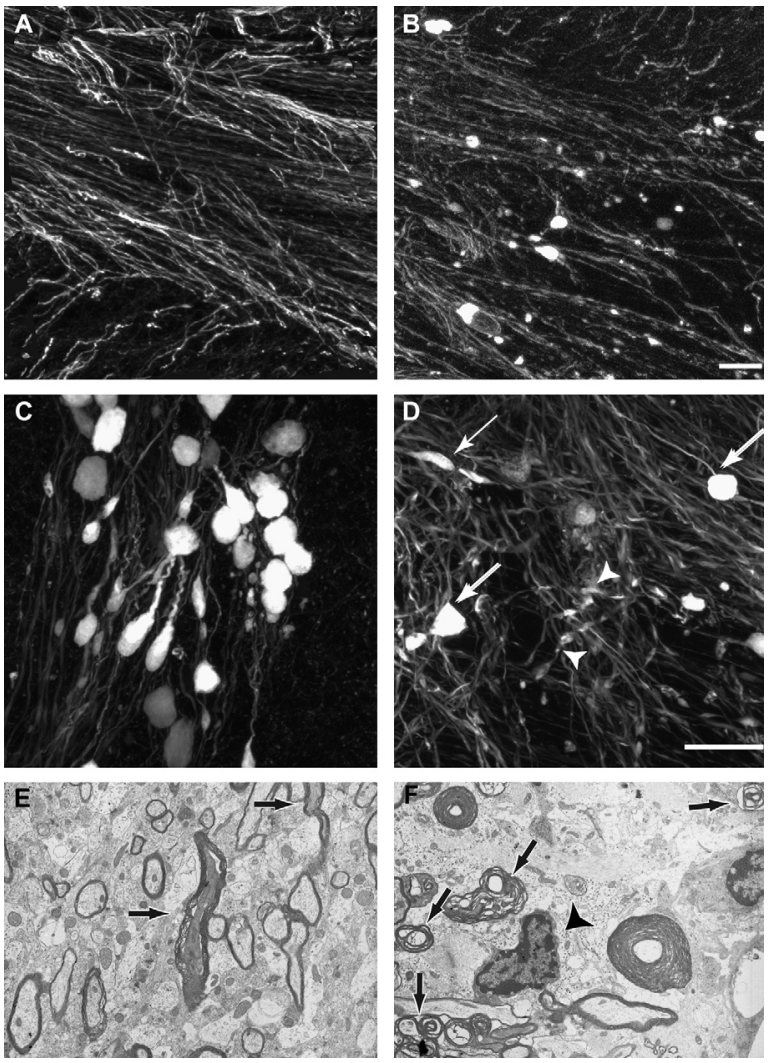

Fig. 5. Axonal damage from ischemic white matter stroke. (A–D) Sections taken from YFP-H line 7 days after stroke. (A) Normal subcortical white matter contains multiple linear axons and axon fascicles. (B) Seven days after white matter stroke axons have dropped out leading to fewer labeled axons in subcortical white matter. Damaged axons contain retraction bulbs seen as bright varicosities. (C) Higher power view of damaged axons and retraction bulbs present in white matter projections through the striatum below the stroke site. (D) Higher power view of retraction bulbs and beaded axons (arrows) in subcortical white matter. (E and F) Electron micrograph of subcortical white matter 1 day after stroke (E) and 7 days after stroke (F). Arrows in (E) show injured axons with electron dense cytoplasm. Arrows in (F) show degenerating axons with vacuoles and separated and fragmented myelin sheaths. Arrowhead in (F) shows cell with microglial morphology adjacent to degenerating axon EM images taken at 4800×. Bar in (B) applies to (A and B) = 40 μm; Bar in (D) applies to (C and D) = 40 μm.

tralateral cortex and subcortical projections from the overlying cortex to striatum, thalamus, brainstem and spinal cord. To map the connections that are damaged by this stroke, the neuroanatomical tracer BDA was co-injected with ET-1. Neurons retrogradely labeled by a BDA injection into subcortical white matter represent cells with damaged axons at the stroke site. However, because of the very limited spatial extent of the subcortical white matter in the mouse, some of the injected BDA was placed into the most superficial aspect of the dorsolateral striatum. There was no difference in the character of the induced stroke between BDA/ET-1 injection and ET-1 alone. BDA-labeled neurons are present in layers II/III and V/VI in cortical areas ipsi- and contralateral to the stroke site (Fig. 6). Neurons are labeled in forelimb and hindlimb somatosensory and motor cortex and whisker (barrel field) somatosensory cortex. Within cortex a mean of 1024 ± 41 neurons are labeled per animal, approximately 0.7% of the cortical neurons from this region. The total number of neurons in the corresponding sections is determined by NeuN staining (total $150{,}995 \pm 6277$ neurons, $n = 3$). The largest single collection of cells that project through the stroke site is in layer V of overlying frontal motor cortex (Fig. 6).

3.6. Glial progenitor responses

In animal models of multiple sclerosis, inflammatory white matter lesions produce a limited regenerative response from OPCs, which divide and differentiate into oligodendrocytes. Staining for the OPC marker NG2 indicates a progressively larger and more intensely stained cell population in white matter stroke, beginning

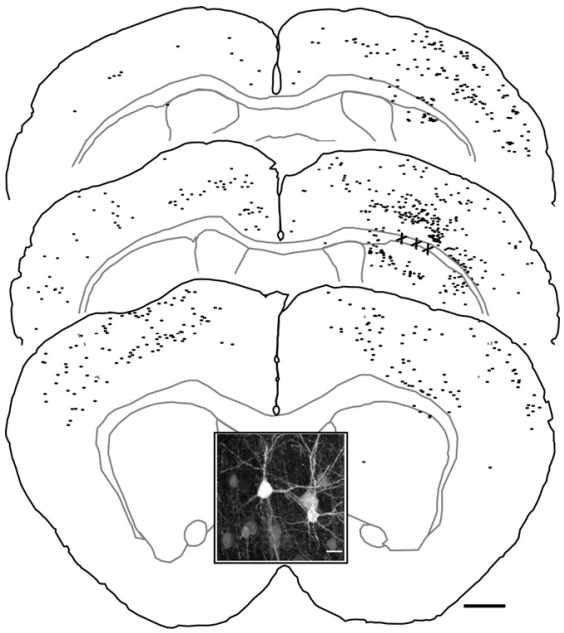

Fig. 6. Neuronal projections through stroke site. Line drawings are from digitized maps of labeled cells from a co-injection of the anatomical tracer BDA with ET-1. The sites of the stroke and BDA injections are indicated with X. The dots represent cells that were retrogradely labeled from the stroke site. Bar = 350 μm. The inset is a high magnification photomicrograph of labeled neurons from the BDA injection. Bar in inset = 20 μm.

at day 3 and progressively increasing to day 14 (Fig. 2G and H). To determine if OPC proliferation occurs in subcortical white matter stroke, mice were administered BrdU for one week after ET-1 injection and sacrificed at days 7 and 28 time points in the early and late phases of neuropathological change in this stroke model. The BrdU pulse-labeling also allowed a preliminary assessment of the fate of these progenitors, as the progeny of the BrdU incorporated cells can be phenotyped by cell-specific markers and their numbers can be compared between time points. BrdU injection through the first week after stroke labeled a population of dividing OPCs that is maximal at day 7 after the stroke, and then declined by day 28 (BrdU/NG2 7 day vs. 28 day 3918.33 ± 238.03, 2150.0 ± 413.54, $p = 0.003$, Fig. 7B). A similar pattern was observed in BrdU incorporated oligodendrocytes, which are products of differentiated BrdU labeled OPCs (BrdU/transferrin 7 day vs. 28 day 3665.0 ± 456.54, 1941.67 ± 677.98, $p = 0.02$, Fig. 7B). Whereas, BrdU administration to the no-injection control mice resulted in BrdU incorporation limited to the SVZ and dentate gyrus. Populations of BrdU/NG2 and BrdU/transferrin cells were randomly selected in several sections and examined with high magnification confocal microscopy and *z* plane reconstruction to confirm that double-labeling was indeed due to colocalization (Fig. 7 A).

4. Discussion

The animal modeling of human stroke subtypes is limited by the lack of a suitable *in vivo* model for subcortical white matter stroke. The available stroke models of large vessel occlusion mostly affect a combination of gray matter and white matter by infarcting much of the cerebral hemisphere, or selectively target striatum or cortex (Carmichael, 2005). These approaches do not provide the specific, isolated white matter infarct that is seen in human subcortical or lacunar strokes. Although the mechanisms of cellular injury in response to ischemia can been studied in *in vitro* white matter preparations, this approach fails to reflect the diverse cellular involvement in cell death and repair mechanisms that occur *in vivo*. Models of subcortical white matter in the mouse would further take advantage of the molecular genetic approaches in this species that allow specific studies of cell types and molecular mechanisms involved in injury and repair. With these issues in mind, an important initial question arises in developing a mouse model of white matter stroke: what type of white matter ischemia should be modeled?

White matter ischemia in humans can be classified into several categories based on imaging and neuropathological findings. Lacunar infarctions result from occlusion of perforating vessels and produce a small stroke cavity on pathology and in MRI (Lammie, 2002; Matsusue et al., 2006). These strokes may cause clinical lacunar syndromes, such as pure motor stroke or hemisensory loss, or may be clinically silent. Lesions without a true stroke cavity appear as subcortical white matter hyperintensites on MRI, and myelin and axon loss and diminished oligodendrocyte staining in pathological studies (Matsusue et al., 2006; Kim et al., 2008). These have also been implicated in lacunar syndromes, but more often are individually asymptomatic and accumulate to produce global cognitive dysfunction (Vinters and Carmichael, 2008). Recent prospective studies indicate these two lesions, subcortical lacunar stroke and subcortical white matter hyperintensities, may represent a spectrum of the same process of subcortical small vessel ischemia (Gouw et al., 2008), although this idea is still controversial (Wardlaw, 2008). This spectrum of subcortical stroke, from a frank infarct cavity to an area of incomplete axonal and myelin damage, is supported by neuropathological grading scales of subcortical stroke, which note a range of cell death and white matter destruction from a true stroke cavity to an area of myelin, axon and oligodendrocyte loss (Lammie, 2002; Udaka et al., 2002; Kim et al., 2008). The present studies indicate that ET-1 injection into subcortical white matter of the mouse models the disease spectrum of lacunar stroke-incomplete white matter damage.

4.1. ET-1 induced ischemia results in focal white matter infarct with secondary myelin and axonal damage

The observed focal white matter infarct contrasts with other recently utilized white matter ischemia models. The model of bilateral common carotid occlusion produces a chronic, diffuse white matter ischemia, however it is maximal in the optic nerve, and also produces patchy neuronal cell death in hippocampus and retina (Pappas et al., 1997). Recent reports of ET-1 injection in white matter tracts of the rat also show white matter infarct cavities (Frost et al., 2006; Lecrux et al., 2008). In one of these models, ET-1 injection into the rat results in a behavioral deficit (Frost et al., 2006). In the present model, there was no obvious forelimb motor deficit on gross observation after a 3-day period from the infarct (unpublished observations). However, this model has the advantage that the extensive array of mouse genetic tools can be applied to the study of mechanisms of white matter cell death and repair. In a careful study of ET-1 effects in mouse, Steinberg and colleagues recently reported the ET-1 injection into the mouse did not produce consistent cerebral infarctions (Horie et al., 2008). This finding varies from the present results, where evidence for cell death and white matter damage were noted across eight different measures of death or damage and through electron microscopic analysis. A major difference between the present study and Horie et al. is that in the present technique ET-1 was slowly pulsed directly into white matter using a very fine glass micropipette, along an axis of white matter axonal cylinder diffusion and not through a vertical approach. This may have allowed local ET-1 concentrations

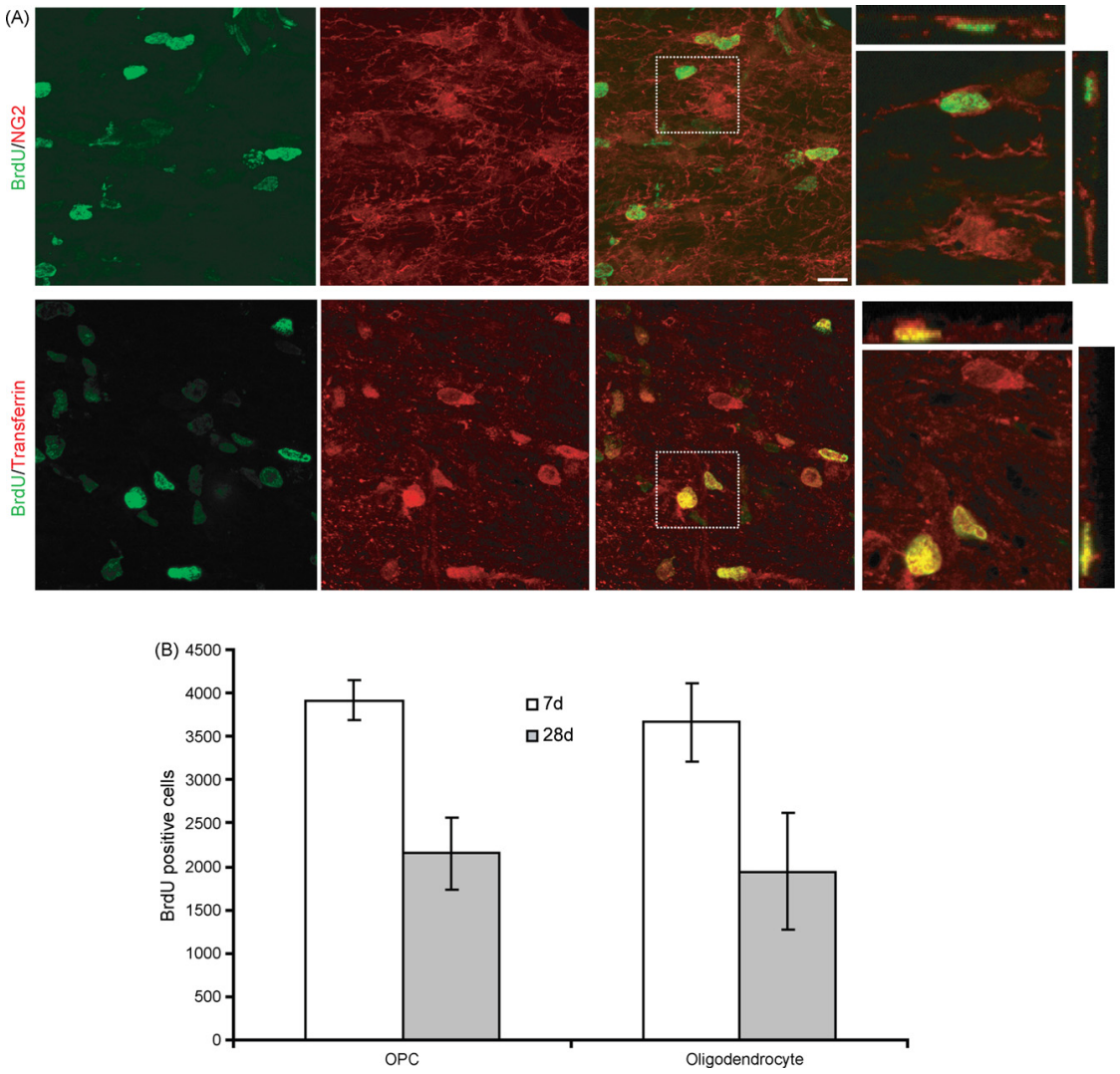

Fig. 7. Early and late response of OPCs and oligodendrocytes following subcortical stroke. BrdU pulse-chase experiment at day 7 and 28 after subcortical stroke. (A) Representative images of BrdU double labeling of oligodendrocyte progenitor cells (OPC) with OPC marker NG2 (top panel), and oligodendrocytes with specific marker transferrin (bottom panel) at day 7. The insets correspond to higher power views. Bar in right middle panel of A = 20 μm. (B) Total number of double labeled cells estimated by stereology: means ± standard deviations. NG2 7 day vs. 28 day 3918.33 ± 238.03, 2150.0 ± 413.54, $p = 0.003$; transferrin 7 day vs. 28 day 3665.0 ± 456.54, 1941.67 ± 677.98, $p = 0.02$.

to remain at a vasoconstricting level for longer. This is supported in the studies in which the tracer BDA was co-injected with ET-1, as staining for BDA indicate diffusion along white matter fascicles within the short distance of the subcortical region below motor cortex.

Following the white matter infarct, secondary axonal and myelin degeneration takes place around the stroke site. Initially, axons are lost in the infarct core. Subsequently, degenerating axonal fibers form dystrophic "end bulbs" in subcortical white matter adjacent to the core and in white matter tracts that extend from the stroke site through the striatum. This stroke thus disconnects widespread neuronal circuits in bilateral sensory and motor cortical areas. The size of the stroke, as evidenced by neurofilament staining, grew over the first month after the ET-1 injection. This may be due to the turnover time of damaged neurofilaments (Millecamps et al., 2007), but it may also represent a potentially treatable evolving degeneration in hypomyelinated and vulnerable peri-infarct axons. Myelin degeneration is evidenced by loss of myelin staining in the infarct core as well as the peri-infarct zone, and separating myelin sheaths observed in electron microscopy preparations. However, regions of peri-infarct white matter display a relative preservation of axonal profiles in regions of diminished myelin staining. This has been reported in a pig model of subcortical stroke (Tanaka et al., 2008) and in pathological study of human ischemic white matter disease (Lammie, 2002; Kim et al., 2008). Similarly, in longitudinal prospective studies of subcortical white matter lesions on MRI, small lacunar infarcts often produce adjacent rims of abnormal white matter (Gouw et al., 2008). Future studies will need to directly address the problem of infarct evolution in white matter stroke.

4.2. ET-1 induced subcortical stroke causes oligodendrocyte apoptosis and activates inflammatory mechanisms

In large artery stroke models and transient forebrain ischemia, oligodendrocyte cell death occurs within the first several days through an apoptotic mechanism (Tanaka et al., 2003). Indeed, in transient forebrain ischemia apoptotic oligodendrocyte cell death occurs before neuronal cell death (Petito et al., 1998). Oligodendrocyte cell death in the present model of white matter stroke follows a similar time course, with nuclear AIF, activated PARP and double stranded DNA nicking in oligodendrocytes at the center of the stroke site maximal 1 day after ET-1 injection. However, in this white matter stroke model apoptotic oligodendrocytes extend away from the stroke core into adjacent white matter areas that will not form part of the stroke cavity. Importantly, the areas of apoptotic oligodendrocytes correspond to areas of relative myelin loss. Oligodendrocyte cell death and secondary demyelination may place axons at risk for subsequent damage (Tekkok and Goldberg, 2001). Microglia/macrophage cells infiltrate the ischemic white matter and localize to SMI-32 positive axons soon after ET-1 injection. The SMI-32 antibody recognizes a dephosphorylated neurofilament protein that is sparsely present in normal brain, but marks areas of axonal damage after injury (Petzold et al., 2008). Such interaction between microglia and degenerating axons was confirmed ultrastructurally through the electron microscopy studies, Interestingly, IBA-1 positive microglia were also present in the contralateral side to the infarct, which may be a remote effect of the subcortical stroke. Lastly, the white matter hyperintensity observed in MRI studies, especially at day 2, very likely corresponds to immune cell infiltration and associated edema.

4.3. Glial cells respond to subcortical stroke by proliferation and differentiation

White matter stroke triggers a response from OPCs and astrocytes. NG2 positive OPCs respond to the ischemic lesion with proliferation within the first week of the stroke. After a month, fewer proliferated NG2 cells are observed. Newly generated oligodendrocytes are also present in substantial numbers one week after the infarct. These findings suggest a robust process of oligodendrocyte regeneration within the first week after white matter stroke and a potential partial reparative response, especially within the region of relative hypomyelination in peri-infarct white matter. Such a proliferative response from NG2 positive OPCs is seen in cortical stab wound injury and in inflammatory lesions of white matter (Hampton et al., 2004; Menn et al., 2007). Quantification of this process suggests that NG2 cells divide early after the stroke and are initiated to differentiate into oligodendrocytes. However, from the present data it is not clear why the number of BrdU-labeled NG2 cells and oligodendrocytes decline over one month after stroke. One possible explanation may be directly related to the astrocytic activation triggered by the stroke. Reactive astrocytes are concentrated in white matter following subcortical stroke and are found in close association with white matter tracts. Astrocytes produce extracellular hyaluronic acid that plays a role in glial scar formation and impairs OPC regenerative response in neonatal ischemia (Back et al., 2005). Hyaluronic acid is also deposited in the glial scar in this adult white matter stroke model, suggesting that local scar formation in white matter stroke may block OPC differentiation into mature oligodendrocytes. More systematic studies of cell fate mapping with inducible transgenic reporter mice (Dimou et al., 2008) might allow this question to be answered and are under way in this model. The contralateral hemisphere to the ET-1 injection displays an increase in hyaluronic acid deposition as well, yet not as pronounced as the peri-infarct area. As the infarct disconnects axonal tracts that carry connections from cell bodies that are located bilaterally, this increase may be secondary to remote astrocyte activation following axonal injury.

In summary, these data define a viable subcortical white matter stroke model in the mouse and suggest clinically relevant aspects of white matter stroke that impact initial death and degeneration or repair such as: the peri-infarct zone of partial damage, a microglial association with axonal degeneration, a glial progenitor response that may be manipulated to enhance repair in the peri-infarct zone, and the effect of a relatively widespread sensorimotor network that is disconnected by ischemic white matter axotomy.

Conflict of interest

The authors declare no conflict of interest.

Acknowledgements

We would like to thank Ms. Caroline Wallner for technical assistance, Ms. Birgitta Sjöstrand for excellent ultrastructural tissue processing, and Andy Frew and Dr. Jeff Alger for assistance in MRI imaging. These studies were supported by the Dr. Miriam and Sheldon G. Adelson, Medical Research Foundation.

Appendix A. Supplementary data

Supplementary data associated with this article can be found, in the online version, at doi:10.1016/j.jneumeth.2009.03.017.

References

Back SA, Tuohy TM, Chen H, Wallingford N, Craig A, Struve J, et al. Hyaluronan accumulates in demyelinated lesions and inhibits oligodendrocyte progenitor maturation. Nat Med 2005;11:966–72.

Bamford J, Sandercock P, Dennis M, Burn J, Warlow C. Classification and natural history of clinically identifiable subtypes of cerebral infarction. Lancet 1991;337:1521–6.

Carmichael ST. Animal models of stroke: size, mechanism and purpose. NeuroRx 2005;2:396–409.

Carmichael ST, Vespa PM, Saver JL, Coppola G, Geschwind DH, Starkman S, et al. Genomic profiles of damage and protection in human intracerebral hemorrhage. J Cereb Blood Flow Metab 2008;28:1860–75.

Dimou L, Simon C, Kirchhoff F, Takebayashi H, Götz M. Progeny of Olig2-expressing progenitors in the gray and white matter of the adult mouse cerebral cortex. J Neurosci 2008;28:10434–42.

Feng G, Mellor RH, Bernstein M, Keller-Peck C, Nguyen QT, Wallace M, et al. Imaging neuronal subsets in transgenic mice expressing multiple spectral variants of GFP. Neuron 2000;28:41–51.

Frost SB, Barbay S, Mumert ML, Stowe AM, Nudo RJ. An animal model of capsular infarct: endothelin-1 injections in the rat. Behav Brain Res 2006;169:206–11.

Fuxe K, Kurosawa N, Cintra A, Hallström A, Goiny M, Rosen L, et al. Involvement of local ischemia in endothelin-1 induced lesions of the neostriatum of the anaesthetized rat. Exp Brain Res 1992;88:131–9.

Gouw AA, van der Flier WM, Pantoni L, Inzitari D, Erkinjuntti T, Wahlund LO, et al. On the etiology of incident brain lacunes: longitudinal observations from the LADIS study. Stroke 2008;39:3083–5.

Hampton DW, Rhodes KE, Zhao C, Franklin RJ, Fawcett JW. The responses of oligodendrocyte precursor cells, astrocytes and microglia to a cortical stab injury, in the brain. Neuroscience 2004;127:813–20.

Hughes PM, Anthony DC, Ruddin M, Botham MS, Rankine EL, Sablone M, et al. Focal lesions in the rat central nervous system induced by endothelin-1. J Neuropathol Exp Neurol 2003;62:1276–86.

Horie N, Maag AL, Hamilton SA, Shichinohe H, Bliss TM, Steinberg GK. Mouse model of focal cerebral ischemia using endothelin-1. J Neurosci Methods 2008;173:286–90.

Kim KW, MacFall JR, Payne ME. Classification of white matter lesions on magnetic resonance imaging in elderly persons. Biol Psychiatry 2008;64:273–80.

Lammie GA. Hypertensive cerebral small vessel disease and stroke. Brain Pathol 2002;12:358–70.

Lecrux C, McCabe C, Weir CJ, Gallagher L, Mullin J, Touzani O, et al. Effects of magnesium treatment in a model of internal capsule lesion in spontaneously hypertensive rats. Stroke 2008;39:448–54.

Matsusue E, Sugihara S, Fujii S, Ohama E, Kinoshita T, Ogawa T. White matter changes in elderly people: MR-pathologic correlations. Magn Reson Med Sci 2006;5:99–104.

Mehta SL, Manhas N, Raghubir R. Molecular targets in cerebral ischemia for developing novel therapeutics. Brain Res Rev 2007;54:34–66.

Menn B, Garcia-Verdugo JM, Yaschine C, Gonzalez-Perez O, Rowitch D, Alvarez-Buylla A. Origin of oligodendrocytes in the subventricular zone of the adult brain. J Neurosci 2007;26:7907–18.
Millecamps S, Gowing G, Corti O, Mallet J, Julien JP. Conditional NF-L transgene expression in mice for in vivo analysis of turnover and transport rate of neurofilaments. J Neurosci 2007;27:4947–56.
Nikolov R, Rami A, Krieglstein J. Endothelin-1 exacerbates focal cerebral ischemia without exerting neurotoxic action in vitro. Eur J Pharmacol 1993;248:205–8.
Ohab JJ, Fleming S, Blesch A, Carmichael ST. A neurovascular niche for neurogenesis after stroke. J Neurosci 2006;26:13007–16.
Pantoni L, Garcia JH, Gutierrez JA. Cerebral white matter is highly vulnerable to ischemia. Stroke 1996;27:1641–6.
Pappas BA, Davidson CM, Bennett SA, de la Torre JC, Fortin T, Tenniswood MP. Chronic ischemia: memory impairment and neural pathology in the rat. Ann N Y Acad Sci 1997;826:498–501.
Paxinos G, Franklin KBJ. Mouse brain in stereotaxic coordinates. San Diego: Academic Press; 2001.
Petito CK, Olarte JP, Roberts B, Nowak Jr TS, Pulsinelli WA. Selective glial vulnerability following transient global ischemia in rat brain. J Neuropathol Exp Neurol 1998;57:231–8.
Petzold A, Gveric D, Groves M, Schmierer K, Grant D, Chapman M, et al. Phosphorylation and compactness of neurofilaments in multiple sclerosis: indicators of axonal pathology. Exp Neurol 2008;213:326–35.
Shannon C, Salter M, Fern R. GFP imaging of live astrocytes: regional differences in the effects of ischaemia upon astrocytes. J Anat 2007;210:684–92.
Tanaka K, Nogawa S, Suzuki S, Dembo T, Kosakai A. Upregulation of oligodendrocyte progenitor cells associated with restoration of mature oligodendrocytes and myelination in peri-infarct area in the rat brain. Brain Res 2003;989:172–9.
Tanaka Y, Imai H, Konno K, Miyagishima T, Kubota C, Puentes S, et al. Experimental model of lacunar infarction in the gyrencephalic brain of the miniature pig: neurological assessment and histological, immunohistochemical, and physiological evaluation of dynamic corticospinal tract deformation. Stroke 2008;39:205–12.
Tekkok SB, Goldberg MP. AMPA/kainate receptor activation mediates hypoxic oligodendrocyte death and axonal injury in cerebral white matter. J Neurosci 2001;21:4237–48.
Udaka F, Sawada H, Kameyama M. White matter lesions and dementia: MRI-pathological correlation. Ann N Y Acad Sci 2002;977:411–5.
van Dierendonck JH. DNA damage detection using DNA polymerase I or its Klenow fragment. Applicability, specificity, limitations. Methods Mol Biol 2002;203:81–108.
Vinters HV, Carmichael ST. The impact of cerebral small vessel disease on cognitive impairment and rehabilitation. In: Stuss DT, Winocur G, Robertson IH, editors. Cognitive neurorehabilitation: evidence and application. Cambridge: Cambridge Univ Press; 2008. p. 360–75.
Veenman CL, Reiner A, Honig MG. Biotinylated dextran amine as an anterograde tracer for single- and double-labeling studies. J Neurosci Methods 1992;41:239–54.
Wardlaw JM. What is a lacune? Stroke 2008;39:2921–2.

References

Arnett HA, Fancy SP, Alberta JA, Zhao C, Plant SR, Kaing S, Raine CS, Rowitch DH, Franklin RJ, Stiles CD (2004) bHLH transcription factor Olig1 is required to repair demyelinated lesions in the CNS. Science 306:2111-2115.

Arsava EM, Rahman R, Rosand J, Lu J, Smith EE, Rost NS, Singhal AB, Lev MH, Furie KL, Koroshetz WJ, Sorensen AG, Ay H (2009) Severity of leukoaraiosis correlates with clinical outcome after ischemic stroke. Neurology 72:1403-1410.

Back SA, Tuohy TM, Chen H, Wallingford N, Craig A, Struve J, Luo NL, Banine F, Liu Y, Chang A, Trapp BD, Bebo BF, Jr., Rao MS, Sherman LS (2005) Hyaluronan accumulates in demyelinated lesions and inhibits oligodendrocyte progenitor maturation. Nat Med 11:966-972.

Cahoy JD, Emery B, Kaushal A, Foo LC, Zamanian JL, Christopherson KS, Xing Y, Lubischer JL, Krieg PA, Krupenko SA, Thompson WJ, Barres BA (2008) A transcriptome database for astrocytes, neurons, and oligodendrocytes: a new resource for understanding brain development and function. J Neurosci 28:264-278.

Canoll PD, Petanceska S, Schlessinger J, Musacchio JM (1996) Three forms of RPTP-beta are differentially expressed during gliogenesis in the developing rat brain and during glial cell differentiation in culture. J Neurosci Res 44:199-215.

Cirstea MC, Levin MF (2000) Compensatory strategies for reaching in stroke. Brain 123 (Pt 5):940-953.

Coman I, Aigrot MS, Seilhean D, Reynolds R, Girault JA, Zalc B, Lubetzki C (2006) Nodal, paranodal and juxtaparanodal axonal proteins during demyelination and remyelination in multiple sclerosis. Brain 129:3186-3195.

Doetsch F, Caille I, Lim DA, Garcia-Verdugo JM, Alvarez-Buylla A (1999) Subventricular zone astrocytes are neural stem cells in the adult mammalian brain. Cell 97:703-716.

Erdmann G, Schutz G, Berger S (2007) Inducible gene inactivation in neurons of the adult mouse forebrain. BMC Neurosci 8:63.

Feng G, Mellor RH, Bernstein M, Keller-Peck C, Nguyen QT, Wallace M, Nerbonne JM, Lichtman JW, Sanes JR (2000) Imaging neuronal subsets in transgenic mice expressing multiple spectral variants of GFP. Neuron 28:41-51.

Frank S, Schulthess T, Landwehr R, Lustig A, Mini T, Jeno P, Engel J, Kammerer RA (2002) Characterization of the matrilin coiled-coil domains reveals seven novel isoforms. J Biol Chem 277:19071-19079.

Franklin RJ, Ffrench-Constant C (2008) Remyelination in the CNS: from biology to therapy. Nat Rev Neurosci 9:839-855.

Fujise K, Stacy L, Beck P, Yeh ET, Chuang A, Brock TA, Willerson JT (1997) Differential effects of endothelin receptor activation on cyclic flow variations in rat mesenteric arteries. Circulation 96:3641-3646.

Gadea A, Schinelli S, Gallo V (2008) Endothelin-1 regulates astrocyte proliferation and reactive gliosis via a JNK/c-Jun signaling pathway. J Neurosci 28:2394-2408.

Gadea A, Aguirre A, Haydar TF, Gallo V (2009) Endothelin-1 regulates oligodendrocyte development. J Neurosci 29:10047-10062.

Gouw AA, van der Flier WM, Pantoni L, Inzitari D, Erkinjuntti T, Wahlund LO, Waldemar G, Schmidt R, Fazekas F, Scheltens P, Barkhof F (2008) On the etiology of incident brain lacunes: longitudinal observations from the LADIS study. Stroke 39:3083-3085.

Huang JK, Ferrari CC, Monteiro de Castro G, Lafont D, Zhao C, Zaratin P, Pouly S, Greco B, Franklin RJ (2012) Accelerated axonal loss following acute CNS demyelination in mice lacking protein tyrosine phosphatase receptor type z. Am J Pathol 181:1518-1523.

Jafari M, Soerensen J, Bogdanovic RM, Dimou L, Gotz M, Potschka H (2012) Long-term genetic fate mapping of adult generated neurons in a mouse temporal lobe epilepsy model. Neurobiol Dis 48:454-463.

Leask A, Abraham DJ (2006) All in the CCN family: essential matricellular signaling modulators emerge from the bunker. J Cell Sci 119:4803-4810.

Malin D, Sonnenberg-Riethmacher E, Guseva D, Wagener R, Aszodi A, Irintchev A, Riethmacher D (2009) The extracellular-matrix protein matrilin 2 participates in peripheral nerve regeneration. J Cell Sci 122:995-1004.

Matzuk MM, Finegold MJ, Su JG, Hsueh AJ, Bradley A (1992) Alpha-inhibin is a tumour-suppressor gene with gonadal specificity in mice. Nature 360:313-319.

Menn B, Garcia-Verdugo JM, Yaschine C, Gonzalez-Perez O, Rowitch D, Alvarez-Buylla A (2006) Origin of oligodendrocytes in the subventricular zone of the adult brain. J Neurosci 26:7907-7918.

Mi S, Hu B, Hahm K, Luo Y, Kam Hui ES, Yuan Q, Wong WM, Wang L, Su H, Chu TH, Guo J, Zhang W, So KF, Pepinsky B, Shao Z, Graff C, Garber E, Jung V, Wu EX, Wu W (2007) LINGO-1 antagonist promotes spinal cord remyelination and axonal integrity in MOG-induced experimental autoimmune encephalomyelitis. Nat Med 13:1228-1233.

Nagaraja AK, Middlebrook BS, Rajanahally S, Myers M, Li Q, Matzuk MM, Pangas SA (2010) Defective gonadotropin-dependent ovarian folliculogenesis and granulosa cell gene expression in inhibin-deficient mice. Endocrinology 151:4994-5006.

Nait-Oumesmar B, Decker L, Lachapelle F, Avellana-Adalid V, Bachelin C, Baron-Van Evercooren A (1999) Progenitor cells of the adult mouse subventricular zone proliferate, migrate and differentiate into oligodendrocytes after demyelination. Eur J Neurosci 11:4357-4366.

Piecha D, Muratoglu S, Morgelin M, Hauser N, Studer D, Kiss I, Paulsson M, Deak F (1999) Matrilin-2, a large, oligomeric matrix protein, is expressed by a great variety of cells and forms fibrillar networks. J Biol Chem 274:13353-13361.

Rivers LE, Young KM, Rizzi M, Jamen F, Psachoulia K, Wade A, Kessaris N, Richardson WD (2008) PDGFRA/NG2 glia generate myelinating oligodendrocytes and piriform projection neurons in adult mice. Nat Neurosci 11:1392-1401.

Robak LA, Venkatesh K, Lee H, Raiker SJ, Duan Y, Lee-Osbourne J, Hofer T, Mage RG, Rader C, Giger RJ (2009) Molecular basis of the interactions of the Nogo-66 receptor and its homolog NgR2 with myelin-associated glycoprotein: development of NgROMNI-Fc, a novel antagonist of CNS myelin inhibition. J Neurosci 29:5768-5783.

Salzer JL (2003) Polarized domains of myelinated axons. Neuron 40:297-318.

Sim FJ, Lang JK, Waldau B, Roy NS, Schwartz TE, Pilcher WH, Chandross KJ, Natesan S, Merrill JE, Goldman SA (2006) Complementary patterns of gene expression by human oligodendrocyte progenitors and their environment predict determinants of progenitor maintenance and differentiation. Ann Neurol 59:763-779.

Sozmen EG, Hinman JD, Carmichael ST (2012) Models That Matter: White Matter Stroke Models. Neurotherapeutics.

Sozmen EG, Kolekar A, Havton LA, Carmichael ST (2009) A white matter stroke model in the mouse: axonal damage, progenitor responses and MRI correlates. J Neurosci Methods 180:261-272.

Tanaka K, Nogawa S, Suzuki S, Dembo T, Kosakai A (2003) Upregulation of oligodendrocyte progenitor cells associated with restoration of mature oligodendrocytes and myelination in peri-infarct area in the rat brain. Brain Res 989:172-179.

Tripathi RB, Rivers LE, Young KM, Jamen F, Richardson WD (2010) NG2 glia generate new oligodendrocytes but few astrocytes in a murine experimental autoimmune encephalomyelitis model of demyelinating disease. J Neurosci 30:16383-16390.

Wang C, Stebbins GT, Nyenhuis DL, deToledo-Morrell L, Freels S, Gencheva E, Pedelty L, Sripathirathan K, Moseley ME, Turner DA, Gabrieli JD, Gorelick PB (2006) Longitudinal

changes in white matter following ischemic stroke: a three-year follow-up study. Neurobiol Aging 27:1827-1833.

Wang Z, Colognato H, Ffrench-Constant C (2007) Contrasting effects of mitogenic growth factors on myelination in neuron-oligodendrocyte co-cultures. Glia 55:537-545.

Windrem MS, Roy NS, Wang J, Nunes M, Benraiss A, Goodman R, McKhann GM, 2nd, Goldman SA (2002) Progenitor cells derived from the adult human subcortical white matter disperse and differentiate as oligodendrocytes within demyelinated lesions of the rat brain. J Neurosci Res 69:966-975.

Yang Y, Lacas-Gervais S, Morest DK, Solimena M, Rasband MN (2004) BetaIV spectrins are essential for membrane stability and the molecular organization of nodes of Ranvier. J Neurosci 24:7230-7240.

Yeh HJ, He YY, Xu J, Hsu CY, Deuel TF (1998) Upregulation of pleiotrophin gene expression in developing microvasculature, macrophages, and astrocytes after acute ischemic brain injury. J Neurosci 18:3699-3707.

Zhu X, Bergles DE, Nishiyama A (2008) NG2 cells generate both oligodendrocytes and gray matter astrocytes. Development 135:145-157.

DISCUSSION

Similar to immune-mediated demyelination, white matter stroke in mice triggers a robust regeneration response by resident OPCs that become “reactive”. NG2 positive OPCs are recruited to the lesion and the surrounding peri-infarct white matter in high numbers within the first week of injury. Furthermore, following white matter stroke OPCs receive proper signals to proliferate as evidenced by EdU incorporation. These results indicate that OPC proliferation and mobilization steps that are necessary for oligodendrogenesis occur normally in the peri-infarct white matter.

White matter stroke differs when it comes to oligodendrocyte generation compared to other forms of experimental demyelination. Despite the robust proliferative response, our results point out a persistent OPC differentiation arrest. White matter stroke environment does not appear to support successful differentiation of the recruited OPC pool given the post-stroke OPC differentiation rate is no different than the non-injured adult white matter. It should be noted that fate-mapping studies found a percentage of reporter cells that could not be phenotyped. This is largely due to a lack of commercially available antibodies for stage-specific markers, particularly to identify premyelinating oligodendrocytes. For this reason, the number of differentiating OPCs in different stages of oligodendrogenesis may be underestimated in this study. At the same time, some of these reporters are likely newly born OPCs that did not sufficiently accumulate NG2 proteoglycan at the time of analysis, which would escape the detection by routine immunohistochemistry. Nevertheless, the lack of newly formed mature oligodendrocytes supports the failure of remyelination after stroke. Such failure is likely not due to a deficiency of OPCs but instead an absence of pro-myelinating signals and/or presence of inhibitory cues acting on OPCs. White matter stroke shows similarities with chronic MS lesions where axonal injury is prevalant, and OPC differentiation failure is common due to numerous inhibitory cues found in the injured white matter.

In search of stroke-specific inhibitory cues, we conducted novel transcriptome studies to determine the molecular mechanisms responsible for OPC differentiation arrest. Due to prominent temporal changes in stroked white matter, we anticipated OPCs to change their repertoire of autocrine and paracrine signaling later in disease compared to the early stages of stroke. This is the first white matter stroke transcriptome study to date and the only example that compared OPCs in the setting of disease. This was proven to be highly challenging for several reasons.

OPC isolation from adult white matter is a challenging task because the routine isolation techniques like FACS requires successful tissue dissociation, which was not possible because compact adult myelin. LCM was used as the next option that allowed OPC isolation from the specific site of interest. LCM isolation was made possible by genetic labeling of OPCs that induced membrane targeted GFP expression. This method allowed cell labeling that could withstand the necessary ethanol dehydration prior to LCM, unlike soluble GFP labels or immunostaining techniques that degrade the RNA. On the other hand, the current method resulted in low yields of start-up material that consequently lead to decreased transcript diversity and poor exon mapping in some of the samples. This was particularly the case for OPCs isolated from healthy brains, which did not contain high number of labeled cells. The diminished labeling is most likely due to lower baseline levels of *PDGFRa* activation compared to injured white matter. As such, the original number of six biological replicates was reduced two per stroke time point. Although the sample size is less than desired, the current data set provided instrumental information regarding the changes in OPCs gene expression in response to the evolving stroke microenvironment.

Most importantly, the OPC transcriptome study revealed two novel targets, Matrilin 2 and Inhibin A, that have opposite implications on OPC differentiation. Matrilin 2 and and its negative regulator Inhibin A have complementary profiles at the tissue level during white matter stroke. Matrilin 2 is found in OPCs and a subset of astrocytes when Inhibin A positive astrocytes had

not yet filled the white matter stroke lesion. Consistently, Matrilin 2 levels were diminished later in the disease. The *in vitro* OPC differentiation assay demonstrated that Inhibin A plays a limiting role in OPC differentiation and maturation of existing oligodendrocytes, both of which would have detrimental effects on post-stroke repair. Matrilin 2 supplementation could overcome some of these effects but had no effect on OPC differentiation per se. Inhibin A is shown to suppress *Matn2* expression in systems outside of CNS (Matzuk *et al*., 1992). Additional studies are needed to elucidate the molecular mechanisms of how Inhibin A interacts with activin receptors and the associated cell surface molecules on OPCs to downregulate gene expression. It is not clear if *Matn2* expression is induced after stroke by activin binding to respective receptors alone. The primary role of inhibins in stroke is anticipated to be antagonistic with activin downstream gene activation that is mediated mainly by Smad complexes. However, the current findings are not sufficient to show if OPCs undergo altered activation of Smads when Inhibin A is produced by astrocytes *in vivo* or in presence of exogenous Inhibin A *in vitro*. It is also possible Matrilin 2 is not the only target of Inhibin A given that exogenous Inhibin A alone limits the differentiation potential of OPCs, whereas Matrilin 2 did not change the rate of differentiaton. It is to be found if Inhibin A maintains OPCs in a progenitor state by limiting the expression of key transcription factors required for OPC differentiation. Our knowledge of activin signaling in the brain aside from neurons is limited. In order to answer these questions, the consequences activin signaling in OPCs need to be elucidated further.

Nonetheless, our results so far indicate downregulation of Inhibin A in stroke astrocytes can have mutiple consequences *in vivo*. Neutralizing Inhibin A can potentially enhance OPC differentiation similar to the culture condition. Alternatively, exogenous delivery of Matrilin 2 or downregulation of Inhibin A itself can potentially promote maturation of premyelinating oligodendrocytes in white matter stroke. Future studies are needed to assess if post-stroke remyelination can be improved by manipulating these two factors.

We had already identified several inhibitory factors before the expression profiles were completed. Changes in Hyaluronan deposition in white matter stroke is indicative of microenvironment changes following astrocyte activation. It is of high interest to antagonize Hyaluronan due to its detrimental effects on OPC differentiation (Back *et al*., 2005). One of the genes that are upregulated in 15 day stroke OPCs is *Hapln4*, which encodes for Hyaluoronan and proteoglycan link protein (Hapln). Consistent with our results, *Hapln2* expression which is another isoform of Hapln, was increased in a recent screen of focal demyelination (Huang *et al*., 2011). It is not known if increased production of this link protein reinforces the inhibitory effect of Hyaluronan on OPCs. Additionally, it is to be determined if the newly born OPCs and the surviving oligodendrocytes express altered levels of known Hyaluronan receptors CD44 or TLR2 in the peri-infarct white matter. Neither proteins were differentially expressed in the present data set but manipulation of Hyaluronan responsiveness through these receptors can be useful in white matter stroke.

Pleiotrophin deposition was also increased in stroked white matter. Pleiotrophin is known to play a role in reinforcement of OPC self-renewal capacity (Sim *et al*., 2006). The main souce of Pleiotrophin after stroke is most likely the reactive microglia within the infarct. One of the known Pleiotrophin receptor, RTPz, was not found in high abundance according to the transcriptome data. Additional experiments are needed to clarify if peri-infarct OPCs interact with deposited Pleiotrophin that can potentially limit their differentiation.

The genomic comparison of OPCs across two stroke time points revealed additional genes that are involved in OPC - immune cell interactions. Namely, *Cxcl13* and *Ccr7* were differentially expressed during the late stroke time point. CXCL13 is a chemokine normally produced by immune cells during inflammation, which is implicated in remyelination failure in EAE induced demyelination (Bagaeva *et al*., 2006). *Cxcl13* was also significantly upregulated in a recent microarray study of rat remyelination (Huang *et al*., 2011). Similar to CCXL13, the chemokine receptor CCR7 is involved in intiation of inflammation. Although CCRs are

commonly found in various types of immune cells, OPCs were shown to express a set of CCR receptors as well (Nguyen and Stangel, 2001; Maysami *et al*., 2006a; Maysami *et al*., 2006b). Particularly, studies in rat OPCs demonstrate that the expression of functional CCR3 and CCR4 by these progenitors leads to diminished capacity for migration, proliferation and differentiation in response to respective ligands (Nguyen and Stangel, 2001; Maysami *et al*., 2006a; Maysami *et al*., 2006b). It is unclear if upregulated *Cxcl13* expression is an artifact due to possible contamination during LCM isolation. On the other hand, increased CCR7 production may be biologically relevant in white matter stroke by modulating microglia/macrophage – OPC interaction. Furher *in vivo* studies have to characterize the exact role of CCR7 activation in stroke OPCs.

We identified Nogo signaling as another system that can influence white matter repair after stroke. When the well-known NgR ligands were sequestered by NgR-OMNI Fc delivery, newly born OPCs could overcome the differentiation arrest. However, axon conduction deficit measured by CAP recordings indicate demyelination is persistent after stroke, despite the modest improvement in the NgR-OMNI Fc injected brains. It is to be determined if remyelination can be enhanced with a higher dose of NgR-OMNI Fc or by constitutive administration of the compound. There are no reports of NgR-OMNI Fc delivery *in vivo* but Nogo signaling has been manipulated by systemic delivery of Nogo siRNA in the EAE model before (Yang *et al*., 2010).

The primary anticipated action of NgR-OMNI Fc is to enhace axonal regeneration. It remains to be determined if new axons are generated following NgR-OMNI Fc delivery, although CAP measurements indicated no significant changes in functional deficit. However, we did observe improved clearance of myelin debris in the NgR-OMNI Fc infused lesions. Increased clearance of myelin is shown to be involved in enhanced remyelination of shadow plaques in MS (Patrikios *et al*., 2006). Previous studies reported that myelin contains a separate set of inhibitory proteins acting on OPCs that are different than the prominent inhibitors of

axonal generation (Syed *et al*., 2008). Currently, it is unknown how NgR-OMNI Fc promotes myelin clearance after white matter stroke.

It is also unclear if NgR-OMNI Fc directly influences OPCs. The NgR complex components such as NgR isoforms, LINGO-1 and p75 were not present in the transcriptome data set, although OPCs were reported to express *LINGO-1* previously (Mi *et al*., 2005). NgR-OMNI Fc has high affinity for Nogo66 that normally binds to Nogo66 receptor/LINGO-1 complex (Mi *et al*., 2004). As such, NgR-OMNI Fc effect can be attributed to diminished LINGO-1 activation. Alternatively, reduction of available NgR ligands can potentially influence Nogo-mediated signaling in premyelinating oligodendrocytes, since NgRs were detected on this cell type in a previous study (Chang *et al*., 2010). Collectively, NgR-OMNI Fc delivery is a promising therapeautic method to enhance post-stroke remyelination. Additional studies are needed to elucidate the mechanisms of action employed by NgR-OMNI Fc in myelin debris clearance, peri-infarct axons and OPC lineage cells.

The transcriptome dataset includes semaphorin genes that are associated with axon outgrowth inhibition and OPC differentiation block. Specifically, *Sema4b* upregulation in OPCs during the early time point may add to the functional deficit. Another OPC-specific semaphorin, Sema 5A, has been shown to induce axon growth inhibition in retinal ganglion cells (Goldberg *et al*., 2004). A number of studies have also described semaphorin-dependent changes in oligodendrocte generation. For instance, MCA occlusion of Sema 4D deficient mice results in enhanced post-stroke oligodendrocyte production compared to wild-type controls (Taniguchi *et al*., 2009). Additionally, exogenous Sema 3A has been implicated in OPC differentiation block *in vitro* (Syed *et al*., 2011). When the data set was screened for known semaphorin receptor genes we found significant upregulation of *Plxna4* in day 5 stroke OPCs. Plexin A4 interacts with class 3 and 6 semaphorins. As such, increased expression of this receptor in OPCs early in disease is suggestive of OPC - semaphorin interactions. Additional studies are necessary to characterize the consequences of semaphorin system activation in stroke OPCs.

Misguided differentiation of OPCs can be another contributing factor in OPC differentiation arrest. Through genetic labeling, we show OPC fate is sometimes diverged into astrocytic lineage. A review of genetic labeling studies so far show conflicting results regarding OPC fate, which may be explained by presence of specific OPC subpopulations that are characterized by differences in NG2 and PDGFRa expression, regional differences or ectopic expression of NG2 in cells other than OPCs. In the adult brain, *Olig 2* is strictly expressed in OPC lineage cells. In contrast, non-OPC cell types utilize NG2 proteoglycan and PDGFRα for motility and survival respectively. Ectopic genetic labeling of non-OPC cells can be diminished by a prolonged wash period following recombination. Since our experimental paradigm utilized such washout period, we do not anticipate this to be an issue. Despite all this, we found a small percentage of OPC reporter cells that were differentiated into astrocytes. The astrocytic transformation of OPCs after demyelinating injury may appear insignificant. Nonetheless, the NgR-OMNI Fc study resulted in markedly diminished OPC-astrocyte transformation that was coupled with enhanced oligodendrocyte generation. Theoretically, any diversion from oligodendrocyte fate in a state of differentiation block can delay white matter repair. As such, post-stroke fate divergence warrants further investigation to determine the underlying molecular mechanisms.

The intrinsic and extrinsic changes responsible for astrocytic transformation is not known in white matter stroke but the answer may lie within the BMP signaling system. A series of *in vitro* studies have indicated high levels of BMPs, specifically BMP2, 4 and 7, are able to induce astroglial differentiation of cultured OPCs while concurrently inhibiting oligodendrocyte generation (Mabie *et al*., 1997). Furthermore, transient exposure of OPCs to BMPs was sufficient to induce such transformation, whereas extented exposure lead to propagation of astrocytes *in vitro* (Mabie *et al*., 1997). These findings suggest that a molecular switch exists controlling astrocyte transformation of OPCs. Normally, OPCs express a unique profile of BMP4 inhibitors to counteract the suppressive effects of BMP4 on Olig gene expression (Sim *et al*., 2006). Indeed, our genomic comparison of early and late stroke OPCs points out one of the

BMP inhibitors, *BAMBI,* was enriched in 5 day post-lesion OPCs. Interestingly, *BMP2* was markedly upregulated later in the disease. Induction of *BMP2* expression would explain the differentiation arrest as well as astroglial transformation of OPCs. This is suggestive of OPC autonomous cell fate regulation following white matter stroke.

In a similar fashion, canonical Notch signaling may be a contributing factor in OPC differentiation arrest. We found *Jag1* expression was significantly upregulated in early stroke OPCs. Previous reports have indicated that canonical Notch pathway activation through Jagged 1 plays a role in remyelination failure in MS (John *et al*., 2002). Although astrocytes were the main source of Jagged 1 in MS lesions, our results suggest Jagged 1 may be involved in autocrine signaling in stroke OPCs. Further investigation is necessary to understand the implications of BMP2 upregulation and Jagged 1 – Notch signaling activation in white matter stroke.

A recent microarray study conducted by Huang and colleagues provided a transcriptional database of genes that were differentially expressed in association with remyelination in rats (Huang *et al*., 2011). This study used toxin-induced focal demyelination that spontaenously remyelinates, and isolated the lesions in its entireity across three time-points during white matter repair. Through this screen, genes associated with Retionoid X receptor gamma (RXRγ) signaling were found differentially expressed. Following experiments identified RXRγ signaling as a novel regulator of remyelination (Huang *et al*., 2011). In our expression data set, we did not encounter any of the RXRγ related genes. This was expected since white matter stroke exhibits vastly different course of disease than the spontaneously remyelinating models of white matter injury.

In conclusion, through the expression profiling experiments presented here, we generated the first white matter stroke transcriptional database that will be a useful resource to understand the stroke-associated changes in white matter. The differentially expressed genes mentioned so

far can potentially alter the remyelination potential after stroke. Of particular interest, Matrilin 2 and Inhibin A are the two novel targets for follow up *in vivo* experiments.

References

Back SA, Tuohy TM, Chen H, Wallingford N, Craig A, Struve J, Luo NL, Banine F, Liu Y, Chang A, Trapp BD, Bebo BF, Jr., Rao MS, Sherman LS (2005) Hyaluronan accumulates in demyelinated lesions and inhibits oligodendrocyte progenitor maturation. Nat Med 11:966-972.

Bagaeva LV, Rao P, Powers JM, Segal BM (2006) CXC chemokine ligand 13 plays a role in experimental autoimmune encephalomyelitis. J Immunol 176:7676-7685.

Chang KJ, Susuki K, Dours-Zimmermann MT, Zimmermann DR, Rasband MN (2010) Oligodendrocyte myelin glycoprotein does not influence node of ranvier structure or assembly. J Neurosci 30:14476-14481.

Goldberg JL, Vargas ME, Wang JT, Mandemakers W, Oster SF, Sretavan DW, Barres BA (2004) An oligodendrocyte lineage-specific semaphorin, Sema5A, inhibits axon growth by retinal ganglion cells. J Neurosci 24:4989-4999.

Huang JK, Jarjour AA, Nait Oumesmar B, Kerninon C, Williams A, Krezel W, Kagechika H, Bauer J, Zhao C, Evercooren AB, Chambon P, Ffrench-Constant C, Franklin RJ (2011) Retinoid X receptor gamma signaling accelerates CNS remyelination. Nat Neurosci 14:45-53.

John GR, Shankar SL, Shafit-Zagardo B, Massimi A, Lee SC, Raine CS, Brosnan CF (2002) Multiple sclerosis: re-expression of a developmental pathway that restricts oligodendrocyte maturation. Nat Med 8:1115-1121.

Mabie PC, Mehler MF, Marmur R, Papavasiliou A, Song Q, Kessler JA (1997) Bone morphogenetic proteins induce astroglial differentiation of oligodendroglial-astroglial progenitor cells. J Neurosci 17:4112-4120.

Matzuk MM, Finegold MJ, Su JG, Hsueh AJ, Bradley A (1992) Alpha-inhibin is a tumour-suppressor gene with gonadal specificity in mice. Nature 360:313-319.

Maysami S, Nguyen D, Zobel F, Heine S, Hopfner M, Stangel M (2006a) Oligodendrocyte precursor cells express a functional chemokine receptor CCR3: implications for myelination. J Neuroimmunol 178:17-23.

Maysami S, Nguyen D, Zobel F, Pitz C, Heine S, Hopfner M, Stangel M (2006b) Modulation of rat oligodendrocyte precursor cells by the chemokine CXCL12. Neuroreport 17:1187-1190.

Mi S, Lee X, Shao Z, Thill G, Ji B, Relton J, Levesque M, Allaire N, Perrin S, Sands B, Crowell T, Cate RL, McCoy JM, Pepinsky RB (2004) LINGO-1 is a component of the Nogo-66 receptor/p75 signaling complex. Nat Neurosci 7:221-228.

Mi S, Miller RH, Lee X, Scott ML, Shulag-Morskaya S, Shao Z, Chang J, Thill G, Levesque M, Zhang M, Hession C, Sah D, Trapp B, He Z, Jung V, McCoy JM, Pepinsky RB (2005) LINGO-1 negatively regulates myelination by oligodendrocytes. Nat Neurosci 8:745-751.

Nguyen D, Stangel M (2001) Expression of the chemokine receptors CXCR1 and CXCR2 in rat oligodendroglial cells. Brain Res Dev Brain Res 128:77-81.

Patrikios P, Stadelmann C, Kutzelnigg A, Rauschka H, Schmidbauer M, Laursen H, Sorensen PS, Bruck W, Lucchinetti C, Lassmann H (2006) Remyelination is extensive in a subset of multiple sclerosis patients. Brain 129:3165-3172.

Sim FJ, Lang JK, Waldau B, Roy NS, Schwartz TE, Pilcher WH, Chandross KJ, Natesan S, Merrill JE, Goldman SA (2006) Complementary patterns of gene expression by human oligodendrocyte progenitors and their environment predict determinants of progenitor maintenance and differentiation. Ann Neurol 59:763-779.

Syed YA, Baer AS, Lubec G, Hoeger H, Widhalm G, Kotter MR (2008) Inhibition of oligodendrocyte precursor cell differentiation by myelin-associated proteins. Neurosurg Focus 24:E5.

Syed YA, Hand E, Mobius W, Zhao C, Hofer M, Nave KA, Kotter MR (2011) Inhibition of CNS remyelination by the presence of semaphorin 3A. J Neurosci 31:3719-3728.

Taniguchi Y, Amazaki M, Furuyama T, Yamaguchi W, Takahara M, Saino O, Wada T, Niwa H, Tashiro F, Miyazaki J-i, Kogo M, Matsuyama T, Inagaki S (2009) Sema4D deficiency results in an increase in the number of oligodendrocytes in healthy and injured mouse brains. Journal of Neuroscience Research 87:2833-2841.

Yang Y, Liu Y, Wei P, Peng H, Winger R, Hussain RZ, Ben LH, Cravens PD, Gocke AR, Puttaparthi K, Racke MK, McTigue DM, Lovett-Racke AE (2010) Silencing Nogo-A promotes functional recovery in demyelinating disease. Ann Neurol 67:498-507.